DOCTORAL THESIS

Lipid rafts in cancer chemotherapy

Mariana Reis Sobreiro

Salamanca, 2013

Centro de Investigación del Cáncer

CSIC-Universidad de Salamanca

Dr. **Faustino Mollinedo García**, Profesor de Investigación del Consejo Superior de Investigaciones Científicas (CSIC) y miembro del Instituto Universitario de Biología Molecular y Celular del Cáncer de la Universidad de Salamanca,

CERTIFICA:

Que el trabajo "**Lipid rafts in cancer chemoteraphy**" presentado por **Mariana Reis Sobreiro**, ha sido realizada bajo su dirección en el Instituto de Biología Molecular y Celular del Cáncer y reúne, a su juicio, originalidad y contenidos suficientes para que sea presentada ante el tribunal correspondiente y optar al grado de Doctor por la Universidad de Salamanca.

Y para que así conste, a efectos legales, expide el presente certificado en Salamanca, a 17 Junio de 2013.

Fdo. Prof. Dr. Faustino Mollinedo

This thesis was financed by Ministério da Ciência, Tecnologia e Ensino Superior, predoctoral fellowship, Fundação para a Ciência e a Tecnologia (FCT), Portugal.

Figure on the front cover: Confocal image of Jurkat cells treated with resveratrol. Lipid rafts (green fluorescence - marker cholera toxin B subunit). Fas/CD95 death receptor (red fluorescence).

Figure on back cover: Jurkat cells treated with resveratrol. Areas of co-localizacion between membrane rafts and Fas/CD95 (merged panels are yellow).

Dedico este trabalho à minha familia

Abbreviations:

A

ACAT	Acyl-coenzyme A:cholesterol acyltransferase
Akt	Protein kinase B
Akti	Akt inhibitor
ALL	Acute lymphoblastic leukemia
AML	Acute myeloid leukemia
APLs	Antitumor alkylphospholipids
ATLs	Antitumor lipids

B

Bad	Bcl-2-associated death promoter
Bcl-X_L	B-cell lymphoma-extra large
Bid	BH3 interacting domain death agonist
BSA	Bovine serum albumin

C

CASMER	Cluster of apoptotic signaling molecule-enriched rafts
CLL	Chronic lymphocytic leukemia
cSMAC	Central supramolecular activation cluster
CTx B	Cholera toxin B subunit

D

DAPI	4′,6-diamidino-2-phenylindole
DHE or HE	Dihydroethidine

$DiOC_6$ (3)	3,3′-dihexyloxacarbocyanine iodide
DISC	Death-inducing signaling complex
DMSO	Dimethyl sulfoxide
DNA-PK	DNA-dependent protein kinase
DR4	Death receptor 4
DR5	Death receptor 5
DRM	Detergent-resistant membranes

E

ECL	Enhanced chemiluminescence
EDLF	Edelfosine
EDTA	Ethylenediamine tetraacetic acid
EGFR	Epidermal growth factor receptor
EGTA	Ethylene glycol tetraacetic acid
EM	Electron microscopy
ER	Endoplasmic reticulum
ERK	Extracelular signal-regulated protein kinase
Eth	Ethidium

F

FADD	Fas-associated death domain-containing protein
FADD-DN	Dominant negative FADD
FasL/CD95L	Fas ligand/CD95 ligand
FITC	Fluorescein isothiocyanate
FRET	Fluorescence resonance energy transfer
FBS	Fetal bovine serum

G

GM1	Ganglioside GM1
G418	Geneticin
GPI	Gycosylphosphatidylinositol
GSK-3	Glycogen synthase kinase-3

H

HDL	High-density lipoproteins
HDAC	Histone deacetylase
HMG-CoA reductase	3-hydroxy-3-methylglutaryl CoA-reductase
HRP	Horseradish peroxidase

I

IFN	Interferon
IGF-1	Insulin-like growth factor 1
IgG	Immunoglobulin G
ILK	Beta-1-integrin-linked protein kinase

J

JK	Jurkat
JIP-1	c-Jun-amino-terminal kinase-interacting protein-1
JNK	c-Jun N-terminal kinase

L

L_d	Liquid disordered
LDL	Low-density lipoproteins
LiCl	Lithium chloride
L_o	Liquid ordered

M

MAPK	Mitogen-actived protein kinase
MCD	Methyl-β-cyclodextrin
MCL	Mantle cell lymphoma
MFI	Mean fluorescence intensity

MM	Multiple myeloma
mTOR	Mammalian target of rapamycin
mTORC1	Mammalian target of rapamycin complex 1
mTORC2	Mammalian target of rapamycin complex 2

P

PAGE	Polyacrylamide gel electrophoresis
PARP	Poly(ADP-ribose) polymerase
PBL	Peripheral blood lymphocytes
PBS	Phosphate-buffered saline
PC	Phosphatidylcholine
PD	PD98059 (ERK inhibitor)
PDK1	3-phosphoinositide-dependent protein kinase-1
PERF	Perifosine
PERV	Pervanadate
PH	Pleckstrin homology
PI	Propidium iodide
PI3K	Phosphoinositide 3-kinase
PIP2	Phosphatidylinositol 4,5-biphosphate
PIP3	Phosphatidylinositol 3,4,5-tristphosphate
PMSF	Phenylmethanesulfonyl fluoride
PRIF	Perifosine
PtdIns	Phosphatidylinositol
PTEN	Phosphatase and tensin homolog

R

Rafts	Lipid rafts
RESV	Resveratrol
ROS	Reactive oxygen species

S

SD	Standard deviation

SDS	Sodium dodecyl sulfate
SE	Standard error
Ser	Serine
SFVT	Single fluorophore video tracking
SHIP	Phosphatidylinositol 3,4,5-trisphosphate 5-phosphatase
SM	Sphingomyelin
SMS	Shingomyelin synthase
SP	SP600125 (JNK inhibitor)
SPT	Single particle tracking
STAT3	Signal transducer and activator of transcription 3

T

TBS	Tris-buffered saline
TBST	Tris-buffered saline with Tween
TCR	T-cell receptor
Thr	Threonine
TNF	Tumor necrosis factor
TRAIL	Tumor necrosis factor-related apoptosis-inducing ligand
Tris	Tris(hydroxymethyl)aminomethene

W

WN	Wortmannin

Z

z-AEVD-fmk	z-Ala-Glu(OMe)-Val-Asp(OMe)-fluoromethyl ketone
z-IETD-fmk	z-Ile-Glu(OMe)-Thr-Asp(OMe)-fluoromethyl ketone
z-VAD-fmk	benzyloxycarbonyl-Val-Ala-Asp(OMe)-fluoromethyl ketone

4E-BP1	4E-binding protein 1
$\Delta\Psi_m$	Mitochondrial membrane potential

Table of contens

1.INTRODUCTION 1
1.1. Cholesterol and cancer 1
1.2. Lipid rafts 3
1.2.1. Historical overview 3
1.2.2. Lipid raft characterization 4
1.2.3. Raft redefinition and function 5
1.2.4. How do proteins sort in lpid rafts? 6
1.3. Rafts and signaling 8
1.3.1. Akt Pathway 8
1.3.2. Fas/CD95 Pathway 9
1.3.3. Additional raft-dependent processes 10
1.4. Changing rafts, changing cancer cell fate: raft-targeting drugs 11
1.4.1. Modulation of Akt signaling by altering cholesterol levels through statins and cholesterol-depletion Agents 11
1.4.2. Anticancer alkylphospholipids (APLs) or antitumor lipids (ATLs) 13
2.HYPOTHESIS 19
3.OBJECTIVES: 21
4.MATERIALS AND METHODS 23
4.1. Reagents 23
4.2. Cell culture 24
4.3. Flow cytometry 26
4.4. Apoptosis quantification by the interaction of Fas/CD95-FasL/CD95L 27
4.5. Western blot 28
4.6. INF-γ treatment 28
4.7. Confocal microscopy 29
4.8. Cholesterol depletion 31
4.9. Lipid raft isolation 31
4.10. Xenograft mouse model 32
4.11. Measurement of caspase-8 and caspase-9 activities 32
4.12. Statistical analysis 32
5.RESULTS 35
5.1. Involvement of mitochondria and recruitment of Fas/CD95 signaling in lipid rafts in resveratrol-mediated antimyeloma and antileukemia actions 35
5.1.1. Introduction 35
5.1.2. Results 36
5.1.3. Discussion 49

5.2. Lipid raft-mediated Akt signaling as a therapeutic target in mantle cell lymphoma..... 53
5.2.1. Introduction.....53
5.2.2. Results.....55
5.2.3. Discussion.....72
5.3. The antitumor lipid edelfosine in combination therapy for multiple myeloma.....77
5.3.1. Introduction.....77
5.3.2. Results.....78
5.3.3.Discussion.....84
*6.*GENERAL DISCUSSION.....87
*7.*CONCLUSIONS.....93
*8.*SPANISH SUMMARY.....95
Lipid rafts como dianas terapéuticas en el tratamiento del cáncer.....95
8.1. Introducción.....95
8.1.1. Colesterol y cáncer.....95
8.1.3. *Lipid rafts*.....96
8.1.4. *Rafts* y señalización.....98
8.1.5. Modulación de *rafts* en células tumorales..... 100
8.2. Objetivos: 103
8.3. Resultados y discusión..... 104
8.3.1. La acción apoptótica del resveratrol sobre células de mieloma múltiple y de leucemia implica a la mitocondria y el reclutamiento de Fas/CD95 en *lipid rafts* . 104
8.3.2. La activación de Akt mediada por *rafts* como diana terapéutica en células de linfoma de manto 109
8.3.3. Edelfosina en terapia combinada en el tratamiento del mieloma múltiple... 115
8.4. Conclusiones..... 117
*11.*AGRADECIMIENTOS 118
*12.*REFERENCES 120

1. INTRODUCTION

1.1. Cholesterol and cancer

Cholesterol content in tumoral tissues has been the topic of investigations since the beginning of 20th century [1-3] (**Fig. 1 A**). The first evidences already showed that cholesterol was greatly increased in cancer cells and in the surrounding tissues, as compared with the normal tissues from which the transformed cells derived [1-3] (**Fig. 1 B**). Nevertheless, it remains unclear whether such changes play a role in disease progression or are merely byproducts of other metabolic changes in cancer cells [4]. In other words, it remains unknow if cholesterol accumulation in transformed tissues promotes cancer appearance, or whether it is consequence of the neoplastic transformation. Only epidemiological studies revealed that prolonged use of lowering cholesterol drugs (statins) can be associated with prevention of some kinds of tumors such as prostate and kidney cancers, then suggesting that cholesterol accumulation could contribute to the appearance of a malignant neoplasm [5,6].

Cholesterol is critical for the synthesis of cell membranes [7], it follows that rapidly proliferating tumor cells require more cholesterol than normal cells [8,9]. In this regard, alterations in cholesterol regulation, have been detected in a wide number of solid and hematological cancers [1,9]. Cancer cells have been reported to show: **1)** enhanced endogenous cholesterol biosynthesis by increased 3-hydroxy-3-methylglutaryl CoA reductase activity (HMG-CoA-reductase; rate-limiting enzyme of the metabolic mevalonic pathway that generates cholesterol); **2)** increased exogenous cholesterol uptake by over-expression of low-density lipoprotein (LDL)-receptor, LDLs being the major bloodstream transporters of cholesterol; **3)** increased cholesterol acyltransferase enzyme activity (ACAT) that mediates cholesterol esterification for intracellular

storage; and **4)** lower cholesterol efflux mediated by high-density lipoproteins (HDL)-receptor [9] (**Fig. 1 C**).

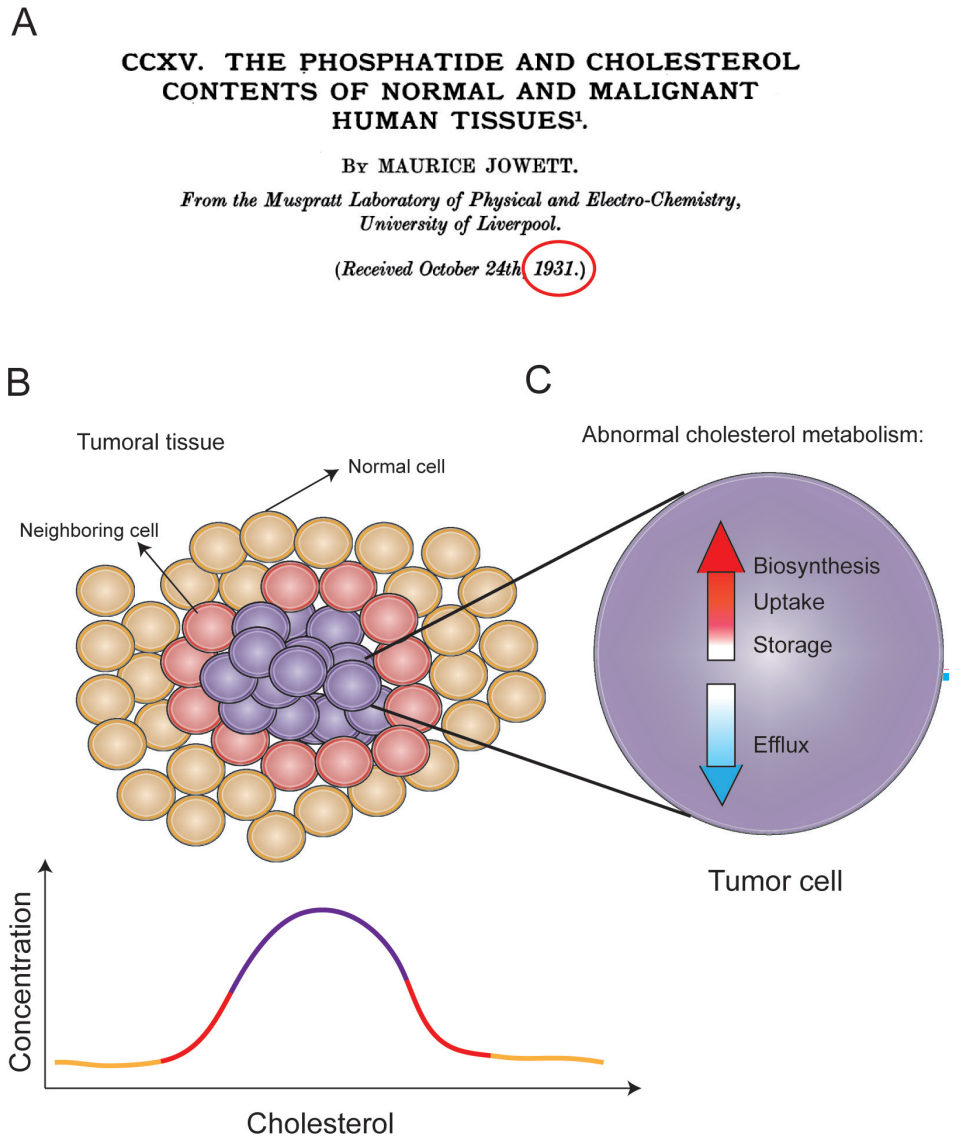

Figure 1- Alterations in the mechanisms that underline the basis of cholesterol regulation in tumoral tissues. (*A*) Report about cholesterol content in cancer cells from the beginning of the 20th century. (*B*) Cholesterol accumulation in tumor cells and surrounding tissues (neighboring cell) has been reported in a large variety of tumor types.(*C*) Deregulation in biosynthesis, uptake, storage and efflux of cholesterol have been detected in cancer cells leading to cholesterol homeostasis breakedown.

The control of cholesterol content is a narrow balance between metabolic processes intrinsic to the cell and the regulation of cholesterol distribution in the organism. Extensive evidences indicate that this complex homeostatic mechanism breaks down not only in cancer, but also in aging tissues [6,10,11]. In addition to the cholesterol implication in cancer cell signaling that we will discuss later, cholesterol is a key component in cell membranes. Cholesterol is a major regulator of lipid organization,

promoting phase separation and stabilizing the formation of microdomains, with closely packed acyl chains of phospholipids, known as lipid rafts [4,5,7] .

1.2. Lipid rafts

1.2.1. Historical overview

Membranes of mammalian cells are composed of a tremendous variety of lipid species still not yet fully identified, including glycerophospholipids, sphingolipids, mono-, di- or triglycerides, fatty-acid and sterol-based structures [12]. Plasma membrane was first defined as a fluid lipid bilayer with floating proteins, considered key components for membrane functionality, and subjected to random mixing -Singer-Nicholson model or "fluid mosaic"- [13,14] (**Fig. 2 A**). It is now clear that far from being disordered, plasma membranes are complex, compartmentalized dynamic structures [15] containing multiple microdomains with specialized functions. These microdomains comprise focal adhesions, tight and adherens junctions, clathrin-coated pits, among others [6]. Non-random distributions of proteins and lipids (assemblies of sphingolipids and cholesterol) were proposed to form microdomains in plasma membranes named as lipid rafts. This hypothesis was postulated in 1997 by Kai Simons and Elina Ikonen [16] (**Fig. 2 B).** The main functions of lipid rafts were initially thought to be related to transport of selected membranes (membrane trafficking) and cellular signaling [12,16] (see Rafts Redefinition and Function).

Lipid raft hypothesis was developed based on epithelial cell polarity and lipid behavior in artificial model membrane studies [16]. A key aspect for lipid raft preliminary models was the observation that assemblies of cholesterol, sphingolipids and glycosylphosphatidylinositol (GPI)-anchored proteins were meant to be delivered to the apical plasma membrane from the Golgi apparatus. This aspect being determinant for epithelial cell differential lipid content in apical (sphingolipid enriched) and basolateral (phosphatidylcoline enriched) plasma membranes –lateral heterogeneity-[16-18]. This was the first indication that cell membranes were also able to segregate different lipid species, as artificial models membranes predicted. Cellular membranes were not just random mixtures of lipids. Despite the complexity of cellular membranes, some insight into their behavior was also anticipated by analyzing lipid mixtures in artificial model membranes that reveled phase separation between sterol-dependent liquid-ordered (L_o), and liquid disordered (L_d) phases, predicting that this phenomena can also occur under physiological conditions [14,19].

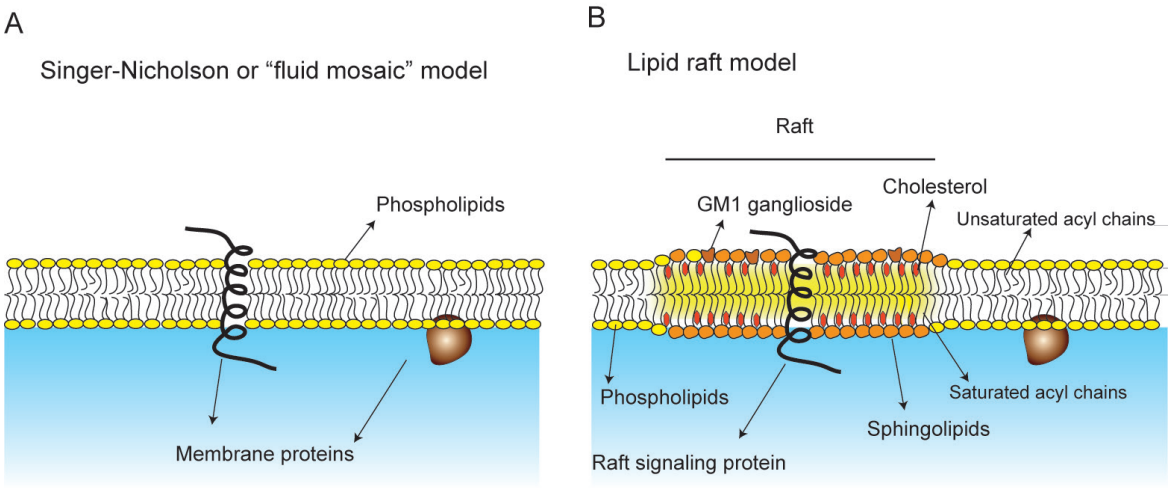

Figure 2- Singer-Nicolson vs. lipid raft model. (*A*) Plasma membranes were first defined as a lipid bilayer with proteins "floating", picturized as a "lipid sea" where lipids could diffuse freely through the membrane. (*B*) Lipid raft hypothesis gives lipids some protagonism, and rafts were first defined as mobile microdomains in the cell membrane specialized in signaling and membrane trafficking, enriched in cholesterol and sphingolipids with saturated acyl chains. Cholesterol fills interstitial spaces between lipids, confers rigidity and closely packs acyl chains promoting phase separation in the lipid membrane. Interaction with cholesterol forces hydrocarbon chains into more extended conformations, increasing membrane thickness. GM1 is a ganglioside associated with rafts currently used as a lipid raft marker.

1.2.2. Lipid raft characterization

After the postulation of lipid raft model, an intense debate emerged in this field; the isolation techniques employed and the impossibility of *in vivo* visualization of rafts were the main topics of controversy [14]. In this sense, raft size is below the resolution of light microscope, the isolation process of rafts is detergent-based, and only after cross-linking with exogenous ligands raft constituents cluster together to form micrometer-size patches able to be detected by light microscopy. All these aspects gave raise to some doubts on whether rafts were a real phenomenon. The knowledge of the precise raft size and dynamics was limited by the available methodology at the time [14].

Rafts are usually referred to as L_o or detergent-resistant membrane (DRM) fractions, leading to some confusion about its meaning. L_o phases were observed in artificial model membranes, enriched with raft components: sphingolipids, cholesterol and saturated lipids. The equivalent structures in biological membranes are called rafts surrounded by a contiguous "sea" of unsaturated lipids equivalent to L_d phase in model membranes. DRMs are the residue that remain insoluble after non-ionic detergent extraction and that includes rafts, clustered rafts and caveolae (**Fig. 3**). Non-ionic detergent extraction and ultracentrifugation in sucrose gradients is the usual biochemical technique for lipid raft isolation. However, this procedure is

not able to discriminate among rafts, clustered rafts and caveolae [12,14,19]. Caveolae are microdomains isolated by the same detergent-based technique, but they are easily detected by electron microscopy (EM) due to their typical "cave" structure. They are characterized also by the presence of the caveolin protein [20]. Caveolae show a more restricted tissue distribution than rafts, which appear to be ubiquitous in eukaryotic cells. Caveolae are abundant in muscle cells, endothelial cells, adipocytes, and fibroblasts, but its presence is rare or absent in lymphocytes and most neuronal cells [13,20]. Although the noncaveolar form of lipid rafts is less defined than caveolae, the biophysical properties of both microdomains are similar. It has been suggested that rafts can supplant caveolae functions in free caveolae tissues [6,21].

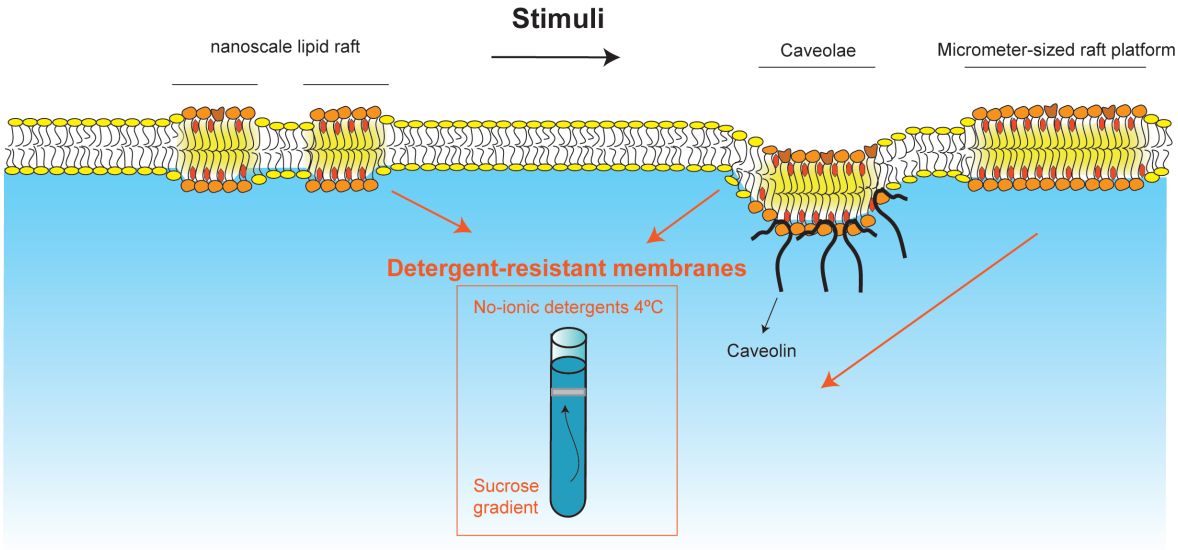

Figure 3 - Detergent-resistant membrane isolation. Lipid rafts are isolated with non-ionic detergents such as Triton X-100 at low temperature (4ºC), followed by ultracentrifugation in sucrose gradients. The membranes isolated by this method are called detergent resistant membranes (DRMs). This is the most common method used for lipid raft isolation, although it does not differentiate between lipid rafts and caveolae domains. Following cell stimulation, rafts can form platforms with sizes able to be detected with conventional microscopy. Caveolae or "little caves" and lipid rafts have been related with many cellular functions as endocytosis and signal transduction. Caveolae microdomains are characterized by the presence of caveolin protein.

Lipid rafts are more abundant at the plasma membrane than in intracellular membranes, being positively correlated with sterol content, but they can also be found in endocytic and secretory pathways; however, the situation for intracellular membranes is less clear [12-14,17].

1.2.3. Raft redefinition and function

The development of new techniques with high temporal and spatial resolution

allowed the visualization/detection of rafts before patches formation, supporting and redefining raft existence [14,22]. These imaging approaches include single particle tracking (SPT), single fluorophore video tracking (SFVT), fluorescence resonance energy transfer (FRET), homo-FRET and EM [19]. In the light of these new approaches, rafts are now described as dynamic, nanoescale, sterol/shingolipid-enriched, ordered assemblies of proteins and lipids, in which the metastable raft resting state can be stimulated to coalesce into larger, more stable raft domains by specific lipid-lipid and protein-protein oligomerizing interactions [14]. Lipid rafts act as a membrane organizing principle in cellular processes, basically, they can facilitate protein-protein interactions by selectively exclude or include proteins. Lipid rafts have been implicated in signal transduction, endo and exocytose, membrane trafficking and viral infection [13,14,19].

The evolution of the lipid raft hypothesis from the original concept of stable pre-existing domains to one of more transient, dynamic platforms has been viewed with some skepticism because of the very short time- and length-scale recordings for nanodomains in living cells [15]. However, John F. Hancock and colleges [15,19] additionally using computational modeling studies, argue that it is precisely the above properties that make lipid rafts (or nanodomains at the light of their dimensions) ideal components for building biological signaling circuits. Thus, nanodomains protect the system from signal degradation during the information transfer across the plasma membrane. They conclude that transient and short life-time protein interactions with small lipid-raft domains facilitate useful biochemical reactions [15,19].

1.2.4. How do proteins sort in lipid rafts?

A number of proteins in different cells show reversible association to rafts in response to appropriate signals [13]. The physical segregation of proteins into lipid rafts may regulate the accessibility of those proteins to regulatory or effector molecules [13]. The precise mechanisms by which proteins sort into rafts are not fully understood. For example, lipid shells hypothesis proposes that specific membrane proteins bind complexes of cholesterol and sphingolipids that confer lipid buoyancy independently of raft/caveolae association. These shells are dynamic within the membrane and they are attracted to lipid raft domains in which shells are miscible [14,23]. However, recent evidences are not compatible with this hypothesis, pointing that raft proteins can function as surfactants, reducing line tension between lipid raft (ordered) and non-raft domains (disordered), with preferential protein localization in the domain boundaries

[19]. In the first instance of lipid raft hypothesis, it was considered that rafts function as protein transporters, promoting protein interactions in the cell membrane. Now, it is believed that proteins help capturing and stabilizing raft domains [19].

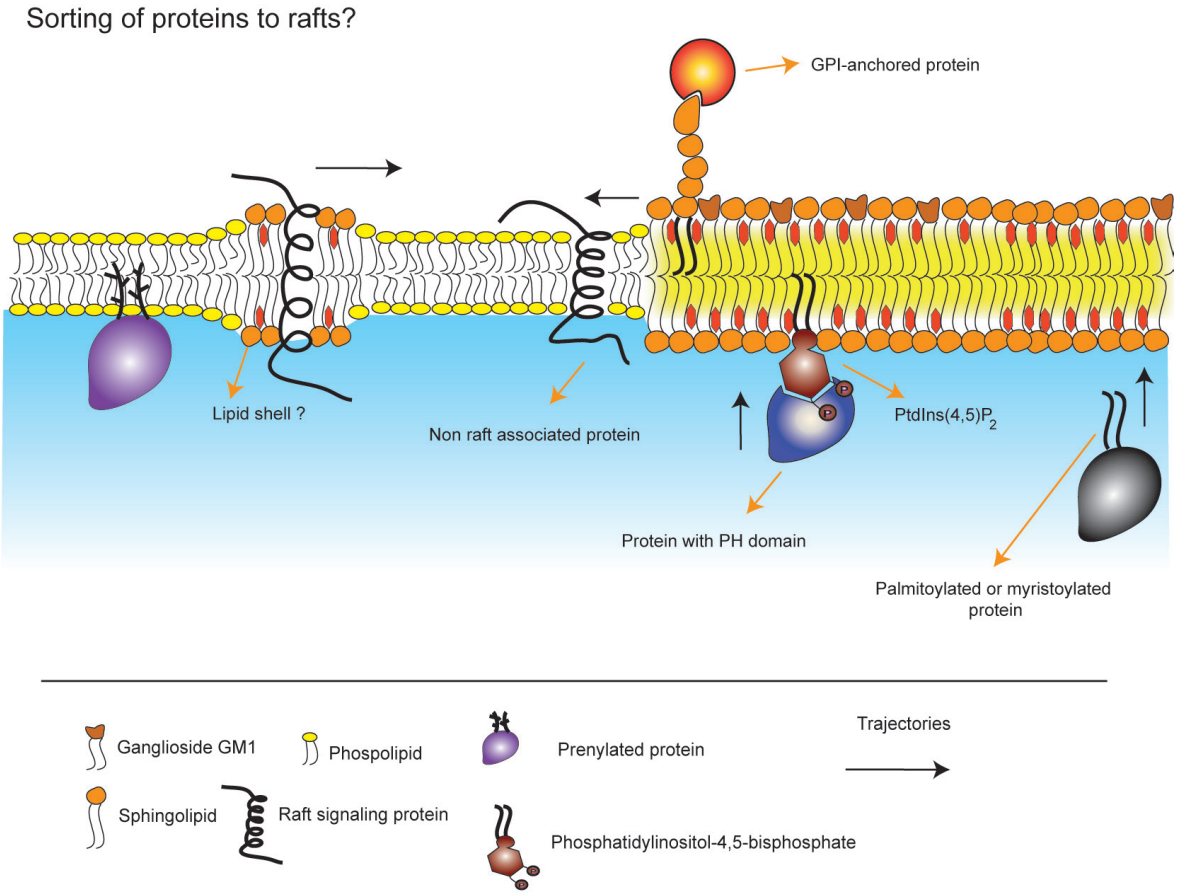

Figure 4- **How proteins are sorted into lipid rafts?** Proteins can be sorted to lipid rafts depending on the length of the hydrophobic transmembrane domains and on the partitioning properties of their "hydrophobic tails". Proteins containing GPI tail as well as myristoylated or palmitoylated tails are signaled for raft incorporation. Prenylated proteins are excluded from rafts. Proteins may be sorted through binding to another raft membrane protein. Proteins with pleckstrin homology domains (PH) can be sorted to lipid rafts as rafts are specially enriched with phosphatidylinositols. "Lipid shell" hypothesis says that proteins with raft destination have shells with a lipid composition similar to raft domains. Cholesterol increases the bilayer thickness and in some extent might affect protein sorting, depending on the transmembrane domain length.

The elevated levels of cholesterol in rafts have been argued to determinate transmembrane protein sorting; cholesterol increases membrane thickness and therefore proteins with short transmembrane domains could be excluded from rafts [4,12,13]. Furthermore, some protein localization in raft domains can be determined by post-translational lipid modifications known as "hydrophobic tails" [13]. For proteins with lipid or fatty-acid anchors, the preference to raft or non-raft domains depends on the properties of the acyl chains. In this regard, GPI-anchored proteins have preference

for lipid rafts because phosphoinositide anchors typically have saturated chains. Likewise, many myristoylated and palmitoylated proteins sort to lipid rafts (**Fig. 4**). In contrast, prenylated anchors tend to disordered domains due to the unsaturation of the isoprenyl groups [4,13,24].

The most important role of rafts at the cell surface may be their function in signal transduction [17,25]. Rafts might form concentrating platforms for individual receptors, where the signaling complex is protected from non-raft enzymes such as membrane phosphatases that otherwise could affect the signaling process. In general, raft binding recruits proteins to a new micro-environment, where the phosphorylation state can be modified by local kinases and phosphatases, resulting in downstream signaling [17,25].

The importance of lipid rafts domains in the transmission of growth promoting and apoptotic signaling will be analyzed in the following chapters. The scope of this Introduction is not to cover all raft molecules mentioned in literature. Instead, it would be briefly summarized the role of lipid rafts in the activation of PI3K/Akt and Fas/CD95 pathways, as prominent examples of cell survival and death signaling pathways, as well as to understand the action of some antitumor compounds, which target cancer cells by a cholesterol-lipid raft-dependent mechanism.

1.3. Rafts and signaling

1.3.1. Akt Pathway

The Akt signaling pathway is one of the most frequently hyperactivated signaling pathways in human cancers, with a wide range of cellular targets [26,27]. The oncogenicity of Akt arises from activation of both proliferative and anti-apoptotic signaling routes. Furthermore, Akt contributes to tumor progression by promoting cell invasiveness and angiogenesis [26,27]. Hyperactivation of Akt protect cancer cells against apoptotic insults, and is found more frequently activated in poorly differentiated tumors that are more invasive, grow faster and respond less to treatment [28]. Thus, the pathological finding of hyperactivated Akt in primary tumors is considered to be a negative prognostic marker for disease outcome [28].

Membrane recruitment is crucial for Akt activation, being promoted by the Akt pleckstrin homology domain (PH) which has high-affinity to membrane inositols [27,29]. In different types of cancer, it has been found a mutation at Akt1 PH domain. This mutation leads to permanent Akt membrane association, then resulting in a constitutive activation of Akt [28,30]. The membrane localization protects Akt from inactivation

by phosphatases [27]. This observation is in agreement with the lipid raft hypothesis which suggests that rafts environment protects protein signaling complexes. In this regard, elevated levels of lipid rafts in cancer cells [31], which are specially enriched with inositols [30,32,33], have been related with oncogenesis by promoting overactivation of Akt signaling pathway [34]. Furthermore, other kinases implicated in Akt activation such as mammalian target of rapamycin (mTOR), phosphoinositide-3-kinase (PI3K) and 3-phosphoinositide protein dependent-kinase-1 (PDK1) have been detected in lipid rafts, reflecting the importance of these domains for Akt pathway regulation [30,32].

An overwhelming evidence of raft implication in Akt pathway regulation comes with the use of high resolution techniques that were able to track Akt *in vivo*. Reports from Lasserre [32] and Gao [34] laboratories maintaining live-cell context, determined that lipid rafts were indispensable for Akt membrane recruitment and activation.

1.3.2. Fas/CD95 Pathway

Cell death can be triggered by several pathways and different kinds of cell death have been described, including, necrosis, apoptosis, lipoptosis, necroptosis, autophagy among others [35]. In some cases, cells show a mixture of the different types of cell deaths. In the simplest and classical way, cell death is usually defined as programmed cell death -apoptosis- or necrotic cell death. In apoptotic cell death, two major pathways have been extensively described, namely: extrinsic pathway, mediated by death receptors and intrinsic pathway mediated by mitochondria [35]. Fas/CD95 is a well known death receptor, and its proper function is essential for the elimination of viral or transformed cells [36].

Signaling of death pathways has been related with lipid rafts, including death-receptor-mediated signaling pathways [22,37-39]. It is still unknown how the strongly raft-disfavoring transmembrane domains of death receptors are arranged with respect to the raft bilayer. Despite it has been described that some death receptors have an "hydrophobic tail", some are palmitoylated proteins, it might be expected that death receptors prefer lipid raft boundaries, positioning their transmembrane domains in disordered domains and their palmitate chains adjacent to raft domains [33].

The death receptor Fas/CD95 and its natural ligand Fas ligand (FasL/CD95L) can be palmitoylated [36,40,41]. In this regard, some reports have shown that the partitioning of both FasL/CD95L and Fas/CD95 into rafts is necessary for efficient cell death signal transduction [36,38-40,42], promoting an efficient Fas/CD95-FasL/CD95L interaction, first described in our group [37,38,41,42]. Upon binding to FasL/CD95L, Fas/

CD95 receptor is activated, then initiating apoptotic signaling cascades in Fas/CD95-expressing cells. However, Fas/CD95 can aggregate and become active in the absence of FasL/CD95L [35,37,43]. It has been proposed that redistribution of Fas/CD95 into lipid rafts is important in the activation of ligand-independent Fas/CD95-induced apoptosis [35,37,44]. The redistribution of this receptor in lipid rafts was firstly described during research conducted with chemotherapeutic drugs that we will discuss later [37-39]. Thus, Fas/CD95 redistribution into lipid rafts can occur naturally promoted by "death cytokines", such as FasL/CD95L, but also by chemotherapeutical agents that have the potential to mimic such cytokine effect [37,45]. In addition, other death receptors, such as tumor necrosis factor-related apoptosis-inducing ligand (TRAIL) receptors, have been reported to be palmitoylated for lipid raft partitioning and proper signal transduction activation [46].

Furthermore, it has also been proposed that ceramide formation from the conversion of sphingomyelin (SM) (a type of sphingolipid) can promote lipid raft platform formation, Fas/CD95 clustering and triggering apoptotic signaling [35,47].

1.3.3. Additional raft-dependent processes

The formation of raft signaling platforms has been extensively reported during T-cell immunological synapse [14]. In this process, T-cell receptors (TCRs) are first engaged and activated in TCR microclusters, then transported towards the central supramolecular activation cluster (cSMAC), where raft-platforms are stabilized and many proteins are involved [14]. Larger and stable platforms seem to be required for protein trafficking endocytosis, and for highly specialized function such as T-cell synapse [14].

Raft clustering seems to be critical as well for Ras signaling [19]. Three different Ras isoforms, H-Ras, N-Ras and K-Ras, have been reported to occupy distinct rafts (nanoclusters) that have different structural requirements for actin, cholesterol and various scaffold proteins. One of the core signaling pathways activated by Ras is the mitogen activated protein kinase (MAPK) cascade that comprise Raf, MEK and extracelular signal-regulated protein kinase (ERK) [15].

Finally, the involvement of rafts in cancer is reaching a new exciting field as they are being related with the invasive capacity of cancer cells. Tumor cell structures named invadopodia are specialized raft-like membrane domains, where cholesterol levels are tightly regulated, and active transport of protease-delivering carriers is required for their function [18].

Lipid rafts may provide an important subcellular microenvironment in which signals are processed, including central signals for tumor cell growth, resistance to apoptotic signals, and other aggressive characteristics [48]. In the following chapter we will discuss the possibility of targeting lipid rafts as a selective therapy for cancer. Summarizing the above data we can envisage that cancer cells are enriched in cholesterol/lipid rafts, and these domains are critical platforms for the signaling of survival pathways.

1.4. Changing rafts, changing cancer cell fate: raft-targeting drugs

1.4.1. Modulation of Akt signaling by altering colesterol levels through statins and cholesterol-depletion agents

Tumor cell survival and death are susceptible to be modulated by altering the cellular cholesterol content. Different kinds of tumors undergo cell death through the inhibition of endogenous cholesterol synthesis by statins [49,50] or by cholesterol depletion from membranes, this lethality being related to the disruption of Akt signaling [31,50-52].

On the other hand, elevated circulating levels of cholesterol have been shown to promote tumor cell growth. Freeman and colleges [49], using *in vivo* models, provide evidences that elevated circulating cholesterol leads to increased cholesterol content in the lipid rafts of cells isolated from xenograft tumors. They also detected increased phosphorylation of Akt and reduced apoptosis in these cells, thus suggesting that some kinds of tumors can become dependent on a cholesterol-regulated Akt pathway for cell survival [48,49] (**Fig. 5 A**).

Despite the above relationship between rafts and Akt upregulation in tumor cells, inactivation of the tumor suppressor PTEN (phosphatase and tensin homolog), the Akt upstream phosphatase, is usually present. However, Akt activity can be regulated by cholesterol, even when PTEN is mutated. Thus, despite Akt overactivation has been typically associated to mutated PTEN, cholesterol depletion can downregulate Akt activity. In this regard, lipid rafts could play a major role for constitutive Akt signaling in tumor cells. Previous reports with statins have shown that these compounds preferentially inhibit Akt phosphorylation at Ser473, that usually takes place in lipid rafts. On these grounds, targeting lipid rafts could be a possible therapeutic approach for Akt downregulation [51].

In this regard, cancer cells with a higher content of cholesterol-rafts have been related with their higher sensitivity to undergo apoptosis by cholesterol-depleting

agents [31]. Interestingly, Akt has been implicated in the transcriptional induction of

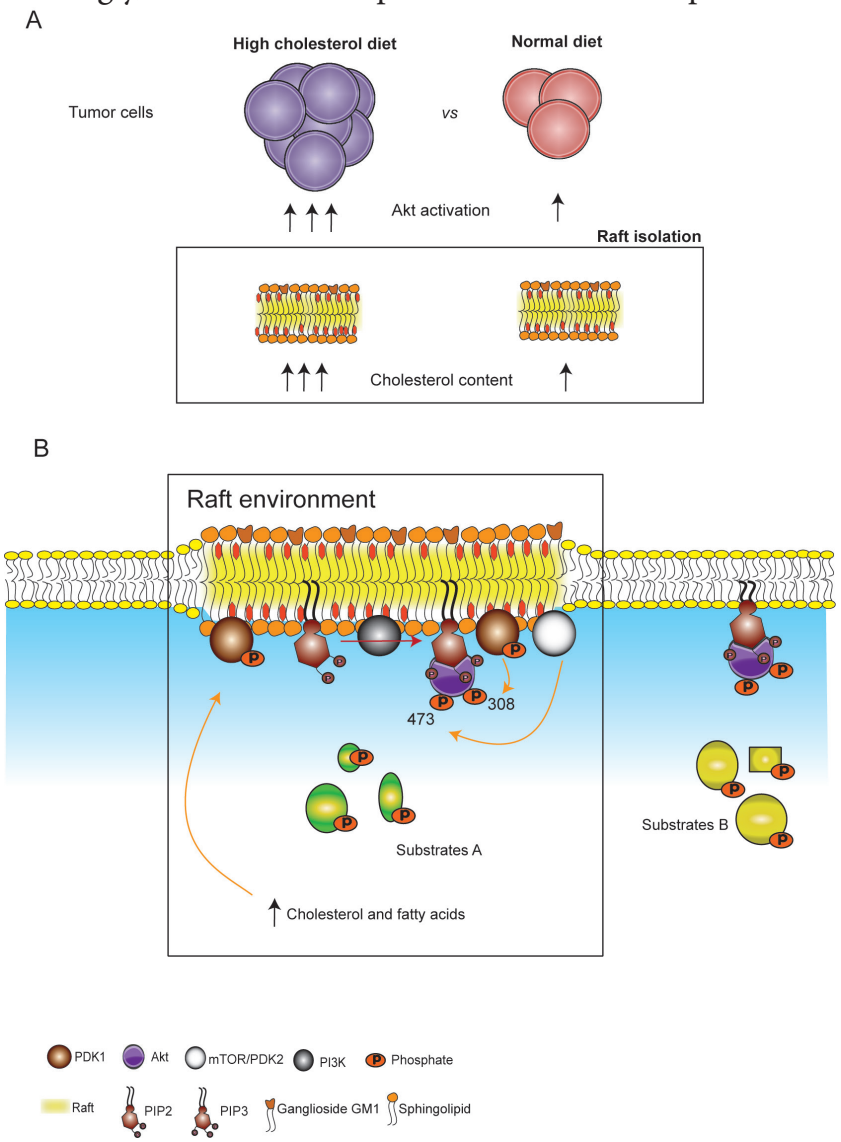

Figure 5- Cholesterol modulates Akt pathway in cancer cells. (*A*) *In vivo* experiments showed that diets with high contents of cholesterol lead to raft expansion and promotes activation of Akt pathway in xenograft tumors. Circulating cholesterol can promote survival signaling. (*B*) Raft environment can affect the affinity of Akt for its substrates, suggesting that differential Akt localizations can lead to different signaling routes. Furthermore, Akt can promote its own activation by regulating the expression of genes involved in the synthesis of raft components such as cholesterol and fatty acids.

enzymes involved in cholesterol and fatty acid biosynthesis, including: HMG-CoA-reductase, HMG-CoA synthase and fatty acid synthase [53]. Therefore, Akt activity may be related with to the mentioned cholesterol accumulation in tumors [53]. Furthermore, Akt can promote its own activation in tumor cells, by supplying substrates for the synthesis of membrane components, including raft components [53]. A positive feedback mechanism seems to exist, whereby signals transmitted by raft-located Akt can lead to enhanced cholesterol synthesis, expansion of the cholesterol-rich compartment, and

increased localization of Akt to rafts [48]. Furthermore, raft-located Akt could promote a distinct Akt-substrate preference, leading to a signal transduction different from that of non-raft Akt [48]. These findings suggest that tumor cells possibly contain discrete Akt populations that trigger distinct signals depending on their subcellular location (**Fig. 5 B**) [48,49]. It has been suggested that antiapoptotic signals are transmitted, at least in part, by raft-resident Akt [48]. In addition, differences in substrate preference might result from a change in conformation of Akt in rafts or from a differential association of Akt with interacting proteins enriched in distinct subcellular compartments [48].Taken together, these results suggest that cholesterol inhibitors may be used for chemoprevention or cancer therapy, likely in combination with other chemotherapeutic drugs [6,48,49].

1.4.2. Anticancer alkylphospholipids (APLs) or antitumor lipids (ATLs)

ATLs are metabolically stable analogs of lysophosphatidylcholine [56-60]. The selectivity and antitumor properties both *in vitro* and *in vivo* of some of these ATLs were first described by Munder and colleges [54,55]. Among these ATLs, edelfosine appeared as a very effective anticancer compound, and become the prototype in antitumor activity trials [56-60]. Edelfosine was found to promote selectively apoptosis in cancer cells, whereas normal cells were spared [59]. The mechanism of action of ATLs differs from classical chemotherapeutic drugs, since their molecular targets are located at the cellular membranes rather than at the DNA. Due to their chemical structure, with essentially one long non-polar hydrocarbon chain, ATLs easily insert into the plasma membrane lipid bilayer [39,56,61,62]. Even though the selective uptake of edelfosine is suggested to be protein-mediated[59], it has been also hypothesized that edelfosine selectivity to tumor cells was, at least in part, affected by its affinity to membrane cholesterol, as there is a geometric compensation of the "cone shape" of sterols and the "inverted cone shape" of edelfosine that leads to the formation of stable bilayers [8,61,63,64]. In this regard, several reports relate ATL antitumor activity with lipid rafts. It has been reported that ATLs accumulate in lipid rafts undergoing a subsequent raft-mediated internalization [56,65,66], and that ATLs can induce raft clustering into larger platforms [37-39,56,57,67].

Van Blitterswijk [68] and colleagues have shown that mouse lymphoma cells resistant to ATLs have no biosynthesis of the raft constituent SM due to the complete downregulation of sphingomyelin synthase (SMS1) [68]. SMS1 is usually located in trans-Golgi network. SMS1 not only produces SM, then facilitating new lipid raft formation, but it is also necessary for membrane raft vesicular trafficking towards (anterograde)

and from (retrograde) the plasma membrane [56].

1.4.2.1. ATLs in hematological malignancies

ATLs can activate apoptosis in cancer cells by multiple signaling pathways, one of them is extensively documented in hematological cancers, and implies the translocation and co-capping of lipid rafts and death receptors [38,64,69,70]. Fas/CD95, a member of the tumor necrosis factor (TNF) receptor gene superfamily, was primarily described to be recruited in tumor cell lipid rafts from tumor cells following ATL incubation, this phenomena being related to the triggering of cell death [37-39,69]. Subsequently, TRAIL death receptors, have also been reported to be recruited in rafts after ATL incubation [64,69]. These findings led to the hypothesis that ATLs were activating apoptosis after redistribution of Fas/CD95 into lipid rafts, independently from its natural ligand FasL/CD95L [37,39,43,71]. The lipid raft localization of Fas/CD95 can promote the recruitment of downstream signaling apoptotic proteins leading to tumor cell death [37,67,69], and to the concept of CASMER (cluster of apoptotic signaling molecule-enriched rafts) [42,72,73] (**Fig. 6**). The stimulation of Fas/CD95 by its natural ligand or by specific cross-linking antibodies results in receptor aggregation, drives the formation of DISC (death-inducing signaling complex), which comprises the adaptor protein FADD (Fas-associated death domain-containing protein) and procaspase-8; then oligomerization drives procaspase-8 activation through self-cleavage, activating downstream effector caspases and leading to apoptosis [37,56]. ATLs not only promoted DISC formation in rafts, but also additional recruitment of downstream apoptotic signaling proteins, including c-Jun N-terminal kinase (JNK), procaspase-10 and BH3 interacting domain death agonist (Bid) [37,67,69,72,74]. Persistent JNK activation is associated with apoptosis, and Bid has been shown to act as a bridge between Fas/CD95 signaling and the mitochondrial-dependent apoptotic pathway [37,73]. In accordance with this Bid localization in rafts, it has been reported a lipid raft connection between extrinsic and intrinsic pathways mediated by ATLs [72]. Redistribution of death receptors into lipid rafts also sensitizes cells to death receptor stimulation by their cognate ligands or agonistic cytotoxic antibodies, despite *de novo* FasL/CD95L synthesis is not essential for the induction of apoptosis [69]. Thus, ATLs promote redistribution of pre-existing Fas/CD95 and FasL/CD95L into clusters [37,39,75].

Activation of the apoptotic machinery in tumor cells constitutes an attractive and promising therapeutic approach for cancer treatment. This strategy takes

advantage of the apoptotic machinery that is still functionally available in tumor cells in order to direct their own demise [37]. The first demonstration of the recruitment of Fas/CD95 in lipid rafts was made in acute lymphoblastic leukemia (ALL) and acute myeloid leukemia (AML) cell lines after edelfosine incubation [38]. Subsequently, similar results were obtained in other hematological malignancies: multiple myeloma (MM) [38,64], mantle cell lymphoma (MCL) [70] and chronic lymphocytic leukemia (CLL) [70].

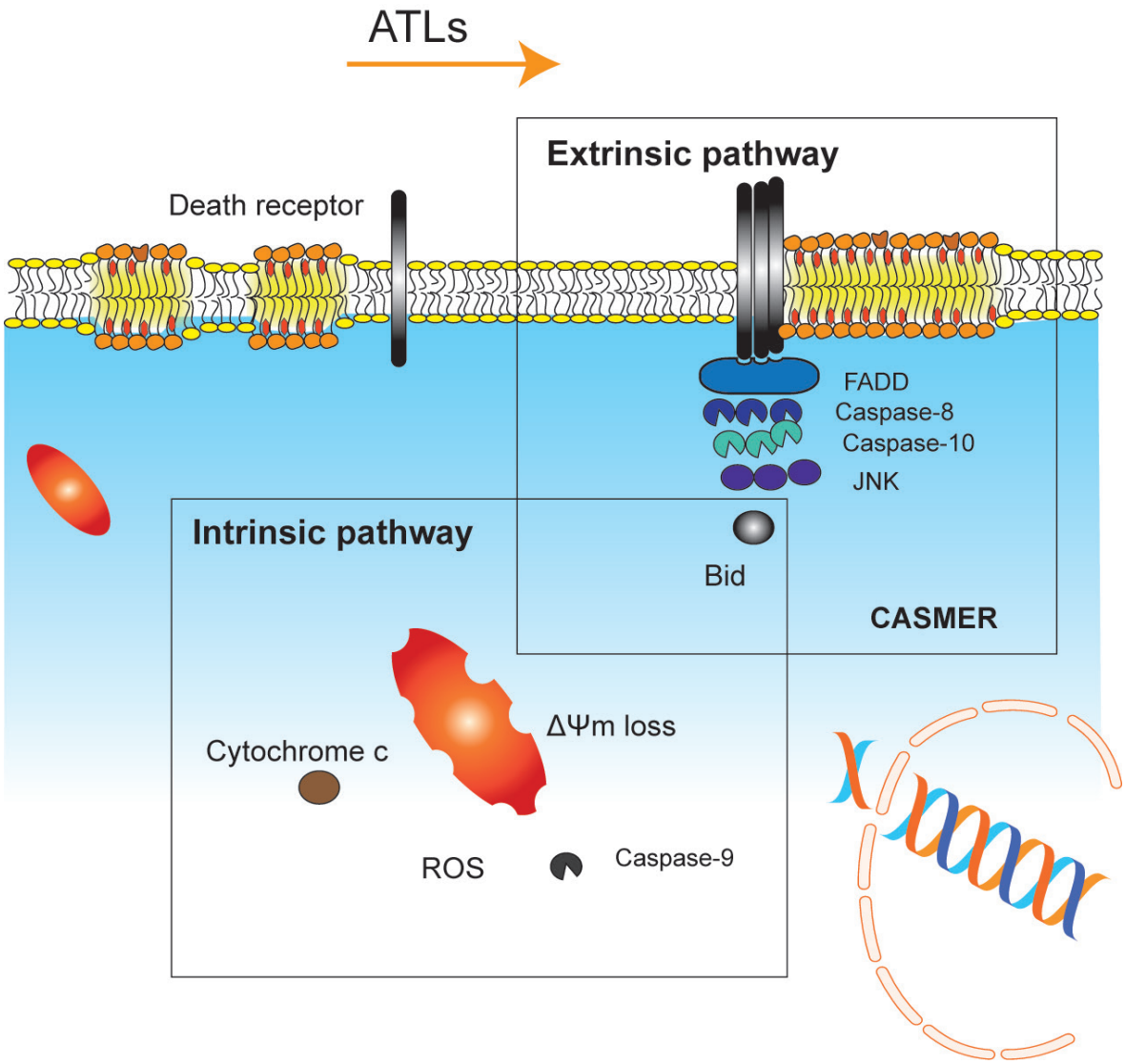

Figure 6- Lipid raft-mediated apoptosis in hematological cancers by the action of ATLs. ATLs can promote the activation of two major apoptotic pathways, namely: mitochondria-mediated intrinsic pathway, which leads to liberation of cytocrome C, formation of reactive oxygen species (ROS), mitochondrial potential loss ($\Delta\Psi_m$ loss) and activation of caspase-9; and extrinsic pathway, mediated by the recruitment death receptors in lipid rafts. ATL incubation leads to co-capping of death receptors and lipid rafts and mobilization of downstream apoptotic signaling molecules. Not just DISC components (Fas/CD95, FADD and procaspase-8), but also JNK and Bid can be recruited in rafts. This accumulation of apoptotic molecules in rafts has led to the notion of the so-called CASMER. ATLs can promote a strong apoptotic response due to the activation of different apoptotic pathways, eventually leading to DNA degradation and cell death.

The Fas/CD95 recruitment in lipid rafts has been reported not only for ATLs and in hematological cancers, but also in solid tumors cells and by the action of distinct compounds. Among others, we can list the following ones: resveratrol in colon cancer cells [76,77], cisplatin in colon cancer cells [78], anandamide in cholangiocarcinoma cells [79], aplidin in leukemic cells [42], and several others that surprisingly do no share similar chemical struture [37].

The Fas/CD95 activation in rafts, can be promoted not only by exogenously added compounds, but the same phenomenon has been observed being induced with the so called "death cytokines". Taking all data together, these findings reinforce the notion that different chemical stressful agents can reactivate a physiological mechanism of cell death that remains "dormant" in transformed cancer cells. Since increasing and accumulating evidence indicates that the clustering of apoptotic molecules in lipid rafts is a general process involved in apoptosis, the concept of CASMER has been proposed to represent a novel lipid raft-based supramolecular entity that seems to play a critical role in the regulation of apoptosis [73,80]. CASMERs act as death-promoting scaffolds where death receptors and downstream signaling molecules are brought together, thus facilitating protein-protein interactions and the transmission of apoptotic signals [73,80].

Additional data suggest that the key molecular target for inhibition of cell proliferation and/or induction of cell death following the action of ATLs may depend on the cell type. Thus, endoplamatic reticulum (ER) accumulation of ATLs and inhibition of phosphatidylcoline synthesis leads to ER-stress and apoptotic induction in several tumor cells [56,57,81,82] (See general discussion). As well as the inhibition of Akt pathway has been implicated the mechanism of action of ATLs [83].

Inhibition of Akt pathway has been implicated in the mechanism of action of ATLs [83]. Once ATLs accumulate in cell membranes it might be envisaged that they could interfere with lipid-dependent signaling process. In this regard, it has been shown that the ATL perifosine can prevent the recruitment of Akt to the membrane [56]. Interestingly, Akt inhibitors can promote Fas/CD95 redistribution and activation in lipid rafts [84].

Since these compounds target membranes of cancer cells instead DNA, ATLs can have synergistic or additive effect in combination with conventional therapy [56,168]. In fact, it has been already shown that ATLs sensitizes tumor cells to radiotherapy[168].

2. HYPOTHESIS

Cholesterol is a critical component for lipid raft formation and function. In the last years, lipid raft investigation in tumor cells has started to establish a link between irregular cholesterol content in cancer cells and unsettled signaling. A number of recent evidences suggest that rafts could be an important target for chemotherapeutic drug action. Rafts can function as gateways and platforms for apoptotic signaling recruitment. Additionally, new data start to reveal that rafts play a role in the metastatic feature of cancer cells. The possibility of targeting cancer cells through rafts in order to induce critical changes on raft proteomic content, driving cancer cells to apoptosis and/or proliferation blockage has been explored as new a framework for cancer therapy. Here, we will analyze how apoptosis can be triggered by agents considered "lipid raft-targeting drugs".

3. OBJECTIVES:

1- Analysis of the role of lipid rafts and Fas/CD95 in the cell death induced by resveratrol in MM and T-cell leukemic cells.

2- Characterization of the role of lipid rafts in Akt activation and cell death induced by ATLs in MCL cells.

3- *In vitro* assessment of combined therapies, between lipid raft-targeting drugs (resveratrol and ATLs) and compounds that do no target lipid rafts (bortezomib, histone deacetylase inhibitors and interferon gamma).

The results generated in this work have led to the following manuscripts:

1. Reis-Sobreiro M, Gajate C, Mollinedo F. Involvement of mitochondria and recruitment of Fas/CD95 signaling in lipid rafts in resveratrol-mediated antimyeloma and antileukemia actions. Oncogene. 2009; 28:3221-3234.

2. Reis-Sobreiro M, Roue G, Mouros A, Gajate C, de la Iglesia-Vicente J, Colomer C, Mollinedo F. Lipid raft-mediated Akt signaling as a therapeutic target in mantle cell lymphoma. Blood Cancer Journal. 2013; 3:e118.

3. Reis-Sobreiro M, Gajate C, Mollinedo F. The antitumor lipid edelfosine in combination therapy for multiple myeloma. *Submitted to publication.*

4. MATERIALS AND METHODS

4.1. Reagents

Resveratrol (RESV; Sigma, St Louis, MO, USA) was prepared as a 100 mM stock solution in dimethylsulfoxide (DMSO). Pancaspase inhibitor z-VAD-fmk (Alexis Biochemicals, Lausen, Switzerland), caspase-8 inhibitor z-IETD-fmk (Calbiochem, San Diego, CA, USA), caspase-10 inhibitor z-AEVD-fmk (R&D Systems, Minneapolis, MN, USA) and JNK inhibitor SP600125 (Calbiochem) were prepared as 10 or 20 mM stock solutions in DMSO. Velcade® (bortezomib) was from Millenium Pharmaceuticals (Cambridge, MA, USA).

Edelfosine (Inkeysa, Barcelona, Spain) and perifosine (Zentaris, Frankfurt, Germany) were prepared as 2 mM stock solutions in culture medium. Anti-CD40 immunoglobulin was a kind gift from Francisco Lozano (Immunology Department, Hospital Clínic-IDIBAPS, Barcelona, Spain). Caspase inhibitor benzyloxycarbonyl-Val-Ala-Asp(OMe)-fluoromethylketone (z-VAD-fmk; Enzo Life Sciences, Lausen, Switzerland) was prepared in DMSO as a 100 mM stock solution. Akt inhibitor 1/2, Akt inhibitor III, Akt inhibitor X (Calbiochem/Merck, Darmstadt, Germany), and PI3K inhibitor wortmannin (Cell Signaling, Irvine, CA, USA) were prepared in DMSO as 10 mM and 2 mM stock solutions. ERK inhibitor PD98059 and JNK inhibitor SP600125 (Calbiochem/Merck) were prepared as 10 or 20 mM stock solutions in DMSO.

SAHA and MS-275 (histone deacetylases inhibitors, Sigma) were prepared as 20 mM, 5 mM and 10 μM stock solutions, respectively. Edelfosine was prepared as

a 2 mM stock solution in culture medium. Velcade® (bortezomib) purchased from Millenium Pharmaceuticals (Cambridge) was prepared as 1 mM stock solution.

4.2. Cell culture

The human acute T-cell leukemia Jurkat cell line; the human MM cell lines: MM1S, MM144, MM1R and U266; the MCL cell lines: Z-138, JVM-2, Jeko-1, HBL-2 as well as the stromal HS-5 cell line were grown in RPMI-1640 culture medium supplemented with 10% (v/v) heat-inactivated fetal bovine serum (FBS; Life Technologies, Carlsbad, CA, USA), 2 mM L-glutamine, 100 U/ml of penicillin, and 100 μg/ml streptomycin at 37°C in humidified 95% air and 5% CO_2.

The Jurkat FADD-DN cell line is a Jurkat-derived clone stably transfected with a pcDNA3 expression vector encoding a dominant-negative form of the FADD protein, was a kind gift from Dr. Lienhard Schmitz (Justus-Liebig-University, Giessen, Germany), and was maintained in complete RPMI-1640/10% FBS medium containing 200 μg/ml G418. Jurkat cells were also transfected with control pcDNA3 empty vector using Lipofectamine 2000 (Invitrogen/Life Technologies, Carlsbad, CA, USA) according to the manufacturer's instructions.

4.2.1. Fas-deficient Jurkat cells

Fas-deficient Jurkat cells were generated following protracted cultures (over 10 months) of parental Jurkat cells.

4.2.2. MM patient-derived cells isolation

Heparinized bone marrow aspirates obtained from patients with newly diagnosed MM and after signing informed consent, were provided by the Hematology Department of the Hospital Clinico Universitario (Salamanca, Spain). The study was approved by the Ethics Committee of the Hospital. Mononuclear cells were isolated by Ficoll-Hypaque (Amersham Biosciences, Upsalla, Sweden) density gradient centrifugation and subjected to positive selection using magnetic cell sorting (Miltenyi Biotec, Bergisch Gladbash, Germany). Purified $CD138^+$ tumor cells (>95% plasma cells) and $CD138^-$ non-transformed cells were isolated as previously described,

resuspended in RPMI-1640/10% FBS medium, and used immediately for experiments.

4.2.3 Isolation of peripheral blood lymphocytes (PBLs)

Mononuclear cells were isolated from fresh human peripheral blood by dextran sedimentation and centrifugation on Ficoll-Paque density gradients. Mononuclear cells at the interface were saved, washed twice with phosphate-buffered saline (PBS), and resuspended in RPMI-1640 culture medium containing 10% (v/v) heat-inactivated FBS, 2 mM L-glutamine, 100 U/ml penicillin, 100 µg/ml streptomycin and 24 µg/ml gentamicin, and incubated overnight at 37°C in the humidified atmosphere of 5% CO_2 and 95% air. Monocytes were depleted by culture dish adherence. After overnight incubation at 37°C, the non-adherent cells (lymphocytes) were washed with PBS and collected. Lymphocyte preparations were typically 67-73% $CD3^+$, 25-28% $CD19^+$, and <0.4% $CD14^+$. To further purify T-cells, the adherent non-adherent cells were washed with PBS and passed twice through a nylon wool column to deplete residual B-cells and monocytes. T-cell purity was checked by flow cytometry analysis. These purified T-cell preparations were typically >95% $CD3^+$, <0.3% $CD14^+$ and <4% $CD25^+$. Further lymphocytes were incubated for 24 and 48 h with RESV at the indicated concentrations.

4.2.4. MM144 transfection with Bcl-X_L

MM144 cells were transfected by electroporation with the SFFV-Neo expression vector containing the human *bcl-x_L* open reading frame driven by the long terminal repeat of the splenic focus-forming virus (pSFFV-*bcl-x_L*). As a control, transfection was performed with empty SFFV-Neo plasmid. MM144 cells (4×10^7) were subjected to electroporation at 500 V, 1700 µF, 72 Ohm in a BTX electro cell manipulator 600 (Biotechnologies & Experimental research, San Diego, CA, USA) and selected by growth in the presence of 400 µg/ml G418.

4.2.5. HS-5 co-culture with patient-derived MCL cells

HS-5 stromal cells (2×10^5) were plated in 24-well plates and left to attach overnight, before adding 5×10^5 MCL patient-derived cells. ATLs were added at10 µM for 6 or 24 h, and then MCL cells were carefully collected and analyzed by western blot or flow cytometry (See flow citometry section).

4.2.6. Isolation and culture of primary MCL cells

Cells from 9 patients diagnosed of MCL according to the World Health Organization classification criteria were studied. Informed consent was obtained from each patient in accordance with the Ethics Committee of the Hospital Clinic (Barcelona, Spain). Cells were cryopreserved in liquid nitrogen in the presence of 10% (v/v) DMSO and 60% (v/v) heat-inactivated FBS. MCL primary cells were cultured immediately after thawing or isolation at a concentration of 1-3 x 10^6 cells/ml in RPMI-1640 medium supplemented with 10% heat-inactivated FBS, 2 mM glutamine, 100 U/ml penicillin and 100 µg/ml streptomycin at 37ºC in a humidified atmosphere containing 95% air and 5% CO_2.

4.3. Flow cytometry

4.3.1. Cell cycle analyses

Cells (2.5-4 x 10^5/ml) were centrifuged and fixed overnight in 70% (v/v) ethanol at 4ºC. Then, cells were washed three times with PBS, incubated for 1 h with 1 mg/ml RNase A and 20 µg/ml propidium iodide at room temperature, and analyzed with a FACSCan flow cytometer (Becton Dickinson; San Jose, DA, USA). Quantitation of apoptotic cells was calculated by flow cytometry as the percentage of cells in the sub-G_1 region (hypodiploidy) in cell-cycle analysis.

4.3.2. Viability and annexin V

To analyze apoptosis by annexin V binding in MCL patient-derived samples and cell lines, 5×10^5 cells were incubated with the indicated agents. Cells were then washed in Annexin-binding buffer and incubated in 50 µl Annexin-binding buffer with allophycocyanin-conjugated anti-CD3 and phycoerythrin-conjugated anti-CD19 antibodies (Becton Dickinson) for 10 min in the dark. Cells were then diluted with Annexin-binding buffer to a volume of 150 µl and incubated with 1 µl FITC-labeled Annexin V (Bender MedSystems, Vienna, Austria) for 15 min in the dark. A total of 10000 stained cells were then analyzed by flow cytometry on a FACSCalibur flow cytometer using CellQuest software (Becton Dickinson).

4.3.3. Cytofluorimetric analysis of mitochondrial transmembrane potential and generation of reactive oxygen species

To evaluate the mitochondrial transmembrane potential ($\Delta\Psi_m$) and the generation of reactive oxygen species (ROS), cells (10^6/ml) were incubated in PBS with 20 nM 3,3´-dihexyloxacarbocyanine iodide [$DiOC_6(3)$]; (green fluorescence; Molecular Probes, Leiden, The Netherlands) and 2 μM dihydroethidine (DHE; red fluorescence after oxidation; Sigma) for 40 min at 37ºC, followed by analysis on a Becton Dickinson fluorescence-activated cell sorting FACSCalibur flow cytometer as previously described.

4.3.4. Cell surface death receptor expression

To analyze Fas/CD95, DR4 and DR5 by flow cytometry assays, cells (2.5 x 10^5) were incubated anti-human Fas SM1/1 IgG_{2a} Mab (Bender MedSystems), or anti human monoclonal anti-DR4 and anti-DR5 (R&D Systems) in PBS (1:150 dilution) for 1h at 4ºC, washed with cold PBS, and incubated for 1 h at 4ºC with fluorescien isotithiocyanate (FITC)-conjugated goat anti-mouse immunoglobulin (Dakopatts, Glostrup, Denmark). After washing, cells were fixed with 1.5% (w/v) formaldehyde, and subject to immunofluorescence flow cytometry in a FACSCan cytofluorometer (MFI values). Percentage of death receptor positive cells were estimated using P3X63 myeloma supernatant as a negative control, provided by F Sánchez-Madrid (Hospital La Princesa, Madrid, Spain).

4.4. Apoptosis quantification by the interaction of Fas/CD95-FasL/CD95L

The possible implication of Fas/CD95-FasL/CD95L interaction in RESV-induced apoptosis was evaluated by using the blocking anti-Fas/CD95 SM1/23 IgG_{2b} monoclonal antibody (Bender MedSystems). Cells (2.5 x 10^5/ml) were preincubated at 4ºC for 30 min in PBS containing 1% (w/v) BSA in the absence (controls) or in the presence of 100 ng/ml of the blocking SM1/23 antibody. Then, cells were resuspended at 2.5 x 10^5/ml in complete RPMI-1640 culture medium containing the same amount of blocking anti-Fas antibody, and treated with 50 ng/ml of cytotoxic anti-Fas CH 11 IgM monoclonal antibody (Upstate Biotecnology, Lake Placid, NY, USA) or 70 μM RESV at 37ºC for 48 h. Then, cells were collected by centrifugation and analyzed for apoptosis by flow cytometry analyses previous described. Experiments performed

with mock-irrelevant isotype immunoglobulins had no effect. Cells were preincubated with 100 ng/ml blocking SM1/23 antibody for 30 min before addition of 50 ng/ml cytotoxic anti-Fas/CD95 CH11 antibody, 100 ng/ml FasL/CD95L or 70 μM RESV for 48 h, or 10 μM edelfosine during 24 h. Untreated control cells and cells incubated only with SM1/23 antibody, CH11 antibody, FasL/CD95L or RESV for 48 h were run in parallel. Apoptosis was then quantitated as percentage of cells in the sub-G1 region by flow cytometry. Average values of two experiments are shown.

4.5. Western blot

Cells (4-5 x 10^6) were lysed with 60 μl of lysis buffer containing (20 mM HEPES, pH 7.5, 10 mM EGTA (ethylene glycol tetraacetic acid), 40 mM β-glycerophosphate, 1% (v/v) NP-40, 2.5 mM $MgCl_2$, 2 mM orthovanadate, 1 mM DTT) supplemented with protease inhibitors (1 mM phenylmethylsulfonyl fluoride, 20 μg/ml aprotinin, 20 μg/ml leupeptin). After 30 min on ice, solubilized proteins were obtained by microcentrifugation at 14000 rpm. Proteins (20-50 μg) were run on SDS-polyacrylamide gels under reducing conditions, transferred to PVDF membranes (Millipore, Billerica, MA, USA) blocked with 5% powdered (w/v) defatted milk in TBST (50 mM Tris-HCl, pH 8.0, 150 mM NaCl, 0.1% (v/v) Tween 20) for 1 h at room temperature, and incubated for 1 h at room temperature or overnight at 4ºC with the following specific antibodies: (See page 30)

Antibody reactivity was monitored with HRP-conjugated anti-rabbit, anti-mouse or anti-goat immunoglobulin G (IgG), using an enhanced chemiluminescence detection system (Amersham Biociences).

4.6. INF-γ treatment

To examine the effect of IFN-γ incubation on protein expression, 4-5 x 10^6 cells were treated with 50 ng/ml IFN-γ (Upstate Biotechnology, Lake Placid, NY, USA) in RPMI-1640/10% FBS complete culture medium for 24 or 48 h and Fas/CD95 and Caspase-8 expression were analyzed by western blot (See western blot section)

To analyze the effect of IFN-γ on apoptosis, cells (4 x 10^5) were pretreated with 50 ng/ml IFN-γ in a final volume of 2 ml for 48 h in RPMI-1640/10% FBS complete

culture medium, before incubation with RESV or edelfosine. Then, the percentage of apoptotic cells was measured by flow cytometry in cell-cycle analysis (see flow cytometry section).

4.7. Confocal microscopy

4.7.1. Fas/CD95 and rafts co-localization

Untreated and RESV, SAHA or MS-275 treated cells (1 x 10^6) were settled onto slides coated with poly-L-lysine, fixed in 4% (v/v) formaldehyde, and then incubated with anti-human Fas/CD95 SM1/23 mouse monoclonal antibody (diluted 1:150 in PBS; Bender MedSystems) for 1 h at room temperature. Samples were washed with PBS and incubated for 1 h with Cy3-conjugated sheep anti-mouse antibody (diluted 1:150 in PBS; Jackson ImmunoResearch, West Grove, PA, USA), washed with PBS and stained with 8 μg/ml FITC-CTx B subunit (Sigma) as a raft marker. Samples were then analyzed by confocal microscopy using a Zeiss LSM510 laser scan confocal microscope (Oberkochen, Germany) for membrane raft and protein visualization as described. Colocalization assays were analyzed by excitation of the corresponding fluorochromes in the same section. Negative controls, lacking the primary antibody or using an irrelevant antibody, showed no staining.

4.7.2. Pervanadate stimulation and p-Akt detection by immunofluorescence

Serum-starved Z-138 cells (4 x 10^5) treated without or with pervanadate (see pervanadate preparation) for 15 min were settled onto poly-L-lysine-coated slides, fixed with 4% (v/v) formaldehyde and permeabilized for 1 min with 0.1% (v/v) Triton X-100 in PBS. Cells were incubated with anti-Ser473 p-Akt rabbit polyclonal antibody (Cell Signaling; 1:100 dilution in PBS/1% BSA) at room temperature for 1 h, followed by incubation with Cy3-conjugated sheep anti-rabbit antibody (Jackson ImmunoResarch; 1:150 dilution in PBS/1% BSA) for 1 h at room temperature, followed by 1 min incubation with 2 ng/ml DAPI (4´,6-diamidino-2-phenylindole) in PBS at room temperature. Samples were then analyzed by using Leica confocal microscope TCS-SP5 (Mannheim, Germany).

Antibody	Dilution	Molecular weigth (kDa)	Company
4-EBP1	1:3000	20-15	Cell Signaling
Akt1/2/3 rabbit polyclonal	1:1000	60	Santa Cruz Biotechnology
Bad monoclonal	1:1000	23	BD Transduction Laboratories
BAP31 goat polyclonal	1:500	29 and 31	Santa Cruz Biotechnology
Bid goat polyclonal	1:500	23	Santa Cruz Biotechnology
Caspase-3 rabbit polyclonal	1:500	20 and 17	BD Pharmingen
Caspase-4 goat polyclonal	1:500	20	Santa Cruz Biotechnology
Caspase-7 monoclonal	1:1000	35,32 and 20	BD Pharmingen
Caspase-8 monoclonal	1:500	18	Oncogene Research Products
Caspase-9 rabbit polyclonal	1:1000	38 and 17	Calbiochem
DR4 goat polyclonal	1:500	56	Santa Cruz Biotechnology
DR5 goat polyclonal	1:500	48	Santa Cruz Biotechnology
ERK2 monoclonal	1:1000	44	Santa Cruz Biotechnology
FADD monoclonal	1:250	24	BD Transduction Laboratories
Fas/CD95 rabbit polyclonal	1:1000	48	Santa Cruz Biotechnology
GSK3 α/β rabbit polyclonal	1:1000	51 and 46	Cell Signaling
JNK1 rabbit polyclonal	1:500	46	Santa Cruz Biotechnology
mTOR rabbit polyclonal	1:1000	289	Cell Signaling
p-4EBP1	1:3000	15-20	Cell Signaling
p-Akt (Ser473) rabbit polyclonal	1:1000	60	Cell Signaling
p-Akt (Thr308) rabbit polyclonal	1:1000	60	Cell Signaling
p-Akt substrate (RXRXXS/T) rabbit polyclonal	1:1000		Cell Signaling
PARP monoclonal	1:2000	116 and 85	BD Pharmingen
p-Bad (Ser136) rabbit polyclonal	1:1000	23	Cell Signaling
PDK1 rabbit polyclonal	1:1000	68-58	Cell Signaling
p-ERK1/2 monoclonal	1:1000	44 and 42	Santa Cruz Biotechnology
p-GSK3 α/β rabbit polyclonal	1:1000	51 and 46	Cell Signaling
PI3K 85 rabbit polyclonal	1:1000	85	Cell Signaling
p-JNK1/2 rabbit polyclonal	1:1000	54 and 46	Cell Signaling
p-PDK1 (Ser241) rabbit polyclonal	1:1000	68-58	Cell Signaling
Procaspase-10 rabbit polyclonal	1:500	58	Oncogene Research Products
Procaspase-8 monoclonal	1:500	55	Oncogene Research Products
α-Tubulina monoclonal	1:1000	60	Calbiochem
β-Actin monoclonal	1:5000	42	Sigma

4.7.3. Pervanadate preparation

Pervanadate (100x) was prepared fresh in PBS (2.12 ml) adding 100 µl of sodium ortovanadate (0.25 M) and 0.28 ml of 30% (v/v) H_2O_2 (Calbiochem/Merck).

4.8. Cholesterol depletion

For cholesterol depletion, 7 x 10^5 cells were washed in serum free medium for three times, and pretreated with 2.5 mg/ml MCD for 30 min at 37ºC in serum-free medium. Cells were then washed three times with PBS and resuspended in complete culture medium before RESV or HDAC addition.

4.9. Lipid raft isolation

Lipid rafts were isolated by using lysis conditions and centrifugation on discontinuous sucrose gradients. Cells (10^8) were washed in ice-cold PBS and lysed for 30 min on ice in TNEV buffer (10 mM Tris-HCl, pH 7.5, 150 mM NaCl, 5 mM EDTA (Ethylenediaminetetraacetic acid), 1 mM sodium orthovanadate and 1% (v/v) Triton X-100) containing 1 mM phenylmethylsulfonyl fluoride. Cells were then homogenized with 10 strokes in a Potter-Elvehjem tissue grinder. Nuclei and cellular debris were pelleted by centrifugation at 1000 rpm for 8 min. Then, 1 ml of cleared supernatant was mixed with 1 ml 85% (w/v) sucrose in TNEV and transferred to the bottom of a Beckman 14 x 95-mm centrifuge tube. The diluted lysate was overlaid with 6 ml 35% (w/v) sucrose in TNEV and finally 3.5 ml 5% (w/v) sucrose in TNEV. The samples were centrifuged in a SW40 rotor at 38000 rpm for 18 h at 4ºC in a Beckman Optima LE-80K ultracentrifuge (Beckman instruments, Palo Alto, USA) and then 1-ml fractions were collected from the top of the gradient. Twelve fractions were colleted. To determine the location of lipid rafts and distinct proteins in the discontinuous sucrose gradient, 20 µl of the individual fractions or a mix between raft fractions 4+5+6 and non-raft fractions 11+12 were subjected to SDS–polyacrylamide gel electrophoresis (PAGE) and immunoblotted as previously described (See western blot section and antibody list). The location of GM1-containing lipid rafts was determined using CTx B subunit conjugated to horseradish peroxidase (1:500 in TBST; Sigma).

4.10. Xenograft mouse model

Female CB17-severe combined immunodeficient (SCID) mice (Charles River Laboratories, Wilmington, MA, USA), were kept and handled according to institutional guidelines, complying with Spanish legislation under a 12/12 h light/dark cycle at a temperature of 22ºC, received a standard diet and acidified water *ad libitum*. CB17-SCID mice were inoculated subcutaneously into their lower dorsum with 10^7 Z-138 cells in 100 µl PBS and 100 µl Matrigel basement membrane matrix (Becton Dickinson). When tumors were palpable, mice were randomly assigned to cohorts of 7 mice each, receiving a daily oral administration, of edelfosine (30 mg/kg body weight), perifosine (26.45 mg/kg body weight), or an equal volume of vehicle (water) for a 21-days period. The shortest and longest diameter of the tumor were measured with calipers at the indicated time intervals, and tumor volume (cm^3) was calculated using the following standard formula: (the shortest diameter)^2 x (the longest diameter) x 0.5. Animals were killed according to institutional guidelines, when the diameter of their tumors reached 3-4 cm or when significant toxicity was observed. Animal body weight and any sign of morbidity were monitored. Mice were killed 24 h after the last drug administration, and then tumors were extirpated, measured and weighed.

4.11. Measurement of caspase-8 and caspase-9 activities

Caspase-8 and caspase-9 activities were determined in the lysates using a colorimetric assay kit (Calbiochem/Merck) according to the manufacturer's protocol. Briefly, the reaction mixture (total volume 100 µl) contained 50 µg of cell lysate and 5 µl of the caspase-8 or caspase-9 substrate Ac-Ile-Glu-Thr-Asp-pNA and Ac-Leu-Glu-His-Asp-pNA, respectively (final concentration of 100 µM), in the assay buffer. Assays were carried out in 96-well plates. Samples were incubated for 90 min at 37ºC, and absorbance was read at 405 nm using a spectrophotometer.

4.12. Statistical analysis

Values are expressed as means ± SD of the number of experiments indicated. Between-group statistical differences were assessed using the Student's t-test. A p

value of < 0.05 was considered statistically significant.

5. RESULTS

5.1. Involvement of mitochondria and recruitment of Fas/CD95 signaling in lipid rafts in resveratrol-mediated antimyeloma and antileukemic actions

5.1.1. Introduction

Hematopoietic malignancies are frequently characterized by a defective apoptosis. MM is a currently incurable B-cell malignancy characterized by the accumulation of plasma cells with a low proliferative index and an extended life span in the bone marrow [85,86]. Thus, a therapeutic potential for MM and additional hematological cancers may lie in potentiating apoptosis [64,87].

A new framework in apoptosis regulation is mediated by coclustering of Fas/CD95 death receptor and lipid rafts [38,72], leading to the concentration of Fas/CD95-downstream signaling apoptotic molecules in membrane rafts that trigger a cell death response [39,67]. This Fas/CD95-raft coclustering plays a key role in the proapoptotic action of some anticancer drugs, including edelfosine, perifosine and aplidin [38,37,39,42,57,69,74]. Chemotherapeutic agent-induced recruitment of Fas/CD95 and downstream signaling molecules in membrane rafts leads to the generation of the DISC in lipid rafts, made up of Fas/CD95, FADD and procaspase-8 [69,72], and eventually to apoptosis. Furthermore, TRAIL receptors are also translocated into rafts following incubation with distinct anticancer drugs [42,69].

Resveratrol (trans-3,4´,5-trihydroxystilbene) is a polyphenolic phytoalexin, abundant in grapes, berries and peanuts [88,89]. Is a toxic compound produced by higher plants in response to infection or other stresses. It was first known as a cardioprotetive agent and then for its manifold beneficicial properties in wide list of diseases including cancer. The mechanism by which resveratrol exerts such a wide rande of beneficial

effects across species and disease models is not yet clear [90].

Resveratrol inhibits the growth of a wide variety of tumor cells and shows chemoprotective properties [88,89], and has been shown to induce redistribution of Fas/CD95 and TRAIL receptors in lipid rafts in colon carcinoma cells [76,91].Resveratrol induces apoptosis in hematological malignant cells, including MM cells [92]. On these grounds, we investigated the role of Fas/CD95 and lipid raft coclustering in the antimyeloma and antileukemic action of resveratrol.

5.1.2. Results

5.1.2.1. Resveratrol induces apoptosis in MM and T-cell leukemia cells, although spares normal lymphocytes

We found that resveratrol induced apoptosis in the human T-cell leukemia Jurkat cell line as well as in the human MM cell lines MM144 and MM1S in a dose response manner (**Fig. 7 A and B**). This apoptotic response was further assessed by caspase-3 activation and cleavage of the typical caspase-3 substrate poly(ADP-ribose) polymerase (PARP), by using a polyclonal anticaspase-3 antibody that recognized the active 20- and 17-kDa subunits of caspase-3, and an anti-PARP monoclonal antibody that detected both the 116-kDa intact form and the 85-kDa cleaved form of PARP (**Fig. 7 C**).

Resveratrol also induced apoptosis in primary cultures of MM cells derived from patients (**Fig. 2 A**), whereas peripheral blood normal lymphocytes from healthy volunteers were spared (<5% apoptosis) (**Fig. 2 B**). These data suggest a rather selective action of resveratrol against MM and T-cell leukemia cells.

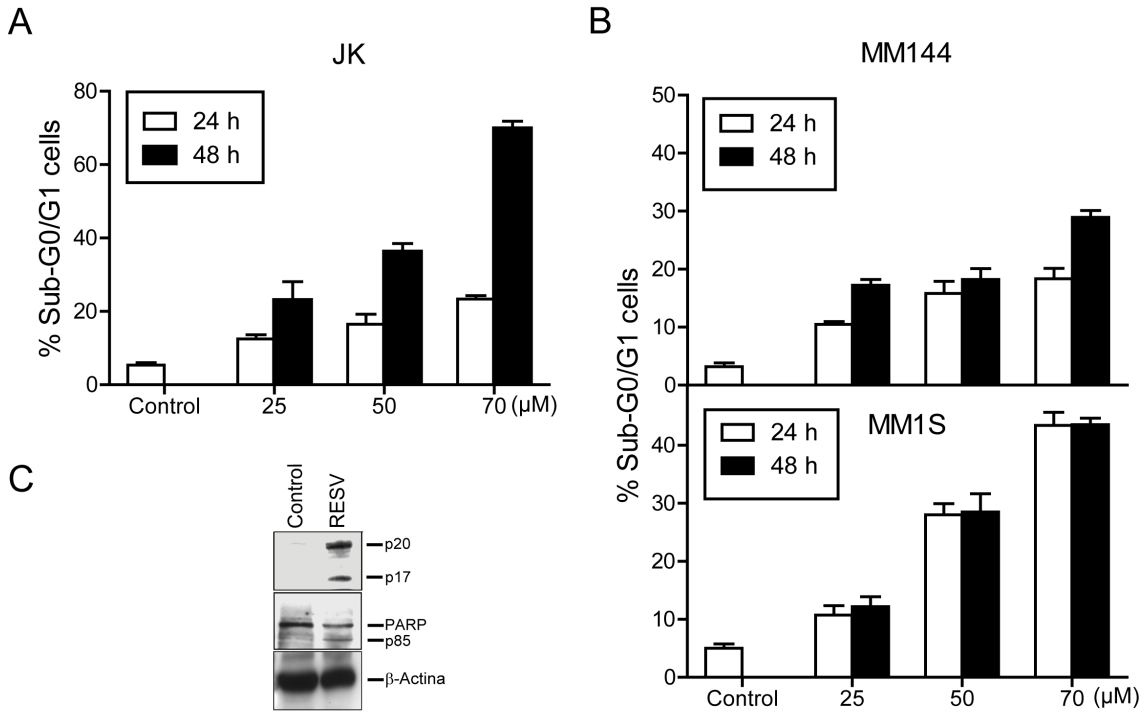

Figure 7. **Induction of apoptosis in leukemic and multiple myeloma (MM) cells by resveratrol.** (*A*) Jurkat cells (JK) and MM cell lines MM1S and MM144 (*B*) were incubated for 24 and 48 h with the indicated concentrations of resveratrol, and apoptosis was then quantitated as the percentage of cells in the sub-G_1 region in cell-cycle analysis by flow cytometry. Untreated control cells were run in parallel and showed similar apoptosis basal values at both 24 or 48 h time points; mean values at these time points are shown means ± s.e. of at least three independent experiments. (*C)* Jurkat cells were untreated (Control) or treated with 70 μM of resveratrol (RESV) for 48 h and then analysed by immunoblotting with anti-caspase-3 (SDS-15% polyacrylamide gels; upper panel) and anti-PARP antibodies (SDS-8% polyacrylamide gels; middle panel). The migration positions of the 20- and 17-kDa subunits of human active caspase-3 as well as of full-length 116-kDa poly(ADP-ribose) polymerase (PARP) and its p85 cleavage product are indicated. Immunoblotting for β-actin (lower panel) was used as an internal control for equal protein loading in each lane. Representative blots of three separate experiments are shown.

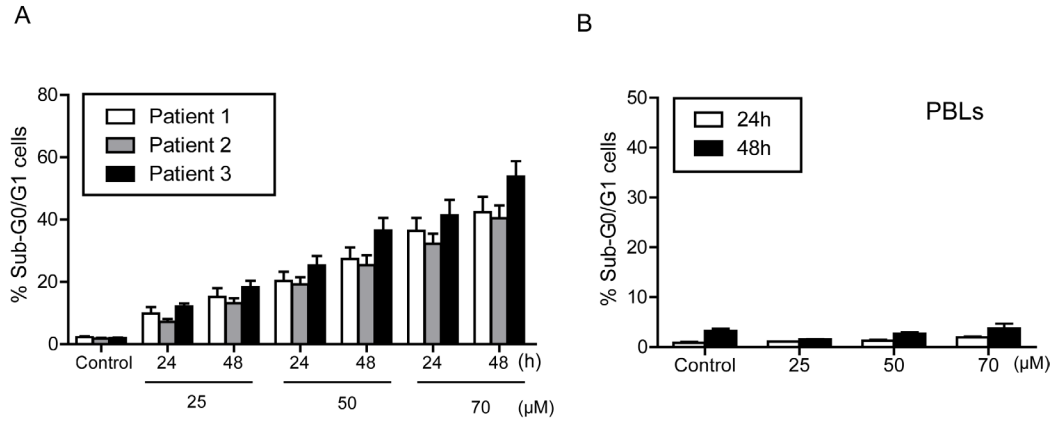

Figure 8. Resveratrol apoptotic effects on MM cells isolated from patients and normal PBLs.(*A*) Freshly isolated tumor MM cells from MM patients were treated with resveratrol for the indicated concentrations and incubation times, and then apoptosis was quantified by flow cytometry. Untreated control cells were run in parallel and showed similar apoptosis basal values at both 24 or 48 h time points.(*B*) Peripheral blood lymphocytes from healthy volunteers were treated with resveratrol for the indicated concentrations and incubation times, and then apoptosis was quantified by flow cytometry. Untreated control cells were run in parallel. Data shown are means ± s.e. of at least three independent experiments.

5.1.1.2. Resveratrol-induced apoptosis in MM and T-cell leukemia cells is mediated by clustering of Fas/CD95 in lipid rafts

Following a time-course analysis, we found that 50 μM resveratrol triggered apoptosis after 15–20 h incubation in Jurkat and MM144 cells. Resveratrol induced coclustering of rafts and Fas/CD95 in both Jurkat and MM144 cells (**Figs. 9 A and B**), as assessed by using the raft marker fluorescein isothiocyanate (FITC)-labeled cholera toxin (CTx) B subunit that binds ganglioside GM1 [93], mainly found in rafts [94] and a specific anti-Fas/CD95 antibody.

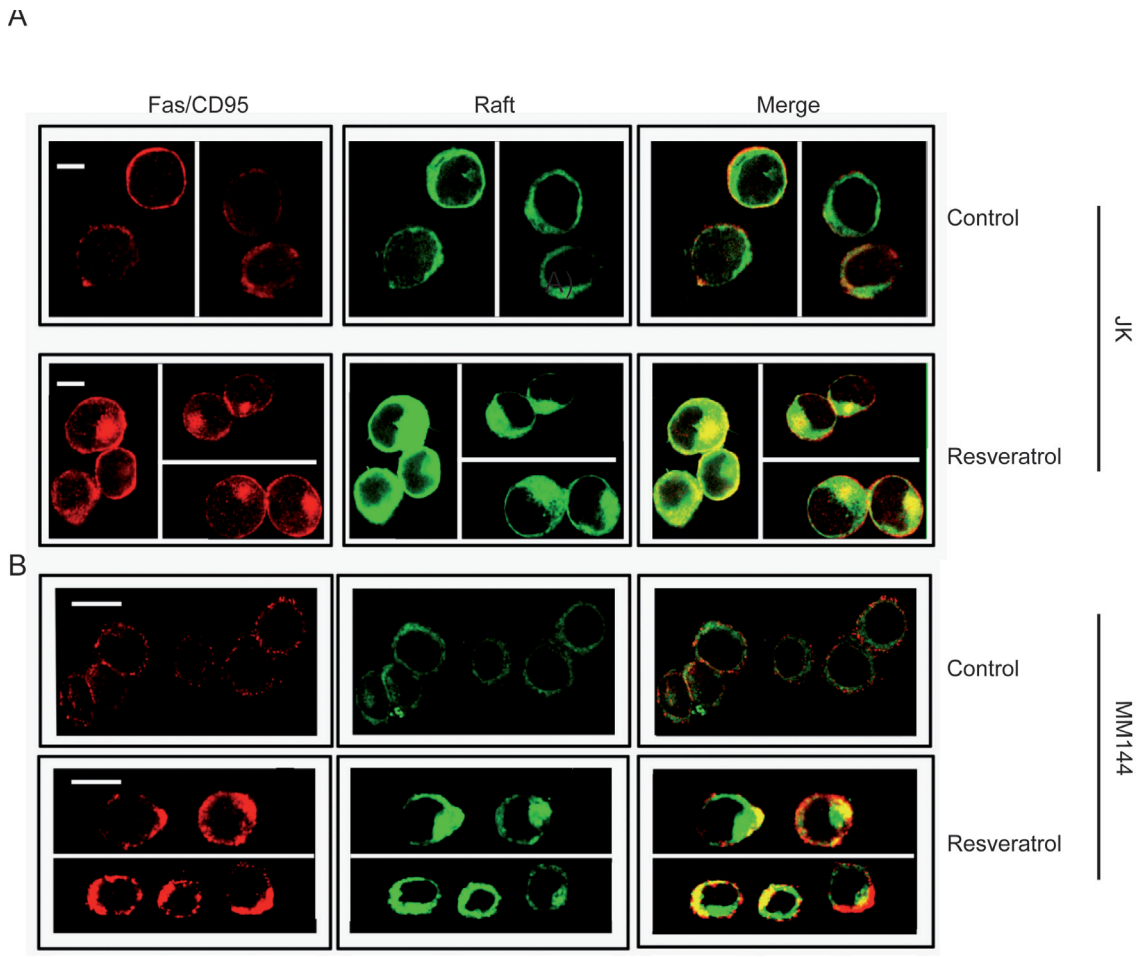

Figure 9- Coclustering of membrane rafts and Fas/CD95 in resveratrol-treated T-cell leukemia and multiple myeloma cells. (*A*) Jurkat (JK) and MM144 (*B*) cells were either untreated (Control) or treated with 50 μM resveratrol (RESV) for 15 h and then stained with a specific anti-Fas/CD95 monoclonal antibody, followed by CY3-conjugated anti-mouse immunoglobulin (Ig) antibody (red fluorescence), and fluorescein isothiocyanate-labeled cholera toxin (FITC-CTx) B subunit to identify lipid rafts (green fluorescence). Areas of colocalization between membrane rafts and Fas/CD95 in the merge panels are yellow. Images shown are representative of three independent experiments. Bar, 10 μm.

Disruption of lipid rafts by cholesterol depletion through methyl-β-cyclodextrin (MCD) treatment [38,95] inhibited resveratrol-induced apoptosis in both T-cell leukemia

and MM cells (**Fig. 10 A and B**). These results indicate that coclustering of Fas/CD95 and membrane rafts mediates the apoptotic action of resveratrol in MM and T-cell leukemia cells.

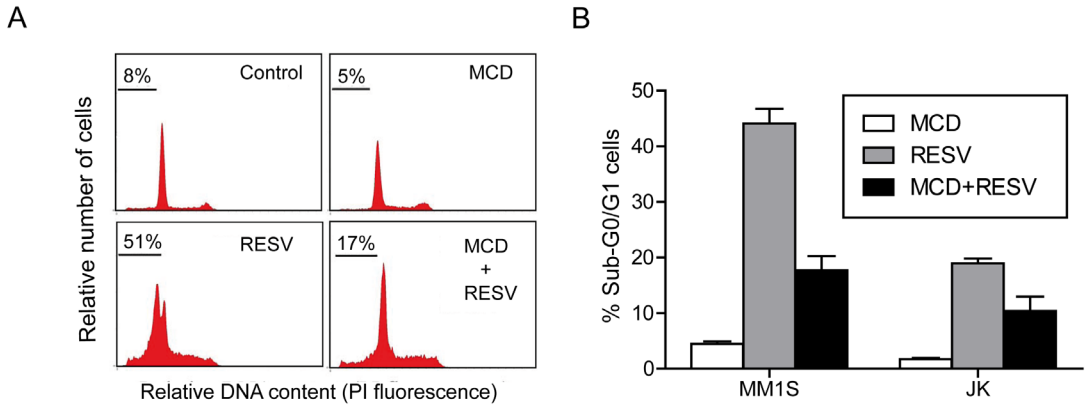

Figure 10 - Involvement of lipid rafts in resveratrol-induced apoptosis. (*A*) MM1S cells were pretreated with methyl-β-cyclodextrin (MCD) and then incubated with 70 μM of resveratrol (RESV) for 24 h. Cells were stained with propidium iodide (PI), and their DNA content was analysed by fluorescence flow cytometry. The percentage of cells with a DNA content less than G_1(sub-G_1) is indicated in each histogram. Control untreated cells and cells treated only with MCD or resveratrol were run in parallel. Data are representative of three experiments performed. (*B*) MM1S and Jurkat (JK) cells were untreated (Control) or pretreated with MCD and then incubated in the absence or in the presence of 70 μM of resveratrol (RESV) for 24 h. Percentage of apoptotic cells was determined by flow cytometry as above. Untreated cells showed apoptosis mean values of <5%. Data shown are means ± s.e. of four independent experiments.

5.1.1.3. Resveratrol induces translocation of death receptors and downstream molecules into lipid rafts in MM and T-cell leukemia cells

The above Fas/CD95 and raft coclustering was further confirmed by isolation of membrane rafts from Jurkat and MM144 cells, untreated and treated with resveratrol (**Fig. 11 A and B**). Lipid rafts were isolated based on their insolubility in Triton X-100 lysis buffer at 4 ºC and fractionated by discontinuous sucrose gradient centrifugation [38] GM1-containing lipid rafts, at the upper part (mostly in fractions 3–5) of the sucrose gradient (**Fig. 11 A and B**), were identified using CTx conjugated to horseradish peroxidase [38]. Fas/CD95 was present in the non-raft fractions (fractions 10–12) of the sucrose gradient in untreated Jurkat and MM144 cells, but resulted dramatically translocated to the raft fractions on resveratrol treatment for 15 h (**Fig. 11 A and B**). MM144 cells express the TRAIL receptors DR4 and DR5, whereas Jurkat cells only express DR5, and all these TRAIL receptors were also translocated to rafts in both cell types following resveratrol treatment, although to a lesser extent than Fas/CD95 (**Fig. 11 A and B**). Death receptor downstream signaling molecules FADD, procaspase-8 and procaspase-10 were also translocated into rafts (**Fig. 11 A and B**). Interestingly, a

portion of the active cleavedcaspase-8 and caspase-10 forms were also found in rafts following resveratrol treatment (**Fig. 11 A and B**), caspase-8 and caspase-10 forms were also found in rafts following resveratrol treatment (**Fig. 11 A and B**), suggesting that triggering of apoptosis is initiated at the membrane rafts.

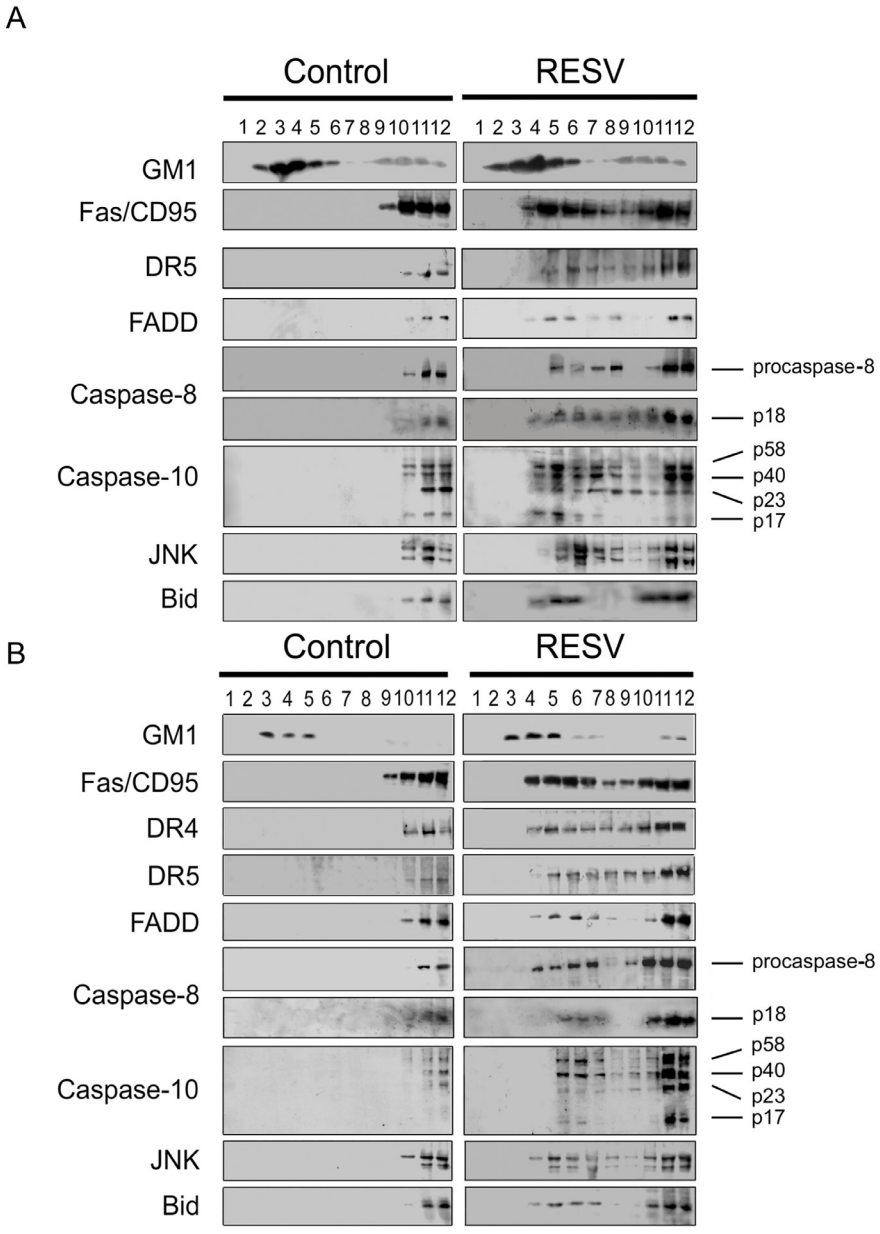

Figure 11- Recruitment of death receptors and downstream signaling molecules in membrane rafts following resveratrol treatment of Jurkat and MM144 cells. (*A*) Untreated Jurkat cells (Control) and Jurkat cells treated with 50 μM resveratrol (RESV) for 15 h were lysed in 1% Triton X-100 and fractionated by centrifugation on a discontinuous sucrose density gradient. An equal volume of each collected fraction was subjected to SDS–polyacrylamide gel electrophoresis (PAGE) before analysis of the indicated proteins using specific antibodies. The migration positions of the 55-kDa procaspase-8 and the cleaved p18 product, as well as of the 58-kDa procaspase-10 and the cleavage products are denoted. Location of GM1-containing lipid rafts was determined using cholera toxin (CTx) B subunit conjugated to horseradish peroxidase. (*B*) Untreated MM144 cells (control) and MM144-treated cells treated with 50 μM resveratrol (RESV) for 15 h were lysed and analysed by western blotting as above. Representative blots of three separate experiments are shown.

These data show that all the constituents of DISC, namely Fas/CD95, FADD and

procaspase-8, are recruited into rafts; and this key apoptotic complex in death receptor signaling is activated in the membrane raft. We also found that Bid, which acts as a bridge between Fas signaling and [96], was translocated into rafts following treatment of Jurkat and MM144 cells with resveratrol (**Fig. 11 A and B**). In addition, JNK was recruited into lipid rafts on resveratrol incubation (**Fig. 11 A and B**). Our results show that resveratrol induces a reorganization of the raft protein content, translocating apoptotic proteins to these detergent-insoluble membrane domains in hematological cancer cells.

5.1.1.4. Involvement of caspases and JNK in resveratrol-induced apoptosis

Incubation with the cell-permeable pan-caspase inhibitor benzyloxycarbonyl-Val-Ala-Asp(OMe)-fluoromethylketone (z-VAD-fmk) abrogated the apoptotic response in resveratrol-treated Jurkat, MM144 and MM1S cell lines (**Fig. 12**). Preincubation with caspase inhibitors showing specificity for caspase-8 (z-Ile-Glu(OMe)-Thr-Asp(OMe)-fluoromethylketone, z-IETD-fmk) and caspase-10 (z-Ala-Glu(OMe)-Val-Asp(OMe)-fluoromethylketone, z-AEVDfmk), involved in the transmission of death receptor signaling, inhibited apoptosis (**Fig. 12**), suggesting their involvement in resveratrol-induced apoptosis. Pretreatment of Jurkat, MM144 and MM1S cells with the JNK inhibitor SP600125 (SP) [97] inhibited resveratrol induced apoptosis to a rather variable degree (22–59% inhibition; **Fig. 12**). This partial inhibition suggests that JNK is acting in parallel to additional signaling pathways to increase cell death, but it does not seem to play an essential role in the apoptosis outcome.

We next examined the effect of overexpressing Bcl-X_L in MM144 cells to analyse the role of mitochondria in resveratrol-induced apoptosis. We stably transfected MM144 cells with pSFFV-*bcl-x*$_L$ (MM144-Bcl-X_L), containing the human *bcl-x*$_L$ open reading frame, or with control pSFFV-Neo plasmid (MM144-Neo). MM144-Neo cells, that behaved similar to nontransfected MM144 cells, expressed small levels of endogenous Bcl-X_L, whereas a high expression of this protein was detected in MM144-Bcl-X_L cells, as previously reported [69].

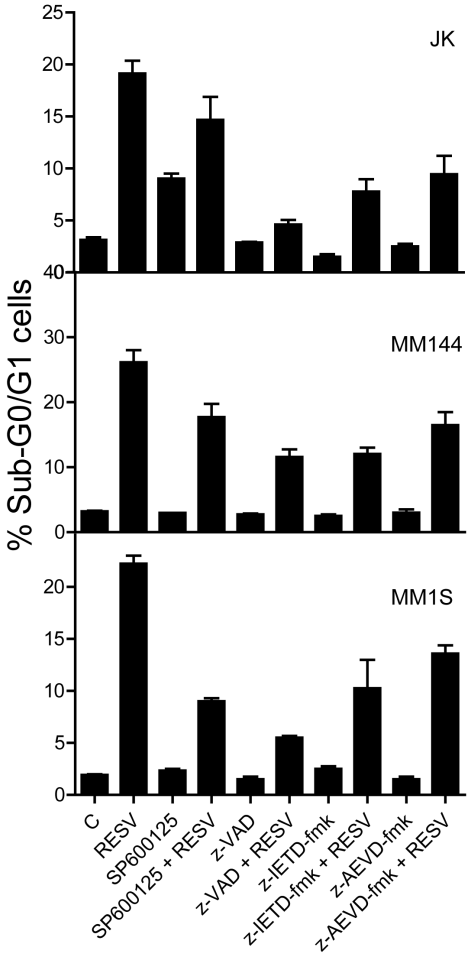

Figure 12. Involvement of JNK and caspases in resveratrol-induced apoptosis. JK, MM144 and MM1S cells were preincubated without or with 20 μM SP600125, 50 μM z-VAD-fmk, 50 μM Z-IETD-fmk or 50 μM z-AEVD-fmk for 1 h, and then incubated in the absence or presence of 70 μM resveratrol (RESV) for 24 h and analysed by flow cytometry to evaluate apoptosis. Untreated control cells (C) were run in parallel. Data shown are means ± s.e. of three independent experiments.

Treatment of MM144-Neo cells with resveratrol led to apoptosis (**Fig. 13 A**) and mitochondrial transmembrane potential ($\Delta\Psi_m$) disruption (**Fig. 13 B and C**). However, overexpression of Bcl-X_L by gene transfer in MM144 cells prevented both resveratrol-induced apoptosis (**Fig. 13 A)** and $\Delta\Psi_m$ loss (**Fig. 13 B and C**). These data indicate that mitochondria are involved in resveratrol-induced MM cell death.

As shown in Figure 13 C, untreated cells showed high $\Delta\Psi_m$ ($DiOC_6(3)^{high}$) and low levels of intracellular reactive oxygen species (ROS; HE-Eth)^{low}. These values were taken as background data. Resveratrol induced an increase in the percentages of $DiOC_6(3)^{low}$/$(HE\text{-}Eth)^{high}$ and $DiOC_6(3)^{high}$/$(HE\text{-}Eth)^{high}$ cells, whereas the ratio of cells with disrupted $\Delta\Psi_m$ and without producing ROS ($DiOC_6(3)^{low}$/$(HE\text{-}Eth)^{low}$) was very small (about 1–2%) on resveratrol incubation (**Fig. 13 C**). Overexpression of Bcl-X_L abrogated well-nigh entirely both $\Delta\Psi_m$ disruption and apoptosis (80–92% inhibition;

Fig. 13 A–C), but did not inhibit the percentage of $DiOC_6(3)^{high}/(HE\text{-}Eth)^{high}$ cells after resveratrol incubation (**Fig. 13 B**).

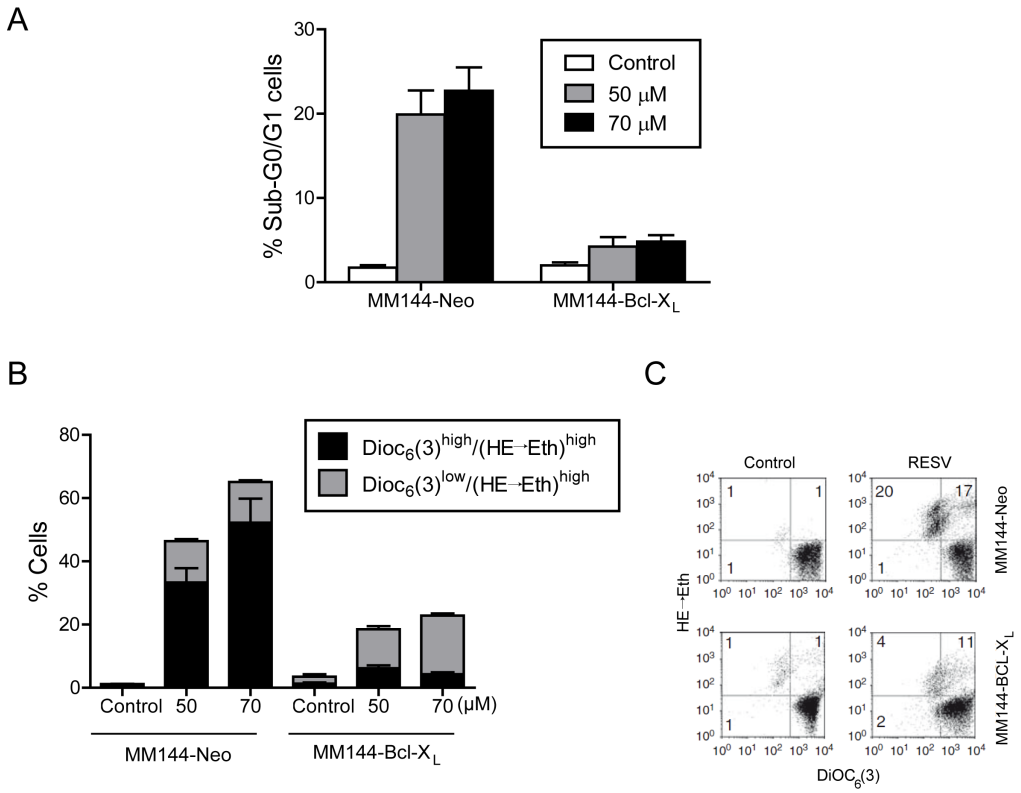

Figure 13. Involvement of $\Delta\Psi_m$ dissipation in resveratrol-induced apoptosis. (*A*) MM144-Neo and MM144-Bcl-X_L cells were treated for 48 h with resveratrol at the indicated concentrations, and then apoptosis was assessed by flow cytometry. Data shown are means ± s.e. of three independent experiments. (*B*) MM144-Neo and MM144-Bcl-X_L cells were untreated and treated with 50 or 70 μM resveratrol for 48 h, and the percentages of cells with disrupted $\Delta\Psi_m$ ($(DiOC_6(3)^{low}$) and generating reactive oxygen species (ROS $(HE\text{-}Eth)^{high}$) were measured as described in Material and methods. Data shown are means ± s.e. of three independent experiments. (*C*) A representative experiment of three performed on the effect of resveratrol (RESV; 70 μM, 24 h) on $\Delta\Psi_m$ disruption ($DiOC_6(3)^{low}$) and ROS generation $(HE\text{-}Eth)^{high}$ in MM144-Neo and MM144-Bcl-X_L cells, assessed by flow cytometry as described in Materials and methods.

These results suggest that $\Delta\Psi_m$ dissipation was critical for resveratrol-induced apoptosis in MM and T-cell leukemia cells, and that a minor portion of ROS may originate from additional sources, apart from mitochondria that plays no essential role in resveratrol-induced apoptosis.

5.1.1.5. Fas/CD95 signaling and mitochondrion connection in resveratrol-induced apoptosis

As the above data showed that both Fas/CD95 and mitochondria signaling were involved in resveratrol induced apoptosis in hematological cancer cells, and the Fas/CD95-mitochondrion bridging molecule Bid was recruited into lipid rafts together

with Fas/CD95 downstream molecules (**Fig. 14**), we wondered whether Fas/CD95 and mitochondrial apoptotic signaling routes were acting in conjunction. Using stable transfection in Jurkat cells of a dominant-negative form of the FADD adapter protein (FADD-DN), which lacks the death effector domain and blocks Fas/CD95 signaling [98], we found that blockade of Fas/CD95 downstream signaling prevented both $\Delta\Psi_m$ loss (**Fig. 14 A and B**) and apoptosis (**Fig. 14 C**). In addition, Fas/CD95-deficient Jurkat cells, that preserved the expression of functional tumor necrosis factor receptor 1 and DR5 [39], were rather resistant to undergo apoptosis on resveratrol treatment (**Fig. 15**). These data suggest a prevailing role of Fas/CD95 in resveratrol-induced $\Delta\Psi_m$ dissipation and apoptosis in Jurkat cells.

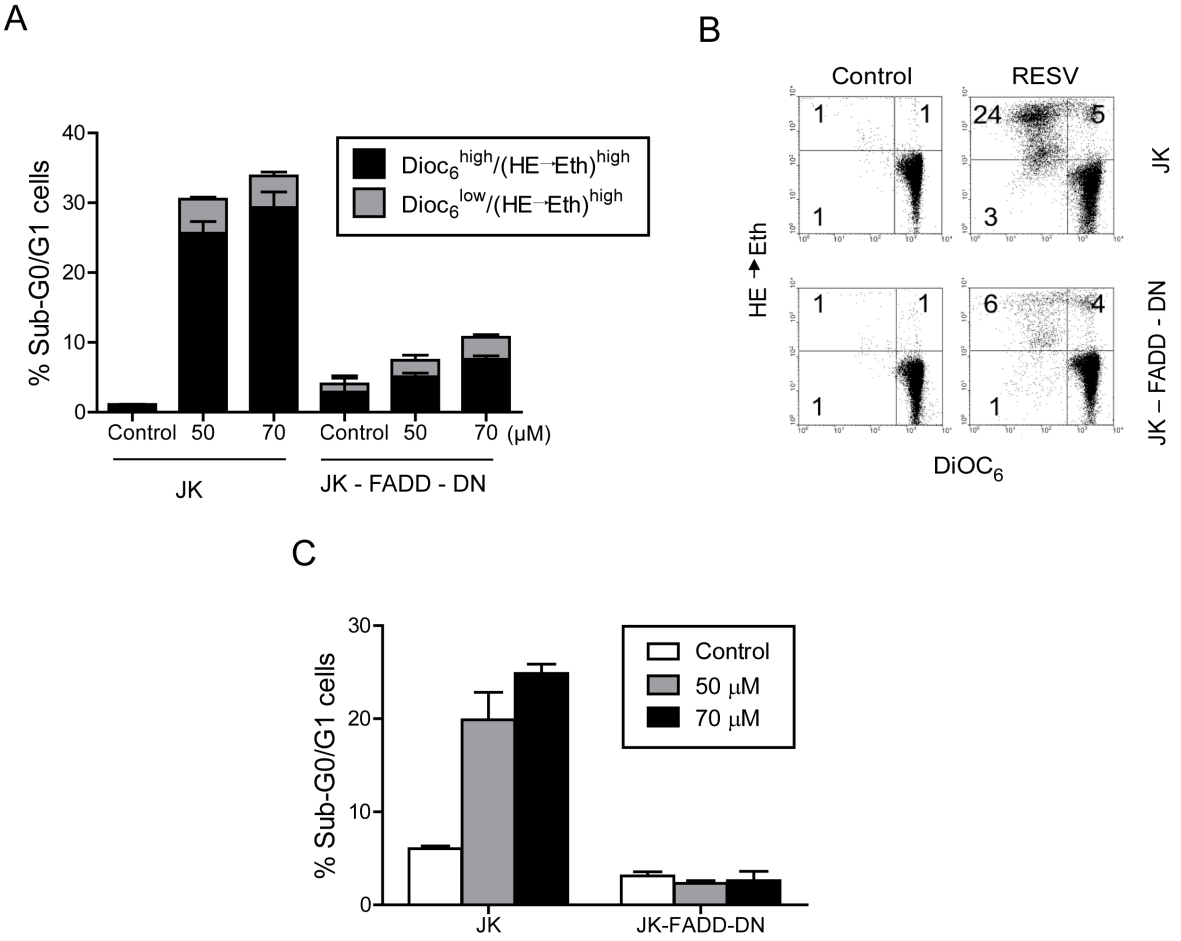

Figure 14. Fas/CD95 signaling regulates mitochondrial downstream events in resveratrol-induced apoptosis. (*A*) Jurkat cells (JK) and Jurkat cells transfected with the dominant-negative form of Fas-associated death domain-containing protein (JK-FADD-DN) were untreated (Control) and treated with 50 or 70 μM resveratrol for 24 h, and the percentages of cells with disrupted ΔΨm ($DiOC_6(3)^{low}$) and generating reactive oxygen species (ROS $(HE\text{-}Eth)^{high}$) were measured as described in Materials and methods. Data shown are means ± s.e. of three independent experiments. (*B*) A representative experiment of three performed on the effect of resveratrol (RESV; 70 μM, 24 h) on ΔΨm disruption ($DiOC_6(3)^{low}$) and ROS generation $(HE\text{-}Eth)^{high}$ in JK and JK-FADD-DN cells, assessed by flow cytometry as described in Materials and methods. (*C*) JK and JK-FADD-DN cells were treated for 48 h with resveratrol at the indicated concentrations, and then apoptosis was assessed by flow cytometry. Data shown are means ± s.e. of three independent experiments.

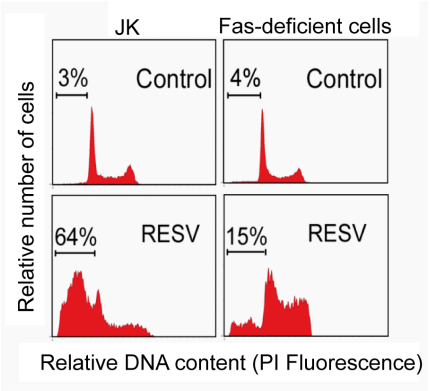

Figure 15. **Fas-deficient Jurkat cells are resistant to resveratrol.** Induction of apoptosis in Jurkat (JK) and Fas-deficient Jurkat cells was determined by flow cytometry after a 48 h incubation with 70 μM resveratrol (RESV). Untreated control cells were run in parallel. Data are representative of three experiments performed.

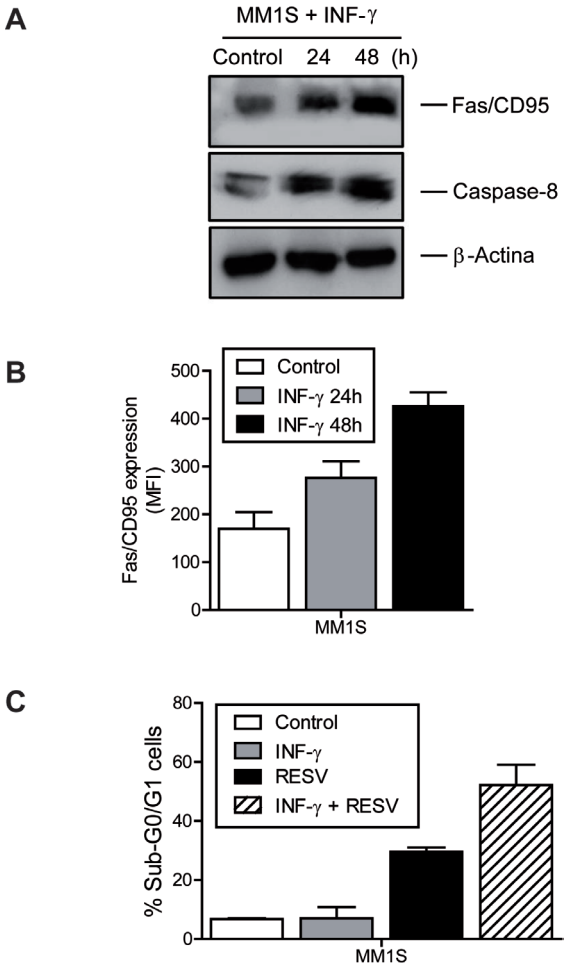

Figure 16. **Effects of interferon (IFN)-γ on Fas/CD95 and procaspase-8 expression and resveratrol-induced apoptosis.** (*A*) MM1S cells were untreated (Control) or treated with 50 ng/ml IFN-γ for the indicated times, and the protein levels of Fas/CD95 and procaspase-8 were determined by western blot. β-Actin was used as a loading control. (*B*) Cell surface expression of Fas/CD95 was determined by immunofluorescence flow cytometry as mean fluorescence intensity (MFI) values in untreated control MM1S cells and MM1S cells treated with 50 ng/ml IFN-γ for the indicated times. Data shown are means ± s.e. of three independent experiments. (*C*) MM1S cells were pretreated with 50 ng/ml IFN-γ for 48 h, and then incubated with 70 μM resveratrol for 24 h. Apoptosis was assessed by flow cytometry as the percentage of cells with DNA content less than G1. Untreated control MM1S cells, and MM1S cells treated only with IFN-γ or resveratrol (RESV) were also analysed for apoptosis. Data shown are means ± s.e. of three independent experiments.

5.1.2.6. Interferon-γ upregulates Fas/CD95 and caspase-8, potentiating resveratrol-induced apoptosis

Following pretreatment of MM cells with interferon (IFN)-γ, we found an increase in both Fas/CD95 and procaspase-8 protein levels by western blot (**Fig. 16 A**). We found that MM cells pretreated with IFN-γ showed an increase in the cell surface expression of Fas/CD95 (**Fig. 16 B**) and were more sensitive to the apoptotic action of resveratrol (**Fig. 16 C**). These data suggest that an increase in Fas/CD95 potentiates the apoptotic response of resveratrol.

5.1.2.7. Resveratrol induces apoptosis and Fas/CD95-raft coclusters in Fas/CD95-resistant U266 cells

The MM cell line U266 expresses Fas/CD95, but addition of the agonistic anti-Fas/CD95 antibody CH11 induces less than 5% apoptosis [99,100]. We found that U266 cells expressed Fas/CD95, DR4 and DR5 at their cell surface (**Fig. 10 A**), and underwent apoptosis following resveratrol treatment (**Fig. 17 B**). Interaction of Fas/CD95 with either the agonistic anti-Fas/CD95 antibody CH11 or the physiological ligand FasL/CD95L did not induce apoptosis in U266 cells (**Fig. 17 C**). Thus, U266 cells are deficient in mounting a Fas/CD95-FasL/CD95L interaction-dependent apoptotic response. Preincubation of U266 cells with the blocking SM1/23 anti-Fas/CD95 antibody, which abrogates Fas/CD95-FasL/CD95L mediated killing [75], failed to inhibit resveratrol-induced apoptosis (**Fig. 17 C**), indicating that resveratrol-induced apoptosis is not mediated by FasL/CD95L. The combination of resveratrol with CH11 or FasL/CD95L slightly potentiated the cell death outcome (**Fig. 17 C**), suggesting that resveratrol might partially circumvent the block in mounting a Fas/CD95-mediated apoptotic signal. Resveratrol induced a potent coclustering of rafts and Fas/CD95 in U266 cells (**Fig. 18 A**). However, disruption of rafts by cholesterol depletion with MCD inhibited only weakly resveratrol induced apoptosis in U266 cells (23.4±2.4 versus 16.8±2.3 apoptosis in untreated and MCD-pretreated cells, respectively, and then incubated with 70 μM resveratrol for 24 h, n=4) (**Fig. 18 B**). Thus, these data suggest that resveratrol is effective in promoting coclusters of Fas/CD95 and rafts, but additional mechanisms must play a role in the induction of apoptosis by resveratrol in U266 cells.

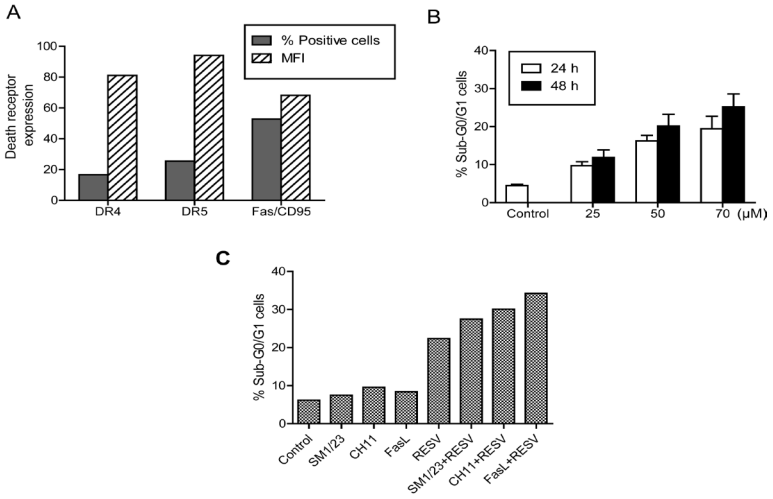

Figure 17. Resveratrol induces apoptosis independently of FasL/CD95L in U266 cells. (*A*) Cell surface expression of DR4, DR5 and Fas/CD95 in U266 cells was determined by flow cytometry as the percentage of positive cells for each death receptor or mean fluorescence intensity (MFI). Average values of two experiments are shown. (*B*) U266 cells were incubated for 24 and 48 h with the indicated concentrations of resveratrol, and apoptosis was then quantitated as the percentage of cells in the sub-G_1 region in cell-cycle analysis by flow cytometry. Untreated control cells were run in parallel and showed similar apoptosis basal values at both 24 or 48 h time points; mean values at these time points are shown. Data shown are means ± s.e. of four independent experiments. (*C*) U266 cells were preincubated with 100 ng/ml blocking SM1/23 antibody for 30 min before addition of 70 μM resveratrol (RESV) for 48 h. Combinations of 50 ng/ml cytotoxic anti-Fas/CD95 CH11 antibody + 70 μM resveratrol (RESV) and 100ng/ml FasL/CD95L + 70 μM resveratrol (RESV) were also assayed for 48 h. Untreated control cells and cells incubated only with SM1/23 antibody, CH11 antibody, FasL/CD95L or resveratrol (RESV) for 48 h were run in parallel. Apoptosis was then quantitated as percentage of cells in the sub-G1 region by flow cytometry. Average values of two experiments are shown.

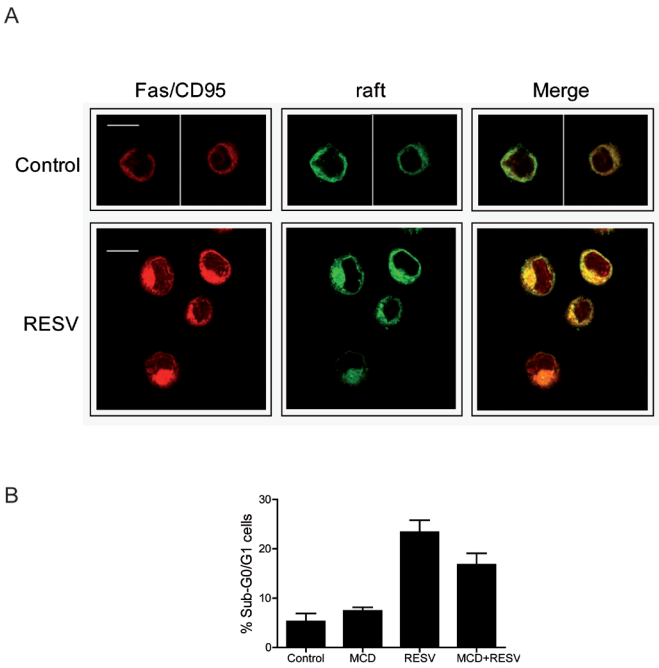

Figure 18. **Resveratrol induces co-clustering of rafts and Fas/CD95 in U266 cells** (*A*) U266 cells were either untreated or treated with 50 μM resveratrol (RESV) for 15 h and then stained with a specific anti-Fas/CD95 monoclonal antibody, followed by CY3-conjugated anti-mouse immunoglobulin (Ig) antibody (red fluorescence), and fluorescein isothiocyanate-labeled cholera toxin (FITC-CTx) B subunit to identify lipid rafts (green fluorescence). Areas of colocalization between membrane rafts and Fas/CD95 in the merge panels are yellow. Images shown are representative of three independent experiments. Bar, 10 μm. (*B*) U266 cells were untreated or pretreated with MCD and then incubated in the absence or in the presence of 70 μM of resveratrol (RESV) for 24 h. Percentage of apoptotic cells was determined by flow cytometry as above. Untreated cells showed apoptosis mean values of <5%. Data shown are means ± s.e.

5.1.2.8. Combination of resveratrol with perifosine or bortezomib potentiates apoptosis

We next analysed the putative potentiation of apoptosis as a result of combining resveratrol with additional drugs acting through similar or distinct mechanisms of action. Perifosine has been reported to induce apoptosis in MM cells through Fas/CD95-raft coclustering [69] and its antimyeloma activity is being tested in clinical trials [101]. The proteasome inhibitor bortezomib is currently used in clinic against MM and other hematological malignancies [102]. We found that the combination of resveratrol and perifosine showed an additive effect, whereas the combination of resveratrol and bortezomib had a synergistic effect on apoptosis (**Figs. 19 and 20**). The additive effect observed following treatment with resveratrol and perifosine suggests that both drugs share, at least in part, similar modes of action. These data would support a mechanism of action mediated by Fas/CD95-raft coclustering. Unlike other assayed cells, U266 cells showed a rather poor additive effect between resveratrol and perifosine (**Figs. 19 and 20**), suggesting that the raft-mediated process is not so critical in cell death induction in this particular cell line. The synergistic effect observed following treatment with resveratrol and bortezomib indicates that both substances act through different mechanisms of action. The combined treatment of resveratrol and bortezomib highly potentiated the apoptosis outcome exerted by each individual drug (**Fig. 20**). Thus, the raft-mediated mechanism of action of resveratrol might be of interest for combination therapy in the treatment of blood malignancies.

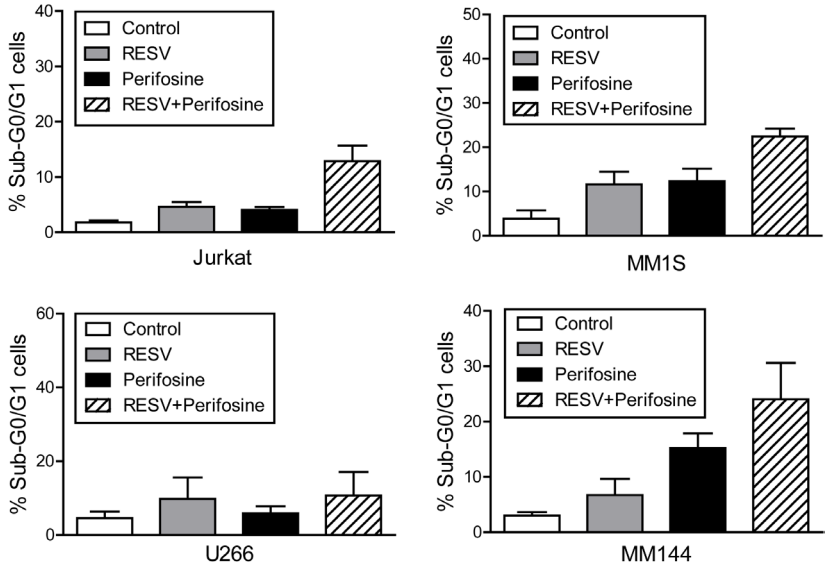

Figure 19. **The combination of resveratrol with perifosine potentiates apoptosis in T-cell leukemia and MM cells.** Jurkat, MM144, MM1S and U266 cells were incubated for 48 h with 10 μM resveratrol (RESV),5 μM perifosine and with a combination of RESV+perifosine or RESV+bortezomib. Untreated control cells were run in parallel. Apoptosis was analysed by flow cytometry as the percentage of hypodiploid (sub-G_1) cells following cell-cycle analysis. Data shown are means ± s.e. of three independent determinations.

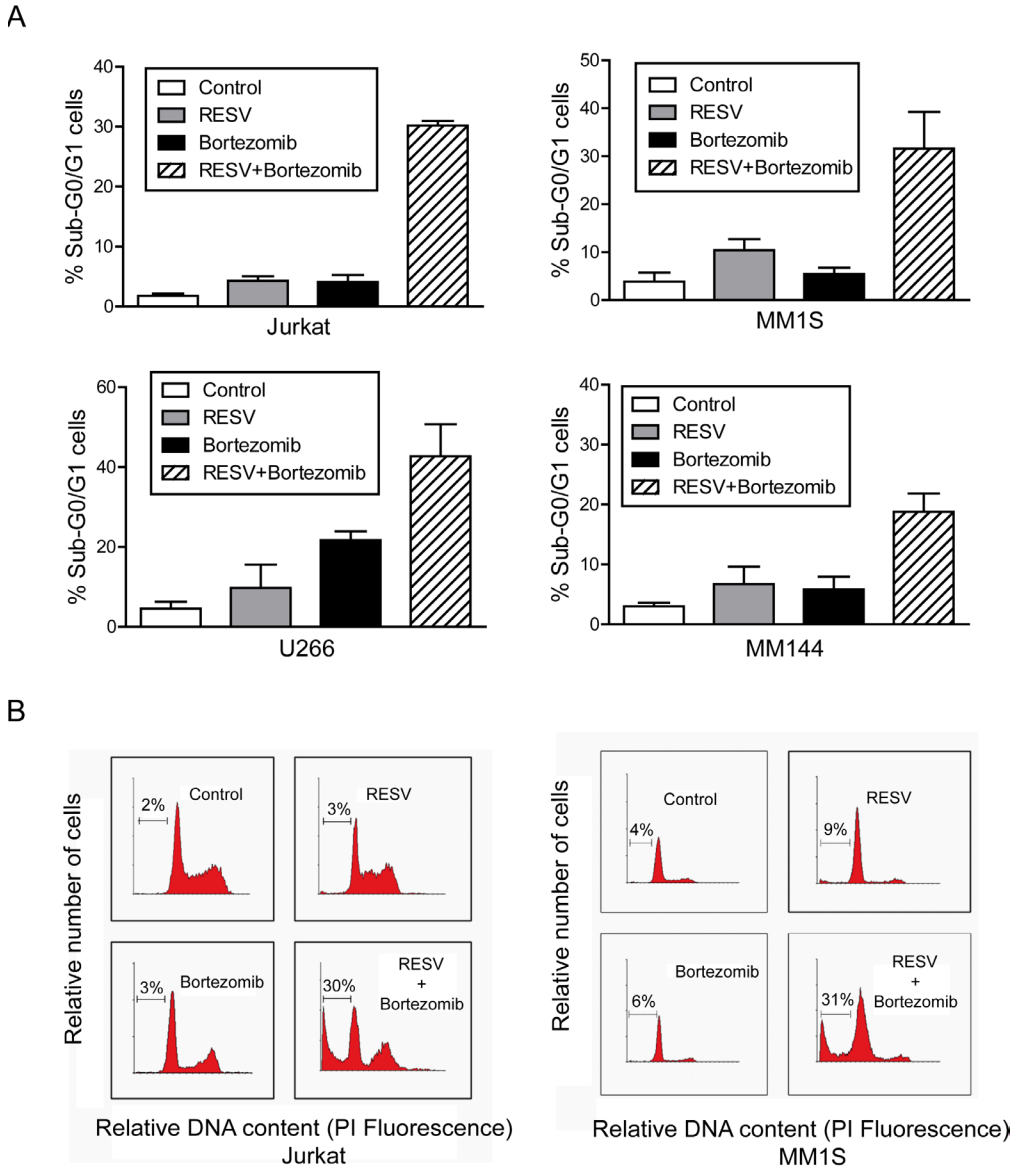

Figure 20. The combination of resveratrol with bortezomib potentiates apoptosis in T-cell leukemia and multiple myeloma cells. (*A*) Jurkat, MM144, MM1S and U266 cells were incubated for 48 h with 10 μM resveratrol (RESV), 10 nM bortezomib, and with a combination of RESV + bortezomib. Apoptosis was analysed by flow cytometry as the percentage of hypodiploid (sub-G_1) cells following cell-cycle analysis. Data shown are means ± s.e. of three independent determinations. (*B*) Jurkat and MM1S cells were untreated (Control), treated with 10 μM resveratrol (RESV), 10 nM bortezomib or the combination of both substances for 48 h, and apoptosis was analysed by flow cytometry. The percentage of apoptotic cells, assessed by a DNA content less than G_1 (sub-G_1) is indicated in each histogram. Data shown are representative of three separate experiments.

5.1.3. Discussion

The data reported here show that resveratrol induces apoptosis in MM and T-cell leukemia cells through the recruitment of Fas/CD95 death receptor and downstream signaling molecules into lipid rafts. Our results demonstrate that Fas/CD95 signaling and mitochondria are required for resveratrol-induced apoptosis, and

there is a sequence of Fas/CD95→mitochondrion in the signaling pathway underlying the apoptotic response triggered by resveratrol in hematological cancer cells. A putative linker between Fas/CD95 signaling and mitochondrion in resveratrol action might be the translocation of Bid to lipid rafts together with Fas/CD95 signaling molecules. Thus, our present data square with the following sequence of events in MM and T-cell leukemia cells that lead to resveratrol-induced apoptosis: coclustering of Fas/CD95 and lipid rafts→ recruitment of Fas/CD95 downstream signaling molecules to membrane rafts→Bid translocation to rafts→ΔΨm disruption→apoptosis (**Fig. 20**). Interference at critical stages of the above scheme, such as disruption of lipid rafts, inhibition of Fas/CD95 signaling by FADD-DN transfection and mitochondria protection by overexpression of Bcl-X_L, prevented resveratrol-induced apoptosis (**Figs. 13 and 15**). As the blockade of Fas/CD95 downstream signaling by FADD-DN overexpression abrogates both $\Delta\Psi_m$ loss and apoptosis, mitochondrial events are downstream of Fas/CD95 signaling in resveratrol-mediated apoptosis. Our data demonstrate that membrane rafts, Fas/CD95 signaling and mitochondria are crucial players in the apoptotic outcome delivered by resveratrol in MM and T-cell leukemia cells.

Resveratrol is effective in inducing the recruitment of Fas/CD95 in raft clusters even in U266 cells, which are resistant to undergo apoptosis on Fas/CD95 stimulation by either FasL/CD95L or agonistic anti-Fas/CD95 antibody. We have previously found that induction of clustering of Fas/CD95 in rafts leads to death receptor activation, independently of its ligand, even in cells that are resistant to undergo apoptosis following Fas/CD95 stimulation through its interaction with FasL/CD95L or agonistic anti-Fas/CD95 antibody [75]. Thus, Fas/CD95 activation by its clustering in rafts seems to be more potent than the receptor activation elicited by its physiological ligand. However, the fact that raft disruption only inhibits about 28% of resveratrol-induced apoptosis in U266 cells suggests that additional mechanisms leading to resveratrol mediated killing are triggered in these particular cells. One of these mechanisms has been reported to involve downregulation of STAT3 and nuclear factor-kB [92]. The present data also show that TRAIL receptors are translocated, in addition to Fas/CD95, into rafts following resveratrol treatment of MM and T-cell leukemic cells. This recruitment and concentration of death receptors in specific domains of the cell surface has clear clinical consequences as it might sensitize cancer cells to death receptor ligands [69]. This is of particular interest for TRAIL-mediated therapy, because TRAIL is under ongoing clinical trials [103]. The recruitment of death receptors and

downstream signaling in membrane rafts promoted by resveratrol treatment may underlie previous observations reporting that this polyphenol sensitizes different cancer cell types to death receptor-mediated apoptosis [104,105].

The findings reported here underline the role of Fas/CD95 recruitment into lipid rafts as a major mechanism in anticancer chemotherapy for the treatment of hematological malignancies. We have recently found that a number of anticancer drugs, including edelfosine, perifosine and aplidin, induce apoptosis in hematological cancer cells by bringing together Fas/CD95 and downstream signaling molecules in membrane rafts [38,39,42,69].

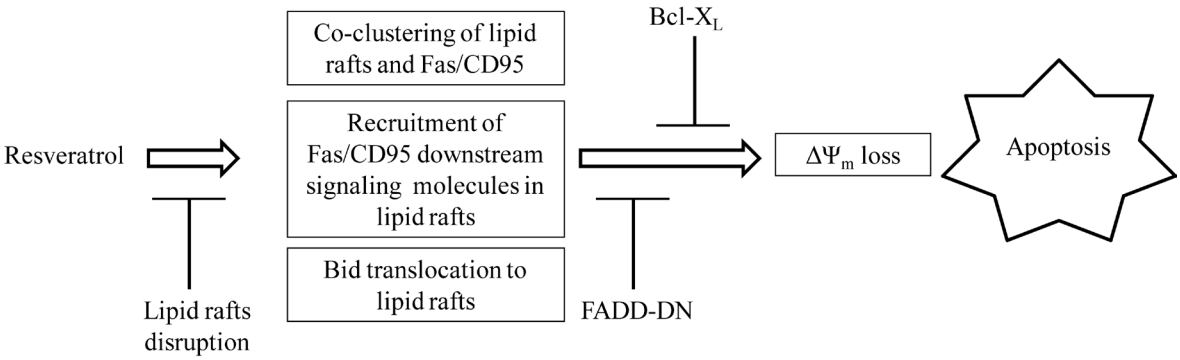

Figure 21. Schematic model for the mechanism of action of resveratrol in the induction of apoptosis in hematological cancer cells. This is a schematic diagram designed to portray the most significant events involved in resveratrol-induced apoptosis. Disruption of lipid rafts and overexpression of dominant-negative form of Fas-associated death domain-containing protein (FADD-DN) or Bcl-X_L prevent resveratrol-induced apoptosis, highlighting the critical role of lipid rafts, Fas/CD95 signaling and mitochondria in the mechanism of action of the polyphenolic phytoalexin. For further details, see the text.

Our data show that IFN-γ enhances the apoptotic response induced by resveratrol in hematological cancer cells, likely through an increase in Fas/CD95 and procaspase-8 levels. On these grounds, the present data suggest that resveratrol is not only effective in killing by itself hematological cancer cells, but also it might be a valuable drug in combination therapy, in particular with agents modulating or activating death receptor signaling. The combination of resveratrol and perifosine, which has been shown to act through raft-Fas/CD95 coclustering [69], resulted in an additive effect, suggesting a shared mode of action for both drugs. In addition, the combination of resveratrol with the proteasome inhibitor bortezomib led to a synergistic apoptotic response. It is tempting to speculate that a putative interaction between raft mediated processes triggered by resveratrol and proteasome inhibition

might lead to a potent cell death response.

Two naturally occurring resveratrol oligomers, ε-viniferin and miyabenol C, have been shown to promote apoptosis in lymphoid and myeloid cell lines at lower doses than resveratrol[106]. Further investigation on the mode of action of these natural oligomers might set new frameworks for cancer treatment.

The mechanistic findings reported here suggest that resveratrol may have a potential in the treatment of MM and T-cell leukemia, and highlight the role of recruitment of Fas/CD95 signaling in lipid rafts in antimyeloma and antileukemia chemotherapy

5.2. Lipid raft-mediated Akt signaling as a therapeutic target in MCL cells

5.2.1. Introduction

MCL is a B-cell-derived neoplasia that constitutes ~6% of all non-Hodgkin lymphomas, and is characterized by the chromosomal translocation t(11;14)(q13;q32) leading to aberrant overexpression of cyclin D1 [107,108]. In addition to this initial oncogenic event, MCL may carry a high number of secondary chromosomal and molecular alterations that influence the aggressive behavior of this neoplasm and a poor survival outcome [107,108]. Although conventional chemotherapy induces high-remission rates, relapse within a few years is common, contributing to a median survival of 5-7 years [109].

Several signaling pathways are deregulated in MCL cells including the constitutive activation of the PI3K/Akt pathway, which mediates the effects of a variety of extracellular signals and is crucial for the maintenance and proliferation of MCL cells [110,111], thus attracting great interest as a possible therapeutic target. PI3K is activated by a wide range of tyrosine kinase growth factor receptors, and is the major activator of Akt, playing a central role in fundamental biological processes including cell growth, proliferation, migration and survival, through phosphorylation of a plethora of substrates [26,110]. Akt is a protein kinase that belongs to the AGC family of serine/threonine kinases and has three conserved domains, namely: PH domain, which binds phosphoinositides with high affinity, as well as catalytic and regulatory domains [29]. Akt suppresses apoptosis by direct phosphorylation of pro-apoptotic proteins such as Bad and pro-caspase-9 [29]. PI3K phosphorylates phosphatidylinositol-4,5-bisphosphate (PIP2) to generate phosphatidylinositol-3,4,5-trisphosphate (PIP3), that binds to Akt PH domain and PDK1, recruiting them to the membrane. Once in the membrane, Akt is phosphorylated at two key residues, Thr308 and Ser473 [28]. Thr308 site is localized in the activation loop and is phosphorylated by PDK1, while Ser473 is localized in the C-terminal hydrophobic motif and is phosphorylated by PDK2 [28]. mTOR has been suggested as the main candidate for PDK2, but DNA-dependent protein kinase (DNA-PK), beta-1-integrin-linked protein kinase (ILK) or even Akt itself through autophosphorylation have also been proposed to act as PDK2 [28,112]. mTOR forms part of two different complexes, mammalian TOR complex 1 (mTORC1) and mTORC2, which exert their actions by regulating a number of

important proteins [113]. mTORC2 acts upstream and is suggested to phosphorylate Akt, whereas mTORC1 acts downstream Akt [113].

Insulin-like growth factor-1 (IGF-1)-mediated activation of Akt has been reported to be dependent on lipid rafts [34,114]. Rafts are membrane microdomains highly enriched in cholesterol and sphingolipids, which act as scaffolds for signaling pathways in the cell membrane [17], and growing evidence shows their potential as therapeutic targets in cancer therapy [8,37,39,42,64,67,69,73,80,115]. An endogenous raft-resident Akt has been reported in LNCaP human prostate cells that showed a different substrate affinity as compared to non-raft Akt, suggesting the presence of distinct Akt populations with differential signaling behavior [48].

The ATLs are a family of compounds, initially synthesized as ether phospholipids and widely referred to as alkyl-lysophospholipid analogs, which are able to selectively induce apoptosis in tumor cells [58-60,64,69,70,75]. These ATLs include the ether lipid edelfosine as well as perifosine, which accumulate in lipid rafts [39,67,116], promote co-capping of Fas/CD95 death receptor and rafts [38,67,84] and inhibit PI3K/Akt survival signaling [83,84,117]. Edelfosine shows affinity for cholesterol [61,63], likely due to geometry compensation of the "cone shape" of sterols and the "inverted cone shape" of edelfosine that leads to a stable bilayer [63]. *In vivo* and *in vitro* experimental approaches have shown that ATLs selectively kill MCL cells as well as additional hematological cancer cells, including patient-derived primary cancer cells, by a lipid raft-dependent mechanism [64,69,70].

In this work we provide evidence that MCL cell survival depends on raft-mediated Akt activation for survival. We show here that ATLs inhibit PI3K/Akt signaling by displacing Akt and key enzyme regulators from lipid rafts, leading to Akt dephosphorylation and apoptosis. In contrast, Fas/CD95 death receptor was recruited to rafts upon ATL treatment. Our data suggest that raft environment is essential for Ser473 Akt phosphorylation in MCL cells. ATL oral treatment inhibited MCL tumor growth in xenograft animal models. Apoptosis induced by either edelfosine or perifosine was not blocked by tumor microenvironmental stimuli in MCL primary cultures and cell lines. These results highlight the importance of raft-mediated PI3K/Akt targeting in MCL therapy.

5.2.2. Results

5.2.3.1. ATLs activate the intrinsic apoptotic signaling pathway and inhibit Akt signaling in MCL cells

We have found that treatment of MCL cell lines Z-138, JVM-2 and Jeko-1 with the ATLs edelfosine and perifosine induced $\Delta\Psi_m$ disruption (**Fig. 22**) and ROS production (**Fig. 23**).Caspase-9 activation was also detected in Z-138 cells after ATLs incubation (**Fig. 24**).

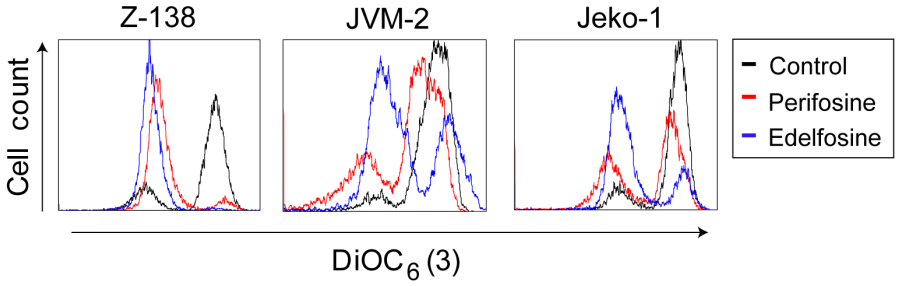

Figure 22. Involvement of the intrinsic apoptotic pathway in the action of ATLs on MCL cells. (*A*) Z-138 cells were untreated (control) or treated with (-)10 μM perifosine or (-) edelfosine for 24 h, and the percentages of cells with disrupted $\Delta\Psi_m$ [$(DiOC_6(3)^{low})$]. Histograms shown are representative of three independent experiments.

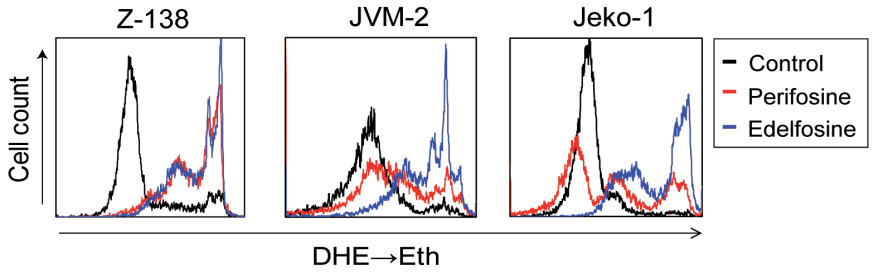

Figure 23. ROS production following ATL treatment in Z-138, JVM-2 and Jeko-1 cells. Cells were untreated (-) or treated with (-) 10 μM perifosine or (-) edelfosine for 24 h, and ROS production (DHE→Eth) was measured as described in Materials and methods. Fluorescence flow cytometryprofiles shown are representative of three independent experiments.

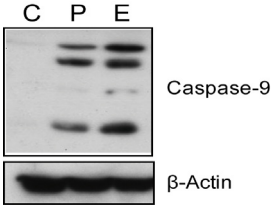

Figure 24. Caspase -9 activation following ATL treatment. Z-138 cells untreated (control, C) or treated with 10 μM of edelfosine or perifosine for 12 h were analyzed by immunoblotting for anti-capase-9 active fragments. Immunoblotting for β-actin was used as an internal control for equal protein loading in each lane.

These events were related to the activation of the intrinsic apoptotic signaling that eventually led to cell death (**Figs. 23 - 25**). Mitochondrial depolarization was one of the first events triggered by ATLs, since this phenomenon was observed as soon as 6 h of treatment (**Fig. 25 A**), prior to the onset of apoptosis after 24-h incubation, as assessed by an increase in the percentage of sub-G_0/G_1 cell population (**Fig. 25 B**). The apoptotic response was caspase-mediated, as preincubation with the cell-permeable pan-caspase inhibitor z-VAD-fmk abrogated ATL-induced apoptosis (**Fig. 26**).

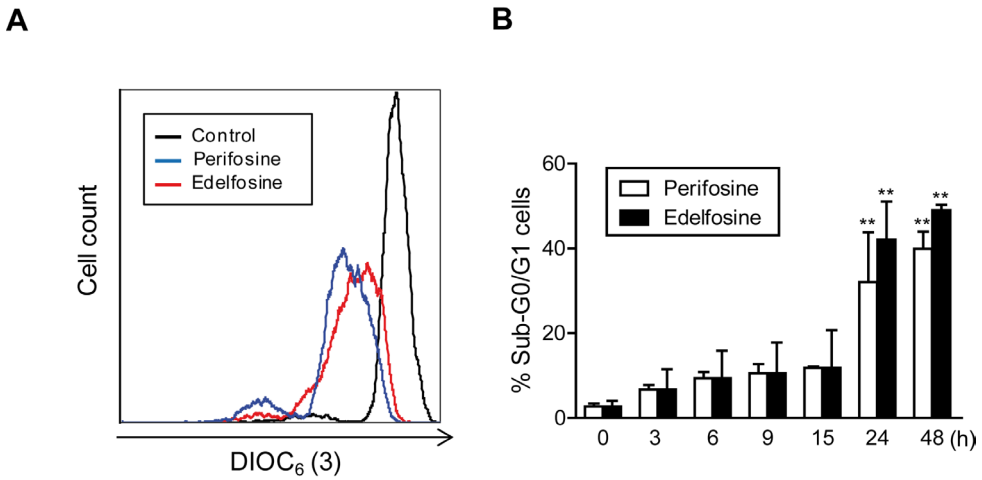

Figure 25. Early loss of mitochondrial transmembrane potential and time course of apoptosis induction following ATL treatment in Z-138 cells.(*A*) Cells were untreated (-) or treated with 10 µM (-) perifosine or (-) edelfosine for 6 h, and loss of mitochondrial transmembrane potential ($\Delta\Psi_m$) was measured as described in Materials and methods using $DiOC_6(3)$. (*B*) Cells were treated with 10 µM perifosine or edelfosine for the indicated times, and then apoptosis was quantitated as the percentage of cells in the sub-G_0/G_1 region following cell cycle analysis by flow cytometry. Data shown are means ± SD or representative experiments of three independent experiments. Asterisks indicate values that are significantly different from untreated control cells at $p < 0.01$ (**) level by Student's t-test.

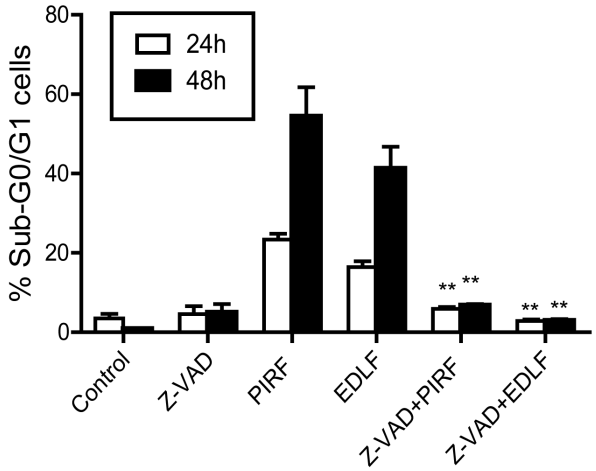

Figure 26. ATL-induced apoptosis in the MCL Z-138 cell line is mediated by caspase activation. Z-138 cells were preincubated without (Control) or with 50 µM z-VAD-fmk for 1 h, and then in the absence (Control) or presence of 10 µM perifosine (PRIF) or edelfosine (EDLF) for 24 h. Apoptosis was quantitated as the percentage of cells in the sub-G_0/G_1 region following cell cycle analyses by flow cytometry. Data shown are means + SD of three independent experiments. Asterisks indicate values that are significantly different from untreated control cells at $p < 0.01$ (**) level by Student's t-test.

Because inhibition of PI3K/Akt signaling has been linked to activation of the intrinsic apoptotic pathway [29], we examined the time-dependent effect of edelfosine, which displayed a higher *in vitro* anti-MCL activity than perifosine (**Fig. 25 B**) [70], on Akt activation, Akt targets and related kinases. While 1-*O*-octadecyl-*rac*-glycero-3-phosphocholine (ETOH), an inactive edelfosine analog [59,118], neither induced apoptosis nor inhibited Akt phosphorylation (**Fig. 27**), edelfosine-treated cells showed a dramatic decrease of Ser473 p-Akt at very early incubation times (3 h), followed by a reduction in Thr308 p-Akt after 15-h incubation (**Fig. 28 A**). Using a specific antibody that recognized p-Akt substrates with the motif RXRXXS/T [119], we detected a decrease in the phosphorylation of most Akt substrates after 3-h incubation (**Fig. 28 A**). However, the level of Ser9/21 glycogen synthase kinase-3 (GSK3) phosphorylation was not inhibited, but slightly activated, and Ser136 dephosphorylation of Bad was detected after 24-h incubation with edelfosine (**Fig. 28 A**), when apoptosis was already triggered (**Fig. 25 B**). These results are in line with our previous observation that MCL cell exposure to ATLs did not modify the expression of cyclin D1 [70], which is physiologically targeted to proteasomal degradation by GSK-3 [110]. In addition, arguing in favor of an Akt-independent regulation of GSK3 signaling in MCL cells, preincubation of Z-138 cells with the GSK3 inhibitor lithium chloride potentiated ATL-induced apoptosis (**Fig. 28 B**), suggesting that ATLs act through a signaling pathway independent of GSK3.

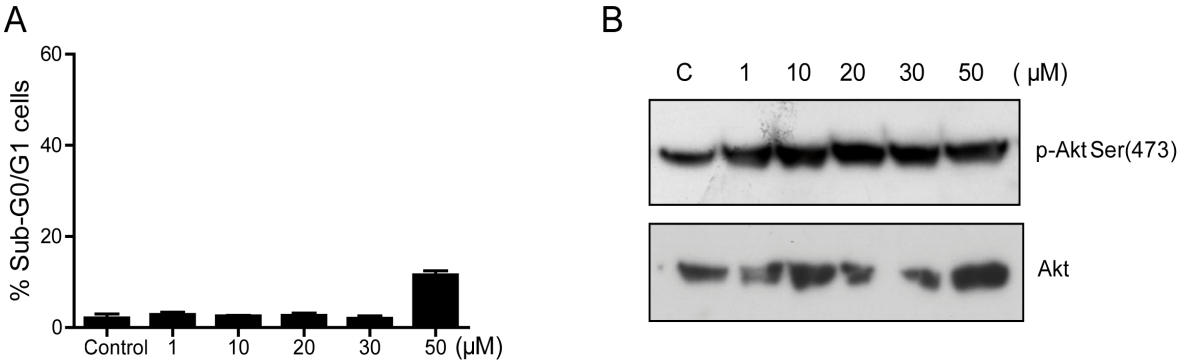

Figure 27. The inactive edelfosine analog ETOH fails to induce apoptosis and to inhibit Akt in Z-138 cells. (*A*) Cells were untreated (Control) or treated with the indicated doses of ETOH for 24 h, and then apoptosis was quantitated as the percentage of cells in the sub-G_0/G_1 region following cell cycle analysis by flow cytometry. Data shown are means ± SD of three independent experiments. (*B*) Cells treated as above were analyzed by immunoblotting for p-Akt Ser473 and Akt protein levels (SDS-12% polyacrylamide gels), after 6 h incubation with ETOH at the indicated concentrations. Untreated control cells (*C*) were run in parallel. Representative blots of three separate experiments are shown.

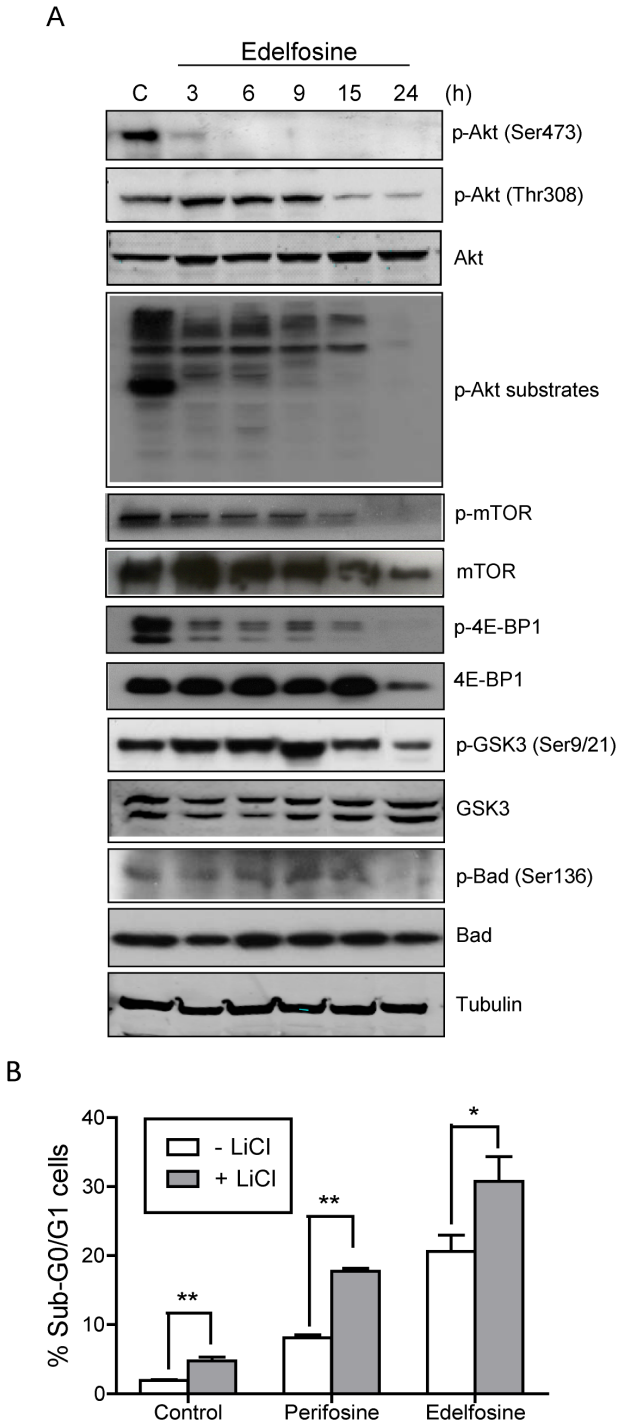

Figure 28. Inhibition of Akt signaling in the action of ATLs on MCL cells. (*A*) Z-138 cells were untreated (control, C) or treated with 10 μM edelfosine for the indicated times, and then analyzed by immunoblotting using specific antibodies against p-Akt (Ser473), p-Akt (Thr308), Akt, p-Akt substrates (RXRXXS/T), p-mTOR, mTOR, p-4E-BP1, 4E-BP1, p-GSK3a/b, GSK3a/b, p-Bad (Ser136) and Bad. Immunoblotting for tubulin was used as an internal control for equal protein loading in each lane. Representative blots of three separate experiments are shown. (*B*) Z-138 cells were preincubated without or with 20 mM lithium chloride for 1 h, and then incubated in the absence (control) or presence of 10 μM perifosine or edelfosine for 24 h, and analyzed by flow cytometry to evaluate apoptosis. Data shown are means±s.d. of three independent experiments (*P<0.05; **P<0.01). The indicated statistically significant differences were between cells untreated and treated with lithium inthe different experimental conditions, but they are equally statistically significant when we subtract the apoptotic percentages of controls with or without lithium from the respective ATL treatments.

We also analyzed the phosphorylation of mTOR, which acts downstream Akt forming the complex mTORC1 [113]. We found that phosphorylation levels of mTOR (p-mTOR), as well as of its direct substrate 4E-BP1 (p-4E-BP1), were rapidly decreased after 3 h incubation with edelfosine (**Fig. 28 A**). The time-course of this inhibition paralleled that of Ser473 p-Akt (**Fig. 28 A**). Both mTOR and 4E-BP1 protein levels were diminished by the time DNA degradation was triggered (**Figs. 28 A and 25 B**).

Next we analyzed the levels of Ser473 p-Akt of distinct MCL cell lines in relationship to their ATL sensitivity. We found that MCL cell lines ranked HBL-2 >> Jeko-1 > Z-138 ≈ JVM-2 for their basal level of phospho-Ser473 Akt (**Fig. 29 A**). This order was inversely related to their sensitivity to ATLs, HBL-2 cells being resistant to their apoptotic action (**Fig. 29 A**). Although ATLs induced a rapid and complete dephosphorylation of Akt in Z-138 sensitive cell line (**Fig. 28 A**), the high levels of p-Akt in ATL-resistant HBL-2 cells were not decreased upon ATL treatment (**Fig. 29 B**).

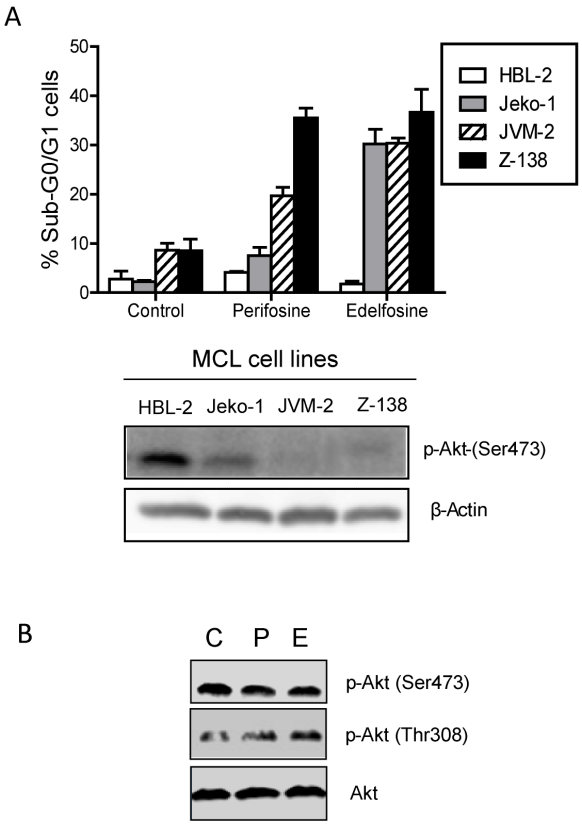

Figure 29. **MCL cell lines sensitivity to ATLs is dependent of p-Akt basal levels.** (*A*, upper) HBL-2, Jeko-1, JVM-2 and Z-138 cell lines were incubated without (control) or with 10 μM perifosine or edelfosine for 24 h, and analyzed by flow cytometry to evaluate apoptosis.Data shown are means±s.d. of three independent experiments. (e, lower) MCL cell lines HBL-2, Jeko-1, JVM-2 and Z-138 were analyzed by immunoblotting for p-Akt (Ser473) and β-actin. Blots were briefly exposed for autoradiography to highlight the high level of p-Akt in HBL-2 cells as compared with the other MCL cell lines.(*B*) HBL-2 cells were untreated (control, C) or treated with ATLs for 6 h, and then analyzed by immunoblotting with specific antibodies against p-Akt (Ser473), p-Akt (Thr308) and Akt1/2/3. Representative blots of three separate experiments are shown.

However, as shown in Figure 28 A and Figure 30, we found a decrease in Ser473 p-Akt levels after ATL-incubation in Z-138, JVM-2 and Jeko-1 MCL sensitive cells after ATL-incubation. These data support the notion that the extent of ATL- induced apoptosis in MCL cells is correlated with and depends on the Akt phosphorylation status at Ser473, suggesting the involvement of Akt dephosphorylation in the mechanism of ATL antitumor activity.

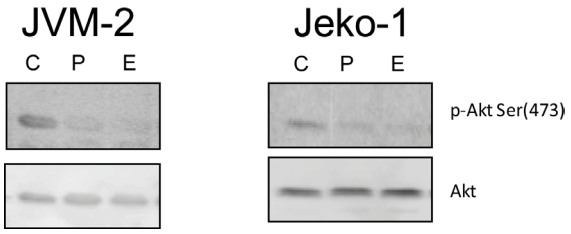

Figure 30. **ATL incubation inhibits Akt in JVM-2 and Jeko-1 cells**. Cells were untreated (C) or treated with 10 μM perifosine (P) or edelfosine (E), and analyzed by immunoblotting for Ser473 p-Akt and Akt protein levels (SDS-12% polyacrylamide gels) after 6-h incubation. Representative blots of three separate experiments are shown.

5.2.3.2. Effect of edelfosine on ERK and JNK phosphorylation in MCL cells

Because JNK signaling has been involved in ATL-induced apoptosis [118] and pathogenesis of MCL [120], and ERK activation has been described as a possible compensatory mechanism in Akt-compromised cells [121], we assessed the phosphorylation status of ERK and JNK activation in Z-138 cells exposed to edelfosine. As shown in Figure 31 A, the level of p-JNK was dramatically increased during edelfosine exposure, whereas the p-ERK level was not modified or resulted slightly enhanced during the first 9 h of treatment, and then decreased following induction of apoptosis. However, despite p-JNK could be efficiently inhibited by JNK inhibitor (SP)(**Fig. 31 B**), these latter inhibitor did not significantly modify the cytotoxicity of ATLs, the same for ERK inhibitor (PD), as assessed by hypodiploidy or Annexin V analyses (**Figs. 31 C and D**).

Altogether, our data suggested that ATL-induced apoptosis in MCL cells involved a rapid and main Akt dephosphorylation at Ser473, rather than at Thr308, with no significant involvement of the Akt targets GSK-3 and Bad, and independently of ERK and JNK signaling.

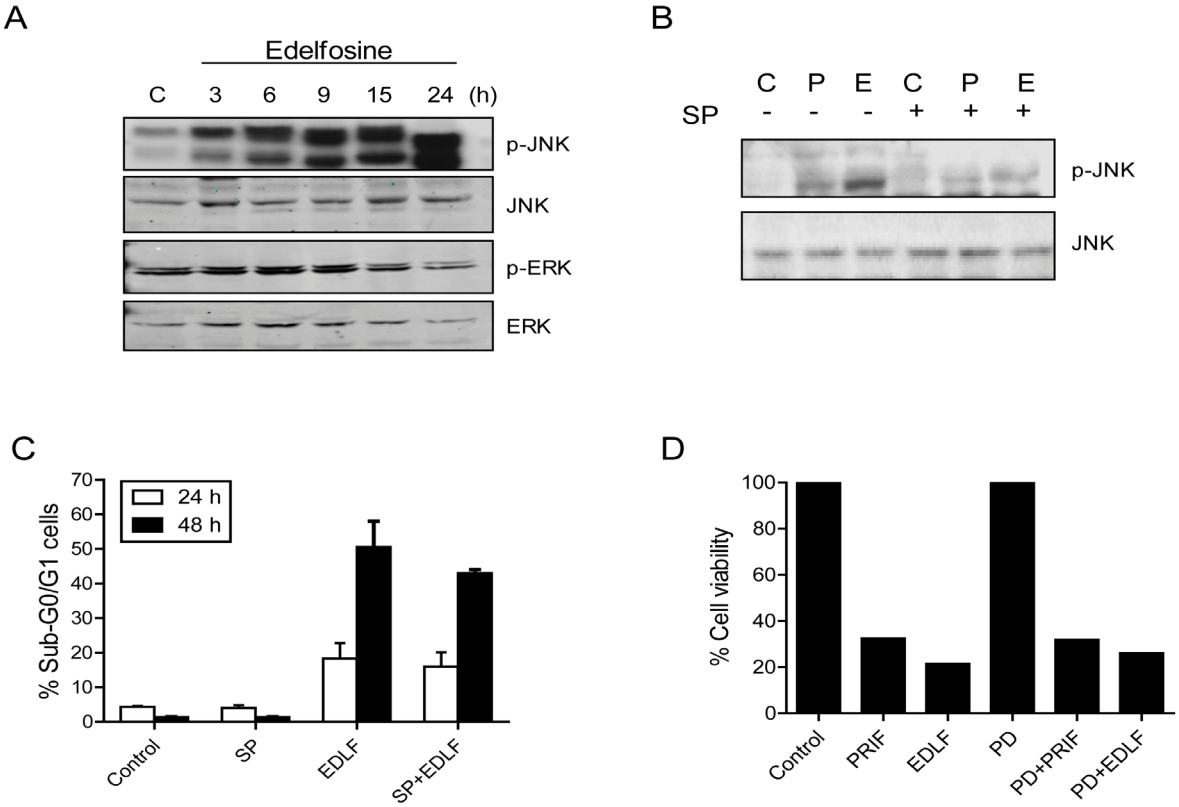

Figure 31. Effect of ATLs on ERK and JNK signaling. (*A*) Cells were untreated (control, C) or treated with 10 μM edelfosine for the indicated times, and then analyzed by immunoblotting for p-JNK, JNK, p-ERK, ERK2. Representative blots of three separate experiments are shown. (*B*) Cells were preincubated without (control, C) or with 1 μM SP600125 for 1 h, and then incubated in the absence or presence of 10 μM perifosine (P) or edelfosine (E) for 6 h, and analyzed by immunoblotting for p-JNK and JNK. Representative blots of three separate experiments are shown. (*C*) Cells were preincubated without or with 1 μM SP600125 (SP) for 1 h, and then incubated in the absence or presence of 10 μM edelfosine (EDLF) for 24 h. Apoptosis was then quantitated as the percentage of cells in the sub-G_0/G_1 region in cell cycle analysis by flow cytometry. Untreated control cells were run in parallel. Data shown are means ± SD of three independent experiments. (*D*) Cells were preincubated without or with 20 μM PD98059 (PD) for 1 h, and then incubated with 10 μM perifosine (PRIF) or edelfosine (EDLF) for 24 h. Cell viability was assessed as non-apoptotic cells in Annexin V analysis by flow citometry. Data are means of 2 independent experiments performed.

5.2.3.3. PI3K inhibition potentiates ATL-induced apoptosis

To further assess the involvement of PI3K/Akt signaling in MCL sensitivity to ATLs, we preincubated MCL cells with the PI3K inhibitor wortmannin before ATL addition. Preincubation of Z-138 cells with wortmannin for 1 h, followed by 24-h incubation with perifosine or edelfosine, potentiated the effect of ATLs on the inhibition of Akt and mTOR phosphorylation after 6-h incubation (**Fig. 32 A**) as well as on apoptosis induction (**Fig. 32 B**), suggesting that inhibition of PI3K/Akt could increase the ATL-mediated apoptotic response.

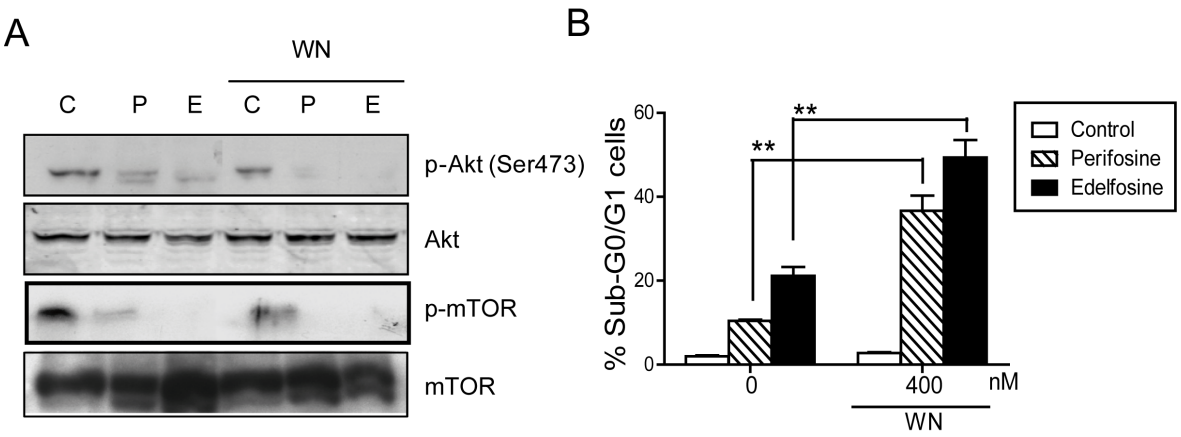

Figure 32. PI3K inhibition potentiates ATL-induced cell death in Z-138 cells. (*A*) Cells were pretreated without (control, C) or with 400 nM wortamnin (WN), and then incubated with 10 μM perifosine (P) or edelfosine (E) for 6 h and analyzed by immunoblotting for p-Akt (Ser473), and Akt1/2/3. (*B*) Cells were preincubated without or with 400 nM wortmannin (WN) for 1 h, and then incubated in the absence or presence of 10 μM perifosine or edelfosine for 24 h, and analyzed by flow cytometry to evaluate apoptosis. Data shown are means ± SD of three independent experiments (**, $P < 0.01$).

5.2.3.4. Akt inhibitors induce apoptosis in the Z-138 MCL cell line

Next we examined the action of specific Akt inhibitors as apoptotic inducers in Z-138 cells, namely: Akti-1/2, an allosteric PH domain-dependent inhibitor; Akt inhibitor III, a substrate-competitive phosphatidylinositol ether analog; and Akt inhibitor X, which prevents phosphorylation of Akt and downstream targets [122,123] (**Fig. 33**). All these Akt inhibitors decreased Ser473 Akt phosphorylation as well as mTOR phosphorylation (**Fig. 34 C**), and induced apoptosis (**Fig. 34 B**) and $\Delta\Psi_m$ disruption (**Fig. 34 C**), in Z-138 cells. In addition, the above Akt inhibitors induced JNK activation and a slight increase in the level of JNK, whereas GSK3 phosphorylation was not inhibited, but slightly activated (**Fig. 35**). These data resemble those obtained with ATLs (**Figs. 28 A and 31 A**), suggesting that Akt inhibitors and ATLs were targeting the same signaling pathway in MCL cells.

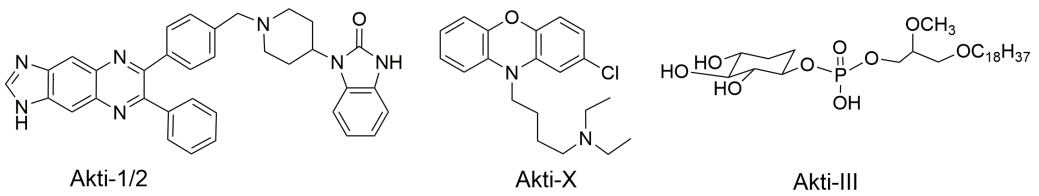

Figure 33. Molecular structure of the Akt inhibitors (Akti) tested in this study.

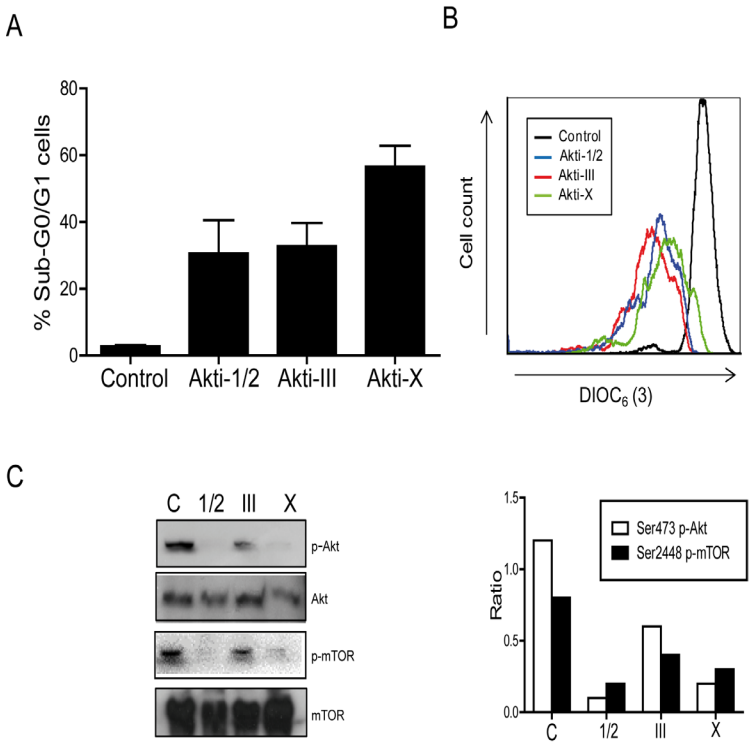

Figure 34. Akt inhibitors induce apoptosis in Z-138 cells. (*A*) Cells were incubated with Akt inhibitors for 24 h, and apoptosis was then quantitated by flow cytometry. Untreated control cells were run in parallel. Data shown are means ± SD of three independent experiments. (*B*) Cells were untreated (Control) or treated with 10 μM Akti-1/2, Akti-III or Akti-X, and disruption of $\Delta\Psi_m$ [$(DiOC_6(3)^{low})$] was measured as described in Materials and methods after 6 h incubation. Histograms shown are representative of three independent experiments. (*C*) Cells were untreated (control, C) or treated with 10 μM of each Akt inhibitor for 6 h, and then analyzed by immunoblotting for p-Akt (Ser473), Akt, p-mTOR and mTOR. (inset, right) Bands from the above gel were quantitated using ImageJ software and phosphorylated/total protein ratio values for p-Akt and p-mTOR relative expression levels were calculated.

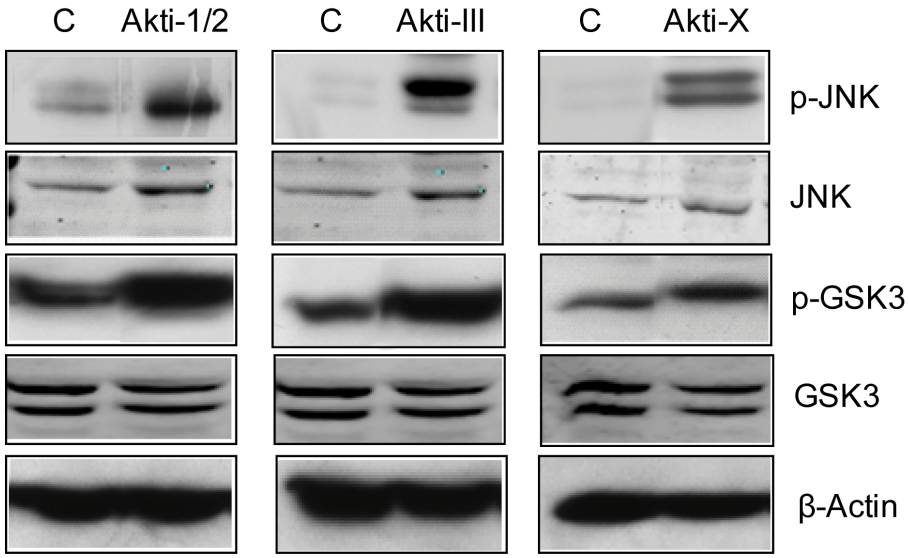

Figure 35. Effect of Akt inhibitors on JNK and GSK3 phosphorylation. Cells were untreated (control, C) or treated with 10 μM Akti-1/2, Akti-III or Akti-X for 24 h and then analyzed by immunoblotting for p-JNK1/2/3, JNK1, p-GSK3, GSK3 and β-actin antibodies (SDS 12% polyacrylamide gels). Immunoblotting for β-actin was used as an internal control for equal protein loading in each lane. Representative blots of three separate experiments are shown.

5.2.3.5. CD40 stimulation does not protect MCL cells from ATL cytotoxicity

The microenvironment, including cytokines, has a central role on MCL survival and drug resistance, and the CD40 system acts as a growth-promoting stimulus [110,122]. In this regard, we preincubated MCL cell lines JVM-2 and Z-138 with anti-CD40 immunoglobulin for 1 h, and then ATLs were added for 24 h, before evaluating apoptosis as assessed by DNA degradation through cell cycle analyses (**Fig. 36 A**). Pretreatment of MCL cells with anti-CD40 immunoglobulins did not prevent perifosine- or edelfosine-induced apoptosis and only a very slight decrease in the ATL-induced apoptotic response was detected (**Fig. 36 A**). Pretreatment of MCL cells with anti-CD40 antibody increased Ser473 p-Akt level (**Fig. 36 B**), but ATLs induced Akt dephosphorylation in both untreated and anti-CD40-treated cells (**Fig. 36 B**). These data suggest that CD40 pro-survival signaling does not affect significantly the ATL proapoptotic activity in MCL cells. Similar results were obtained by using Annexin V binding assays to quantify apoptotic cells (**Fig. 37**).

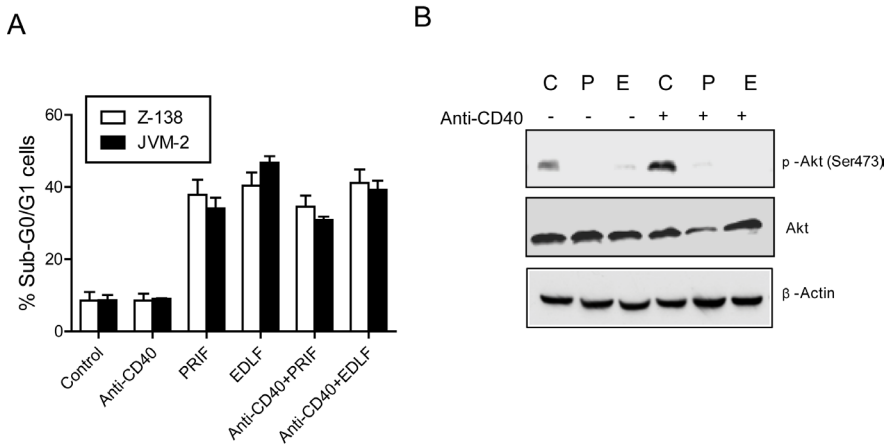

Figure 36. ATL-induced apoptosis in MCL cells is independent of microenvironmental stimuli. (*A*) JVM-2 and Z-138 MCL cell lines were preincubated without or with 500 ng/ml anti-CD40 antibody, and then incubated in the absence or presence of 10 μM perifosine (PRIF) or edelfosine (EDLF). After a 24-h treatment, apoptosis was then quantitated by flow cytometry. Untreated control cells were run in parallel. Data shown are means±s.d. of three independent experiments. (*B*) Z-138 cells were pretreated without (control, C) or with 500 ng/ml anti-CD40antibody, and then incubated with 10 μM perifosine (P) or edelfosine (E) for 6 h, and analyzed by immunoblotting with specific antibodies against p-Akt (Ser473) and Akt. Immunoblotting for β-actin was used as an internal control for equal protein loading in each lane. Representative blots of three separate experiments are shown.

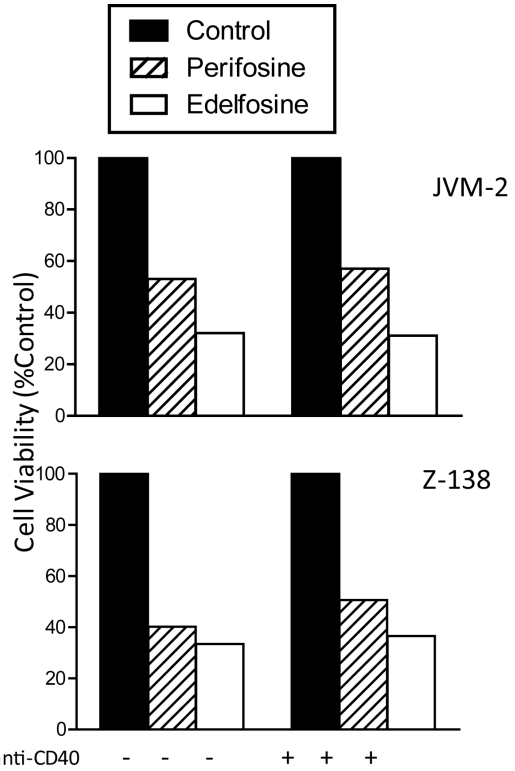

Figure 37. **ATL-induced apoptosis in MCL cells is independent of microenvironmental stimuli.** JVM-2 and Z-138 MCL cell lines were preincubated without or with 500 ng/ml anti-CD40 antibody, and then incubated in the absence or presence of 10 μM perifosine or edelfosine for 24 h. Cell viability was assessed as non-apoptotic cells in Annexin V analysis by flow cytometry. Data shown are means of two independent experiments.

5.2.3.6. Localization of PI3K/Akt signaling in MCL cell lipid rafts

Because the PI3K/Akt pathway is constitutively activated in MCL cells [110,111], and proper activation of Akt has been suggested to be dependent on lipid rafts [34,114], we isolated lipid rafts from Z-138, JVM-2 and Jeko-1 cells based on their insolubility in Triton X-100 lysis buffer at 4°C [39]. GM1-containing lipid rafts, were identified using CTx B subunit conjugated to horseradish peroxidase (**Figs. 38 and 39**). Raft and non-raft fractions, prepared as described in Materials and methods, were analyzed. We observed that rafts from untreated control Z-138 cells were highly enriched in a subpopulation of Akt that was fully activated (Ser473 and Thr308 phosphorylation) (**Fig. 38**). Additional Akt signaling regulatory kinases were also detected in lipid rafts, including PI3K, PDK1 full active form (i.e. phosphorylated on Ser241), and mTOR. Non-phosphorylated Akt and PDK1, unlike their phosphorylated forms, were equally distributed in raft and non-raft fractions (**Fig. 38**). These data suggest that raft membrane domains can serve as key platforms for PI3K/Akt activation in MCL cells.

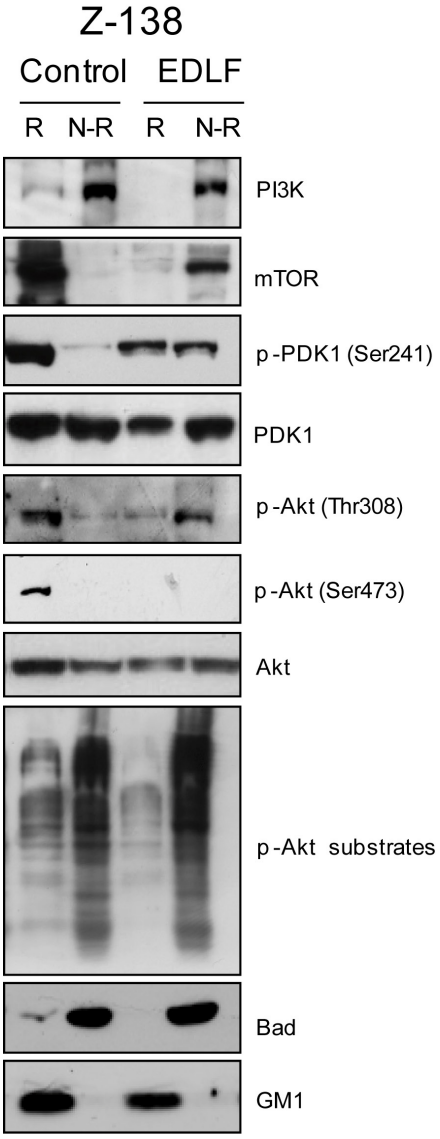

Figure 38. Involvement of raft-mediated Akt signaling in edelfosine-induced apoptosis in MCL cells. Z-138 cells untreated (control) and treated with 10 μM edelfosine (EDLF) for 15 h were lysed in 1% Triton X-100 and fractionated by centrifugation on a discontinuous sucrose density gradient. Equal volumes of collected raft (R) and non-raft (NR) fractions were subjected to SDS-polyacrylamide gel electrophoresis before analysis of the indicated proteins using specific antibodies. The migration positions of PI3K, mTOR, p-PDK1 (Ser241), PDK1, p-Akt (Thr308), p-Akt (Ser473), Akt, p-Akt substrate (RXRXXS/T) and Bad were examined by immunoblotting using specific antibodies. Location of GM1-containing lipid rafts was determined using cholera toxin (CTx) B subunit conjugated to horseradish peroxidase.

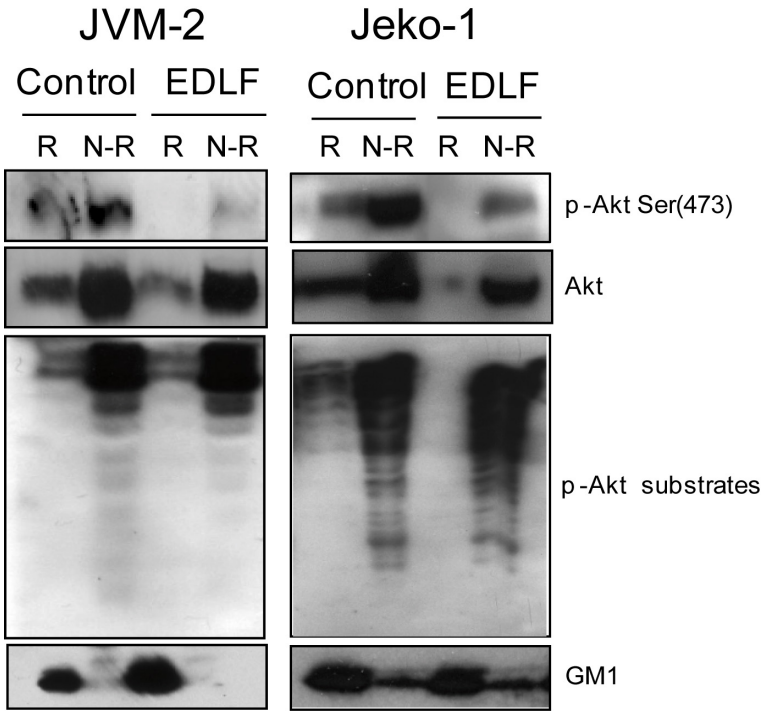

Figure 39. Involvement of raft-mediated Akt signaling in edelfosine-induced apoptosis in MCL cells. JVM-2 and Jeko-1 cells untreated (control) and treated with 10 μM edelfosine (EDLF) for 15 h were fractionated as above to isolate raft (R) and non-raft (N-R) fractions. The migration positions of p-Akt (Ser473), Akt and p-Akt substrates (RXRXXS/T) were examined by immunoblotting. Location of GM1-containing lipid rafts was determined using CTx B subunit conjugated to horseradish peroxidase.

5.2.3.7. Regulation of raft-mediated Akt signaling is critical for MCL survival

ATLs target lipid rafts and reorganize their protein composition [67,75,116]. Following edelfosine incubation, we detected a dramatic displacement of upstream Akt kinases PI3K and p-PDK1, as well as mTOR to non-raft fractions (**Fig. 38**). Akt was also partially displaced from raft fractions upon edelfosine treatment (**Figs. 38 and 39**). Interestingly, we found that edelfosine treatment inhibited p-Akt and the phosphorylation of Akt downstream substrates present in the raft fractions of Z-138 cells (**Fig. 38**). Bad was mainly localized in non-raft fractions (**Fig. 38**), suggesting that its inhibition occurs at a later stage as shown in Figure 28A. Ser473 p-Akt was also inhibited in the raft fractions of the JVM-2 and Jeko-1 cell lines, together with a displacement of Akt from raft fractions (**Fig. 39**). These data suggest that edelfosine incorporation in rafts blocks PI3K/Akt signaling by displacing Akt and its regulators from rafts.

Next, we examined the subcellular localization of Ser473 p-Akt by immunofluorescence imaging of Z-138 cells treated with pervanadate, the most potent known Akt activator [123], in order to facilitate p-Akt visualization in the cell.

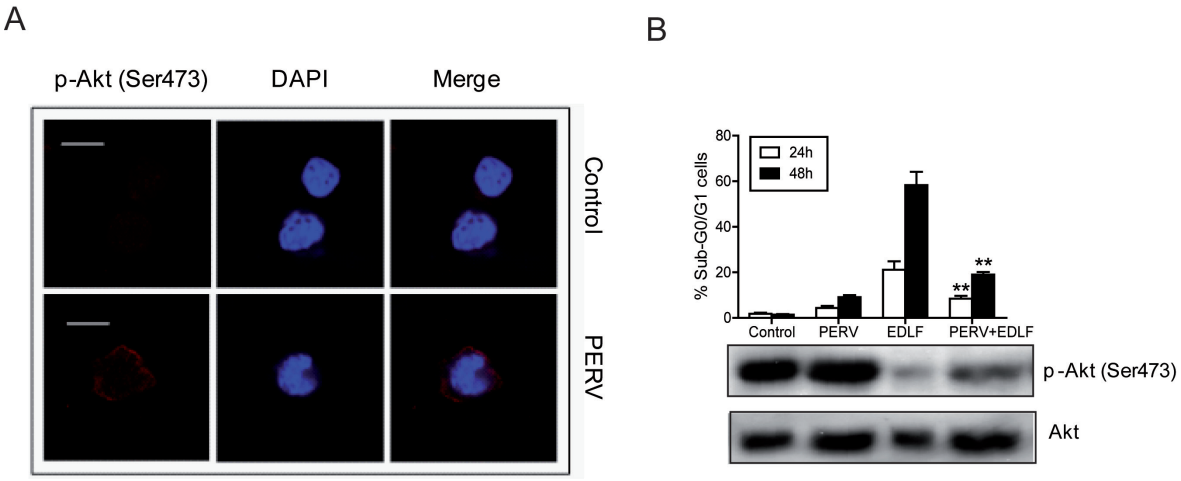

Figure 40. Pervanadate prevents edelfosine-induced apoptosis. (*A*) Serum-starved Z-138 cells untreated (control) or treated with pervanadate (PERV) for 15 min were incubated with anti-p-Akt (Ser473) antibody, and then with CY3-conjugated secondary antibody (red fluorescence) and 40,6-diamidino-2-phenylindole (blue fluorescence), as described in Materials and methods. Bar, 10 μm. (*B*) Z-138 cells were preincubated without (control) or with pervanadate (PERV) for 15 min at 37 ºC, and then incubated in the absence or presence of 10 μM edelfosine (EDLF) for 24 h to evaluate apoptosis induction by flow cytometry (d, upper), or in the presence of 10 μM edelfosine (EDLF) for 6 h to analyze p-Akt (Ser473) and Akt protein levels by immunoblotting (d, lower). Data shown are means ± s.d. Asterisks indicate values that are significantly different from edelfosine-treated cells at P<0.01 (**) level by Student's t-test

Under basal conditions, localization of p-Akt was difficult to detect, but p-Akt Ser473 was readily visualized at the cell plasma membrane following pervanadate treatment (**Fig. 40 A**). Preincubation of MCL cells with pervanadate allowed to overcome edelfosine-mediated inhibition of Ser473 p-Akt and to abrogate almost totally the apoptotic effect of edelfosine (**Fig. 40 B**), thus supporting that membrane p-Akt downregulation is a crucial step in ATL-mediated cell death. In addition, we found that incubation of MCL cells with both edelfosine and perifosine induced recruitment of Fas/CD95 death receptor to rafts (**Fig. 41**). Thus, ATLs displaced survival Akt signaling from rafts, whereas apoptotic Fas/CD95 death receptor was translocated to these membrane domains. However, despite Fas/CD95 translocation to rafts, when we incubated Z-138 cells with agonistic cytotoxic CH-11 anti-Fas monoclonal antibody following edelfosine pretreatment, only a slight increase in apoptosis was detected, which was not statistically significant when compared to cells treated only with the ether lipid (**Fig. 41**).

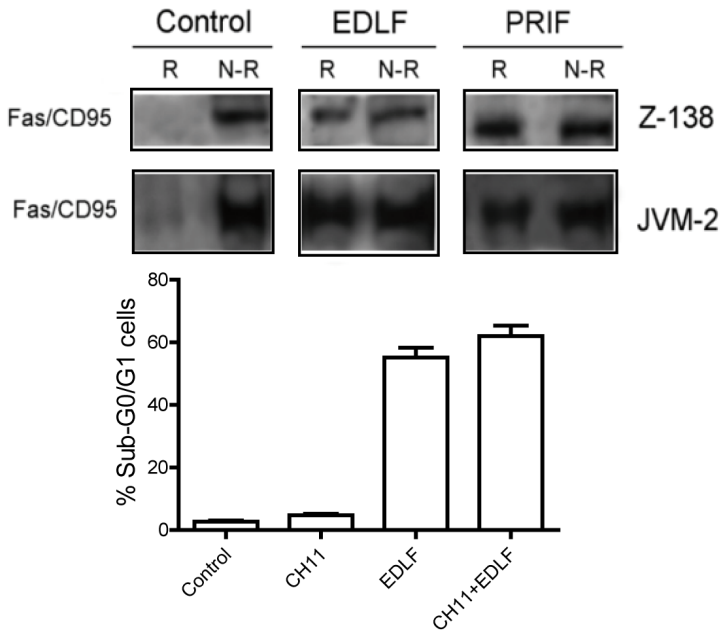

Figure 41. **Recruitment of Fas/CD95 in membrane rafts following edelfosine treatment.** (upper) Z-138 and JVM-2 cells were untreated (control) or incubated with 10 μM edelfosine (EDLF) or perifosine (PRIF) for 15 h, and then raft and non-raft fractions were obtained as above, and analyzed for Fas/CD95 using specific antibodies. (lower) Z-138 cells were preincubated for 1 h with edelfosine (EDLF), followed by treatment with 50-ng/ml CH-11 for 48 h, and then apoptosis was quantitated by flow cytometry. Data shown are means±s.d.

5.2.3.7. In vivo efficacy of edelfosine and perifosine in MCL treatment

By using a xenograft MCL-bearing CB17-SCID mouse model, we found that daily oral treatment for 3 weeks with ATLs (30 mg/kg edelfosine, molecular mass, 523.70 g/mol; 26.45 mg/kg perifosine, molecular mass, 461.67 g/mol) inhibited the growth of MCL cells. Serial caliper measurements were made to determine tumor growth, and showed a significant anti-MCL activity for both ATLs (**Fig. 42 A**). A comparison of tumors, isolated from drug-free control and ATL-treated MCL-bearing mice, at the end of treatment rendered a dramatic reduction of tumor weight and volume in mice treated with edelfosine or perifosine (**Fig. 42 A and B**). These results highlight the effectiveness of both edelfosine and perifosine in treating MCL in mice. No significant differences in mean body weight were observed between drug-treated and control animals during the *in vivo* assay (3-7% of body weight loss in the treated groups *versus* control groups), suggesting a low toxicity exerted by these two ATLs. This observation is in agreement with a previous report showing lack of significant toxicity of edelfosine in a rat model [124].

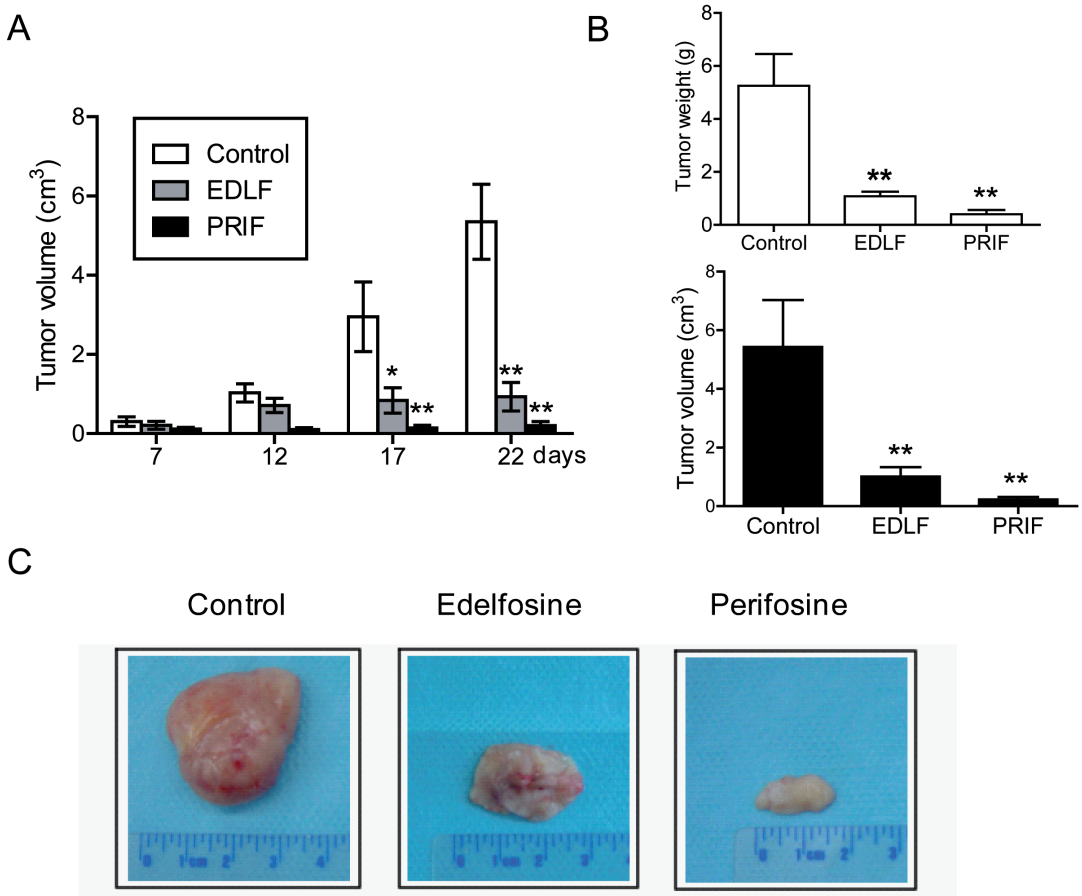

Figure 42. In vivo anti-MCL activity of edelfosine and perifosine. (*A*) CB17-severe combined immunodeficient mice were inoculated subcutaneously with 10^7 Z-138 cells, and once palpable tumors were detected, mice were orally treated with vehicle (control), 30 mg/kg edelfosine (EDLF) and 26.45 mg/kg perifosine (PRIF) for 3 weeks. Tumor size was recorded at the indicated times during drug treatment. (*B*) After completion of the in vivo assay, control mice and animals treated with edelfosine (EDLF) or perifosine (PRIF) were killed, and tumors were isolated and measured (weight and volume). Data in (A) and (B) are shown as mean values±s.d. (n=7). Asterisks indicate significant differences with respect to drug-free control values, at *P<0.05 and **P<0.01. (*C*) A notable reduction in tumor size was observed after edelfosine or perifosine treatment.

5.2.3.8. ATLs induce Akt inhibition and cell death in MCL patient-derived cells

In an attempt to extrapolate the above data to patient-derived cells, primary samples from nine MCL patients (**Table 1**) were incubated for 24 h with the ATLs perifosine and edelfosine at concentrations ranging from 1 to 50 μM, and cell viability was determined by cytofluorimetric quantification of Annexin V-negative cells. LD_{50} values for perifosine and edelfosine were then calculated. As shown in Table 1, we observed a great variability in the capacity of ATLs to promote cell killing of MCL primary cultures, seven out of nine primary cultures being sensitive to ATL concentrations below 20 μM, whereas 2 cases (nos. 8 and 9) were resistant to 50 μM ATL. Concentrations of ATLs as low as 10 μM induced a remarkable cytotoxicity (between 25% and 95%) in most of the patient-derived tumor cells (**Fig. 43 A**).

Table 1.- Characteristics of MCL patients

Patient no.	Age/ Gender[1]	Disease status	% tumor cells*	*P53* status†	Perifosine LD_{50} at 24h (μM)	Edelfosine LD_{50} at 24h (μM)
MCL no.1	64/M	Relapse	95	del/mut	18.2	6.2
MCL no.2	79/M	Diagnosis	85	wt	8.8	6.6
MCL no.3	57/F	Diagnosis	95	wt	3.7	2.1
MCL no.4	81/M	Diagnosis	88	del/mut	7.4	4.0
MCL no.5	76/M	Diagnosis	69	del/mut	7.2	4.1
MCL no.6	77/M	Diagnosis	80	wt	18.5	14.0
MCL no.7	70/M	Relapse	70	wt	13.8	16.8
MCL no.8	76/M	Diagnosis	83	wt	not reached	not reached
MCL no.9	85/M	Diagnosis	85	wt	not reached	not reached

M indicates male; F, female; del, deleted; mut, mutated; wt, wild-type.
*% of CD19 positive tumor cells quantified by flow cytometry.
†*P53* mutational status assessed by fluorescent *in situ* hybridization (FISH) and direct sequencing.

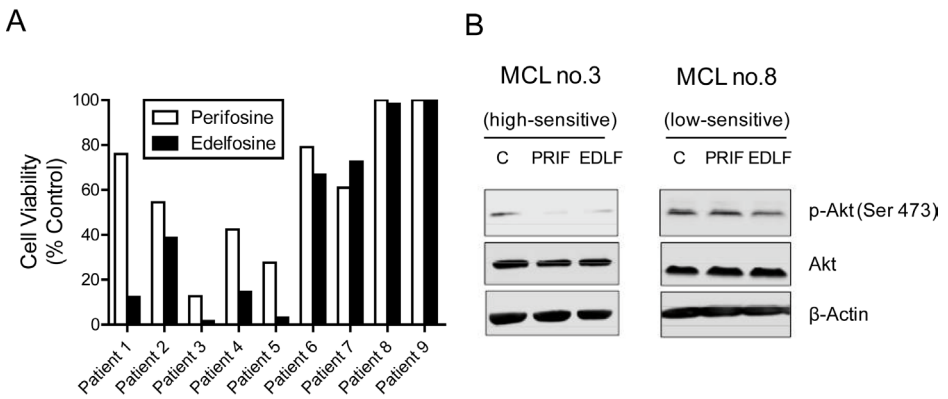

Figure 43. Effect of ATLs on MCL patient-derived cells. (*A*) Isolated primary tumor MCL cells from nine patients were treated with 10 μM perifosine or edelfosine for 24 h. Non-apoptotic cells were quantified as Annexin V-negative cells by flow cytometry, as described in Materials and methods. Untreated controls were run in parallel, and data are represented as percentage of cell viability (means of two experiments) with respect to each untreated control. (*B*) MCL cells derived from patient no. 3, showing high-sensitivity to ATLs, and from patient no. 8, showing low sensitivity to ATLs, were incubated without (control, C) or with 10 μM perifosine (PRIF) or edelfosine (EDLF) for 6 h, and then analyzed by immunoblotting for p-Akt (Ser473) and Akt.

ATL cytotoxicity was closely linked to Akt dephosphorylation, as shown by comparing ATL-sensitive with ATL-resistant MCL cells (**Fig. 43 B**). We also co-cultured primary patient-derived MCL cells with the human bone marrow stromal cell line HS-5, which has been reported to be tumor cell protective against spontaneous and drug-induced apoptosis [125], in the absence or presence of edelfosine or perifosine, and stroma-related protection toward spontaneous and ATL-induced apoptosis was evaluated. About 60-70% of spontaneous tumor cell apoptosis was reversed by MCL co-culture with HS-5 cells, but this value decreased to 25-35% in the presence of perifosine or edelfosine, thus suggesting that the presence of stroma did not prevent the killing of MCL patient-derived cells by ATLs.

5.2.3. Discussion

Here, we have found for the first time the presence of the PI3K/Akt signaling pathway in the lipid rafts of MCL cells, and provide evidence for the critical role of raft-mediated PI3K/Akt signaling in MCL survival. Oral treatment with the ATLs edelfosine and perifosine at an equimolar concentration of 57.3 μmol/kg body weight achieved a strong anti-MCL activity in xenograft animal models, and the killing activity of ATLs was not prevented by tumor microenvironment stimuli. Our findings suggest that a major event in the ATL-induced cell death in MCL cells lies in the displacement of Akt and its upstream regulators PI3K, p-PDK1 and mTOR from lipid rafts. Figure 7 depicts a plausible model for the role of raft-mediated Akt activation in the control of cell survival and in the mechanism of action of edelfosine-induced apoptosis in MCL cells, based on the results reported here. Edelfosine has been shown to accumulate in cholesterol- and sphingolipid-rich rafts, in part due to its high affinity for cholesterol [61,63]. According to our model (**Fig. 44**), the interaction of edelfosine with lipid rafts would launch the following sequence of events leading eventually to apoptosis: edelfosine incorporation into rafts → displacement of Akt and the kinases PI3K, PDK1, and mTOR from rafts → inhibition of Akt phosphorylation → inhibition of Akt substrate phosphorylation → loss of mitochondrial potential → DNA degradation.

Akt pathway has been shown to affect the intrinsic apoptotic pathway through inhibition of pro-apoptotic proteins, by phosphorylation of Bad and caspase-9 on Ser136 and Ser196, respectively [29,126]. Here, we found that incubation of ATLs with MCL cells led to caspase 9 activation, $\Delta\Psi_m$ loss, and ROS production, compatible with

an effect of ATLs on the mitochondrial intrinsic pathway. Because there is an apparent connection between the extrinsic and intrinsic apoptotic pathways through lipid rafts [65,72], the action of ATLs on the intrinsic signaling route could be secondary to the action of ATLs on lipid rafts. Inhibition of PI3K/Akt pathway can induce apoptosis in tumor cells through the recruitment of death receptors to lipid rafts [84]. In this regard, we found that ATL treatment in MCL cells displaced Akt signaling from rafts, while recruited Fas/CD95 death receptor to rafts. Inhibition of Bad phosphorylation by ATLs was detected after rather long incubation times, and was concomitant with the triggering of apoptosis. This raises some doubts on the role of Bad in ATL-mediated apoptosis in MCL cells, either as a cause or consequence in the apoptotic response. In this regard PI3K/Akt-dependent survival in hematopoietic cells has been suggested to proceed independently of Bad phosphorylation [112]. Lipid rafts have been shown to act as scaffolds for the recruitment of Fas/CD95 death receptor and downstream signaling molecules, playing a major role in the killing activity of ATLs against a number of hematological malignancies, including MCL [38,39,64,70]. Thus, the action of ATLs on raft membrane domains leads to the inactivation of Akt survival signaling and activation of death receptor apoptotic signaling. However, we did not detect a statistically significant sensitization of MCL cells to the subsequent agonistic activation of Fas/CD95 receptor. Previous reports have shown a deficient apoptotic response to the external stimulation of Fas/CD95 by agonistic anti-Fas/CD95 antibodies or FasL/CD95L in tumor B cells [127,128]. In this regard, it is interesting to note that unlike the natural ligand Fas/CD95L or agonistic anti-Fas/CD95 antibodies that act through their interaction with the extracellular portion of the Fas/CD95 receptor, edelfosine induces activation of Fas/CD95 from within the cell in a FasL/CD95L independent manner [39,43,75]. In fact, our previous data suggest that edelfosine is even more efficient than FasL/CD95L in promoting apoptosis through Fas/CD95 activation by its recruitment in membrane rafts enriched in downstream signaling molecules [39,43,69,75], leading to the formation of clusters of apoptotic signaling molecule-enriched rafts [39,67,69,72], named CASMERs [42,72,73,80], which could trigger an apoptotic response in the absence of death receptor ligand. Thus, edelfosine could promote Fas/CD95 activation, although the receptor is hardly triggered by its natural ligand or agonistic antibodies. This could explain the herein reported lack of significant further sensitization of MCL cells to FasL/CD95L or agonistic antibodies after edelfosine treatment.

Although ATLs inhibited PI3K/Akt pathway, inducing dephosphorylation of

Akt and downstream substrates, we failed to detect dephosphorylation of GSK3, a typical substrate of Akt, thus suggesting that the raft-mediated PI3K/Akt pathway can act independently of GSK3 in this case. In this context, GSK3 has also been shown to be regulated by phospholipase C/protein kinase C in B cells [129]. The fact that the GSK3 inhibitor lithium potentiates ATL-induced apoptosis further suggests that ATLs act through a GSK3-independent pathway. In prostate carcinoma cell lines, overexpression of myristoylated Akt, which bypasses the requirement for PH domain-mediated membrane recruitment, abrogated perifosine effects [130]. This oncogenic myristoylated Akt has been reported to locate in rafts, displaying no GSK3 affinity and a distinct substrate preference as compared with cytosolic non-raft Akt [48]. Thus, the results reported here suggest that ATLs inhibit raft-mediated Akt that might regulate apoptosis, but not GSK3 phosphorylation. On these grounds, our findings suggest that part of the tumor traits of MCL cells could depend on the raft-located Akt signaling pathway which shows a particular substrate profile, and could be exacerbated by pervanadate-mediated activation. Our data suggest that ATL resistance in MCL seems to be related to raft-dependent Akt activation and overexpression.Specific Akt inhibitors, with different molecular structures and targeting distinct parts of the Akt molecule, reproduced ATL-mediated apoptotic events, suggesting that they target the same Akt signaling crucial for MCL cell survival as ATLs. Interestingly, Akt inhibitor III has a similar structure to edelfosine, but replacing the choline group for inositol (**Fig. 33**). These data further support the involvement of PI3K/Akt pathway in MCL survival.

Because lipid rafts are known to be enriched in PI(4,5)P2 and PI(3,4,5)P3 [131], they provide a permissive milieu for the interaction between PDK1 and Akt. ATLs have been found to accumulate in lipid rafts in a number of hematological malignancies, altering the raft protein and lipid composition [39,69]. Thus, it is tempting to envisage that ATLs might inhibit proteins with PH domains. The levels of PIP2 and Ser473 phosphorylation are more predictors of Akt activation state than Thr308 phosphorylation [112]. In this regard, Ser473 phosphorylation of Akt seems to be more dependent on its location in lipid rafts, and to play a critical role in Akt activation. In fact, Akt Ser473 kinase activity has been identified associated to plasma membrane rafts [132]. These data support the results reported here of a rapid inhibition of Ser473 p-Akt following ATL action in MCL cells, whereas inhibition of Thr308 p-Akt was a secondary effect that required longer ATL incubation times. Likewise, higher levels of

Ser473 p-Akt than Thr308 p-Akt have been shown in mouse lymphoma ATL-resistant cells [133]. Taking together, these data implicate a critical role for lipid rafts in Ser473 Akt phosphorylation in MCL. In this regard, we found a dramatic displacement from rafts of mTOR (**Fig. 38**), which could form the complex mTORC2, suggested to be PKD2, involved in the Ser473 phosphorylation of Akt [113], following edelfosine treatment. Thus, ATLs might inhibit the PI3K/Akt signaling pathway at the very early stages of the route leading to the series of downstream events reported here. Our data highlight raft-mediated PI3K/Akt signaling as a major target in MCL therapy, thus supporting a new raft-mediated strategy for MCL treatment. Inhibition of raft-mediated PI3K/Akt signaling could lead to a decreased apoptotic threshold and to the induction of apoptosis.

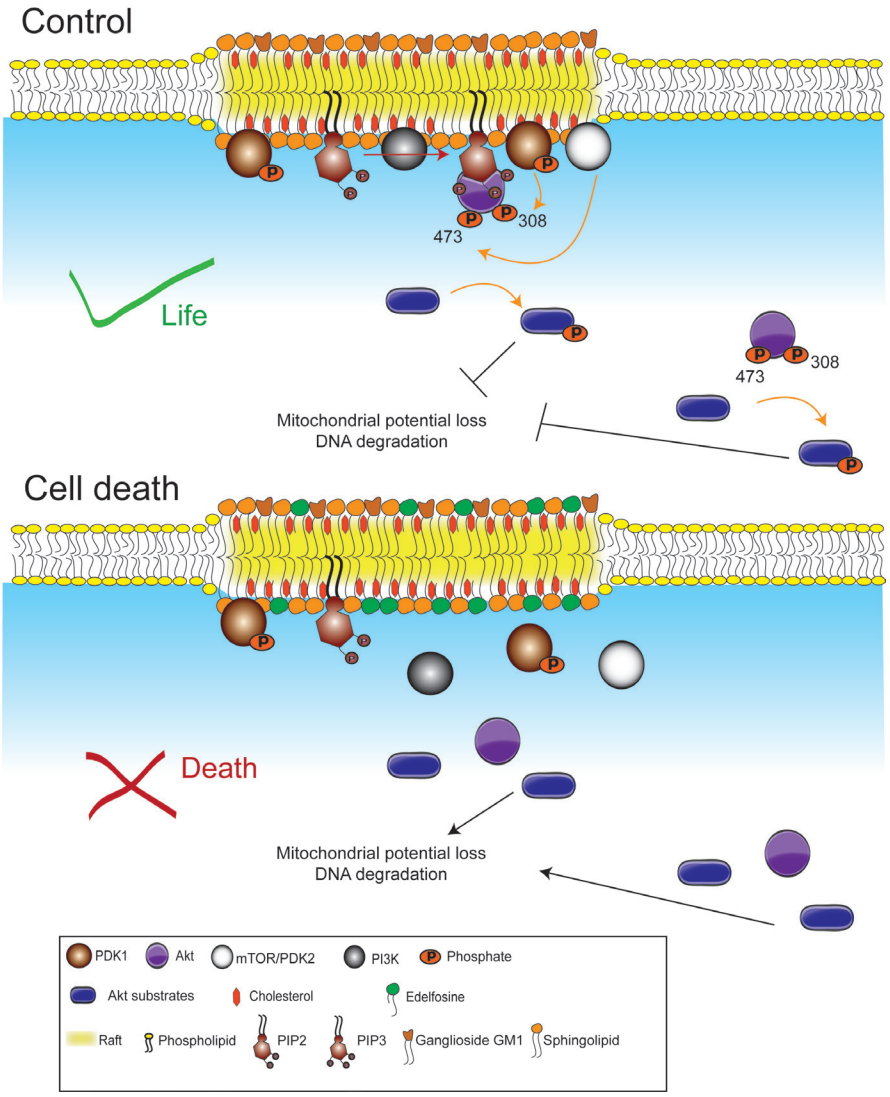

Figure 44. Schematic model of raft-mediated Akt signaling in the regulation of cell survival and death in MCL cells during edelfosine treatment. This scheme highlights the importance of lipid raft membrane domains for PI3K/Akt pathway activation in the regulation of MCL cell survival or death, based on the data reported here. For further details, see the text.

5.3. The antitumor lipid edelfosine in combination therapy for MM

5.3.1. Introduction

MM is characterized by the accumulation of plasma cells in the bone marrow with a low proliferative index, an extended life span and a defective apoptosis [85-87]. With an estimated overall survival rate of 54.4% and an event-free survival of 49.3% after 5 years, MM is still considered an incurable disease [136,137]. At present, treatment for MM focuses on the reduction of tumor growth and the treatment of symptoms [137]. Because resistance to apoptosis may play a crucial role in pathogenesis and resistance to treatment of MM, a therapeutic potential lies in circumventing antiapoptotic signals and/or potentiating apoptosis [87]. The current clinical treatment in MM includes the combination of different agents, which has been shown to improve treatment for MM with rapid progression or aggressive relapse [137,138].

The ATLs, are a family of compounds that target cell membranes and are able to selectively induce apoptosis in tumor cells, including MM cells [58,59,64,69,101]. Edelfosine, considered as the prototype molecule of ATLs, has been shown as the most potent ATL in selectively killing hematological cancer cells *in vitro* and *in vivo*, including MCL, CLL and MM [64,69,70]. Edelfosine shows affinity for cholesterol [61,63], accumulates in lipid rafts and promotes apoptosis by co-capping of Fas/CD95 death receptor and rafts in MM and additional cancer hematological cells [37-39,64,69,70]. The initial studies conducted with edelfosine on lipid raft reorganization have led to consider membrane rafts as a promising novel target for apoptotic induction in hematopoietic cancer cells, as they can act as platforms for the recruitment of Fas/CD95 death receptor and proteins involved in apoptotic signaling [37,39,42,64,67,69,70,73,80,115,139]. In the last few years, increasing accumulating evidence has shown that lipid rafts can be an important target for cancer therapy [8,73,80]. The recruitment and aggregation of death receptors in lipid raft domains also enhance the proapoptoic responses elicited by their death ligands [69]. The mechanism of co-clustering of rafts and Fas/CD95 is also observed after treatment with the death cytokines FasL [140] and CD28 [141,142], suggesting that ATLs could be reactivating a physiological apoptotic mechanism [37,45]. Due to the peculiar action of ATLs in reorganizing rafts and recruiting death receptors and downstream molecules in raft domains, ATLs might be promising agents in combined therapy. They can be used in combination with either conventional therapies or additional anticancer agents promoting cell death. In this regard, have been shown that ATLs

increase cancer cells sensitive to radiotherapy *in vitro* and *in vivo* [56].

This work explores the possibility of using the raft-targeting-edelfosine as an adjuvant chemotherapeutic in MM. Here, we report that edelfosine can be an interesting antitumor drug for combination therapy in the treatment of MM, following its combined use with the proteasome inhibitor bortezomib and histone deacetylase (HDAC) inhibitors. Bortezomib is currently used in clinic, and has significantly improved the response and survival of patients in the last decade [102,143,144]. HDAC inhibitors induce apoptosis in MM cells, show a synergistic effect with proteasome inhibitors and are in clinic evaluation for MM treatment [137,145-149]. In addition, we have found that up-regulation of Fas/CD95 following IFN-γ treatment potentiates the anti-myeloma activity of edelfosine.

5.3.2. Results

5.3.2. 1. HDAC inhibitors induce apoptosis in MM cells by a raft independent mechanism

Here, we found that the HDAC inhibitors SAHA (10 μM) and MS-275 (1 μM) induced apoptosis in the human MM cell lines MM144 and MM1S, as assessed by an increase in the sub-G_0/G_1 population by cell cycle analysis (**Fig. 45 A**). As well as by caspase-3 activation and cleavage of the its typical substrate PARP, using a polyclonal antibody anti-caspase-3 that recognized the active 17-kDa subunit of caspase-3, and an anti-PARP monoclonal antibody that detected both the 116-kDa intact form and 85-kDa cleavage form of PARP (**Fig. 45 B**). We also detected the activation of caspases 8 and 9, measured by colorimetric substrate degradation following HDAC inhibitors treatment (**Fig. 45 B**). The faster and higher activation of caspase-9 rather than 8, after SAHA incubation in time-course analyses, suggested that HDAC inhibitors activated preferentially the intrinsic apoptotic pathway rather than the extrinsic signaling (**Fig. 45 C**).

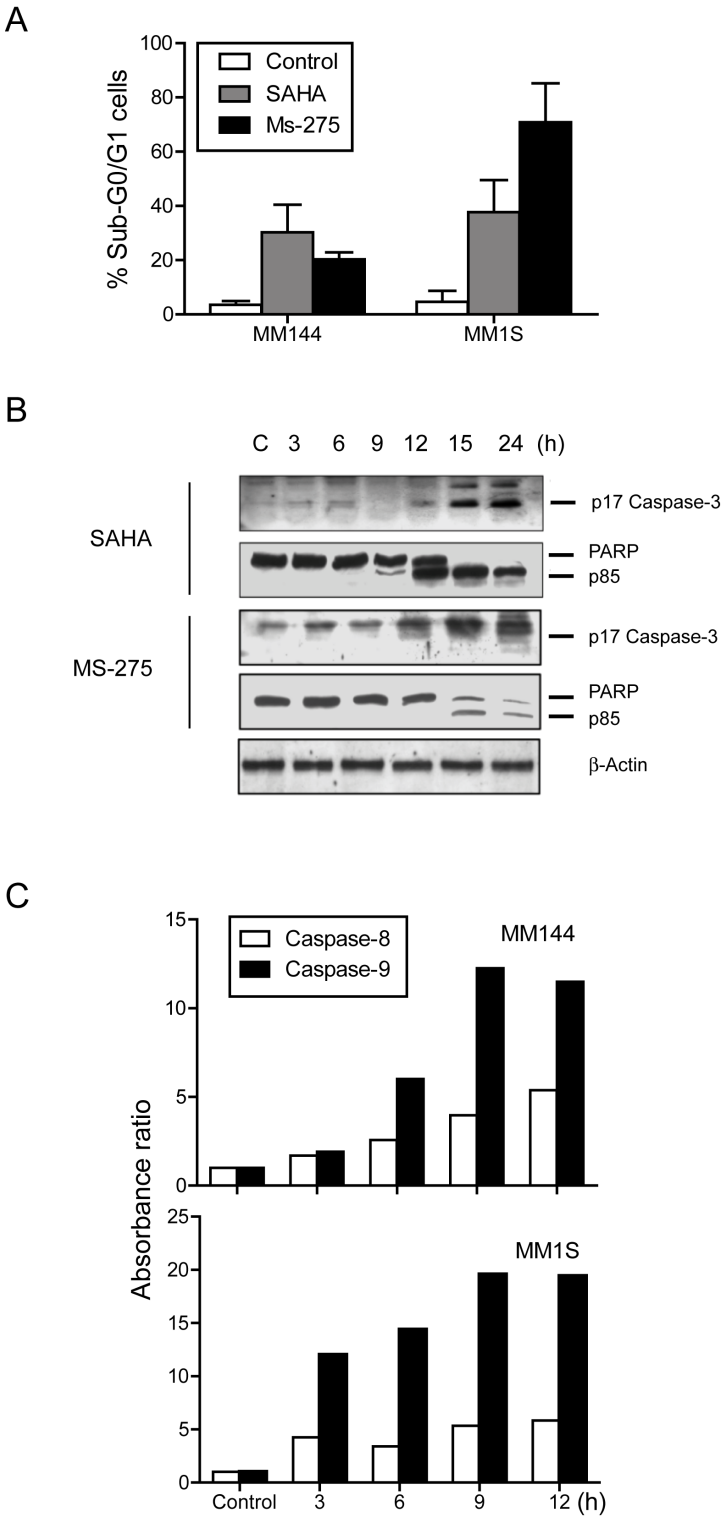

Figure 45. HDAC inhibitors induce apoptosis in MM cell lines. (*A*) MM144 and MM1S cells were untreated or treated with 10 μM SAHA or 1 μM MS-275 for 48 h, and then apoptosis was quantitated as the percentage of cells in the sub-G_0/G_1 region (hypodiploidy) following cell cycle analyses by flow cytometry. Data shown are means ± SD of three independent experiments. (*B*) MM1S cells were untreated or treated with 10 μM SAHA or 1 μM MS-275 for the indicated times and then analyzed by immunoblotting using specific antibodies for the indicated proteins. β-Actin was used for equal protein loading in each lane. Representative blots for three separated experiments are shown. (*C*) Caspase-8 and caspase-9 activities were measured in MM1S cells untreated or treated with 10 μM SAHA at the indicated times by a colorimetric assay described in material and methods. Data shown are means of two experiments performed.

Edelfosine has been reported to induce apoptosis in MM cells through co-clustering of lipid rafts and Fas/CD95 [69,70] . This was further confirmed by the formation of big co-clusters of Fas/CD95 and rafts in edelfosine-treated MM144 cells (**Fig. 46 A**). However, in contrast to edelfosine, neither SAHA nor MS-275 induced rafts and Fas/CD95 co-clustering in MM144 cells (**Fig. 46 A**), as assessed by using specific anti-Fas/CD95 antibody and FITC-CTx B subunit that binds ganglioside GM1 [93], mainly found in rafts [94]. Furthermore, disruption of lipid rafts by MCD, which depletes cholesterol[95], did not inhibit MS-275-induced apoptosis (**Fig. 46 B**), further supporting that HDAC inhibitors-induced apoptosis in MM cells is not lipid raft-mediated.

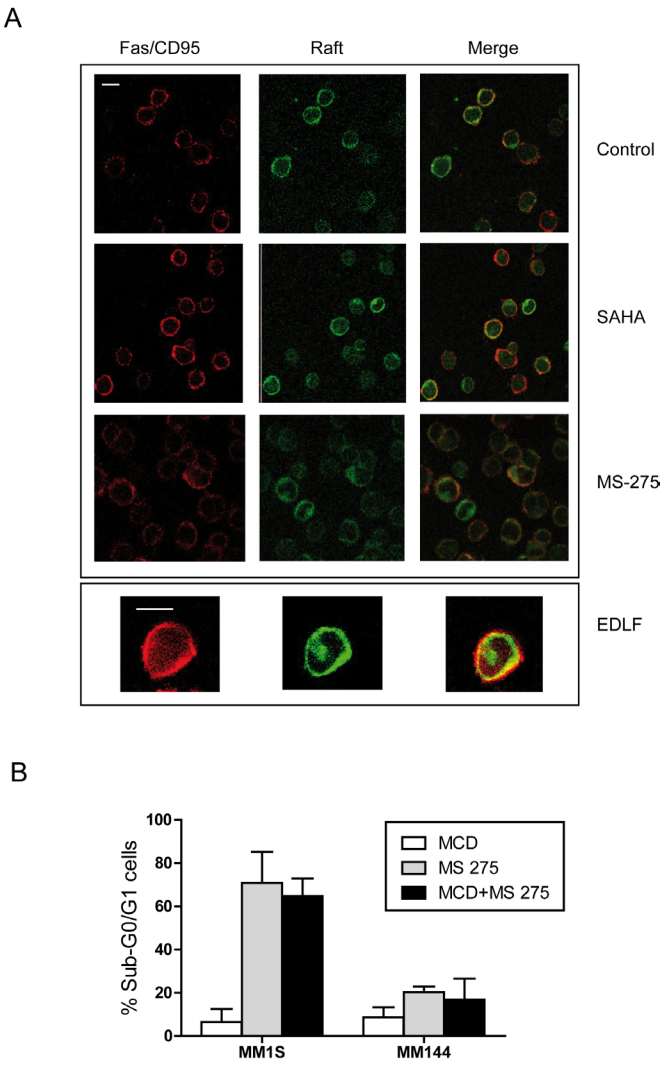

Figure 46. HDAC inhibitors induce apoptosis in MM cells by a lipid raft independent mechanism. (*A*) MM144 cells were either untreated (Control) or treated with 10 μM SAHA and 1 μM MS-275 for 24 h, and then stained with FITC-CTxB subunit to identify lipid rafts (green fluoresce) and specific Fas/CD95 monoclonal antibody, followed by CY3-conjugated anti-mouse immunoglobulin (red fluorescence). Areas of colocalization between membrane rafts and Fas/CD95 in the merge panels are yellow. Images showed are representative of three independent experiments. (*B*) MM1S and MM144 cells were pretreated with 2.5 mg/ml MCD and then incubated with 1 μM MS-275 for 48 h. Percentage of apoptotic cells was then determined by flow cytometry as the percentage of cells at the sub-G_0/G_1 region. Untreated cells showed apoptosis mean values of <5% . Data shown are means ± SD of three independent experiments.

5.3.2.1. Combination of edelfosine and HDAC inhibitors potentiates apoptosis in MM cells

Because edelfosine and HDAC inhibitors seem to act through distinct molecular mechanisms, we tested whether the combination of both types of compounds could potentiate the apoptotic activity against MM cells. By combining low concentrations of edelfosine and HDAC inhibitors compounds, namely 5 μM edelfosine with 5 μM SAHA or 0.5 μM MS-275, we found an increase in the apoptotic response in MM1S cells, as assessed by the an enhancement in the sub-G_0/G_1 population by cell cycle analysis (**Fig. 47 A**). This was clearly supported by the early activation in MM1S cells of caspase-3 and PARP degradation following the co-treatment of MS-275 + edelfosine and SAHA + edelfosine, as compared to the single treatment of HDAC inhibitors or edelfosine (**Fig. 47 B**).

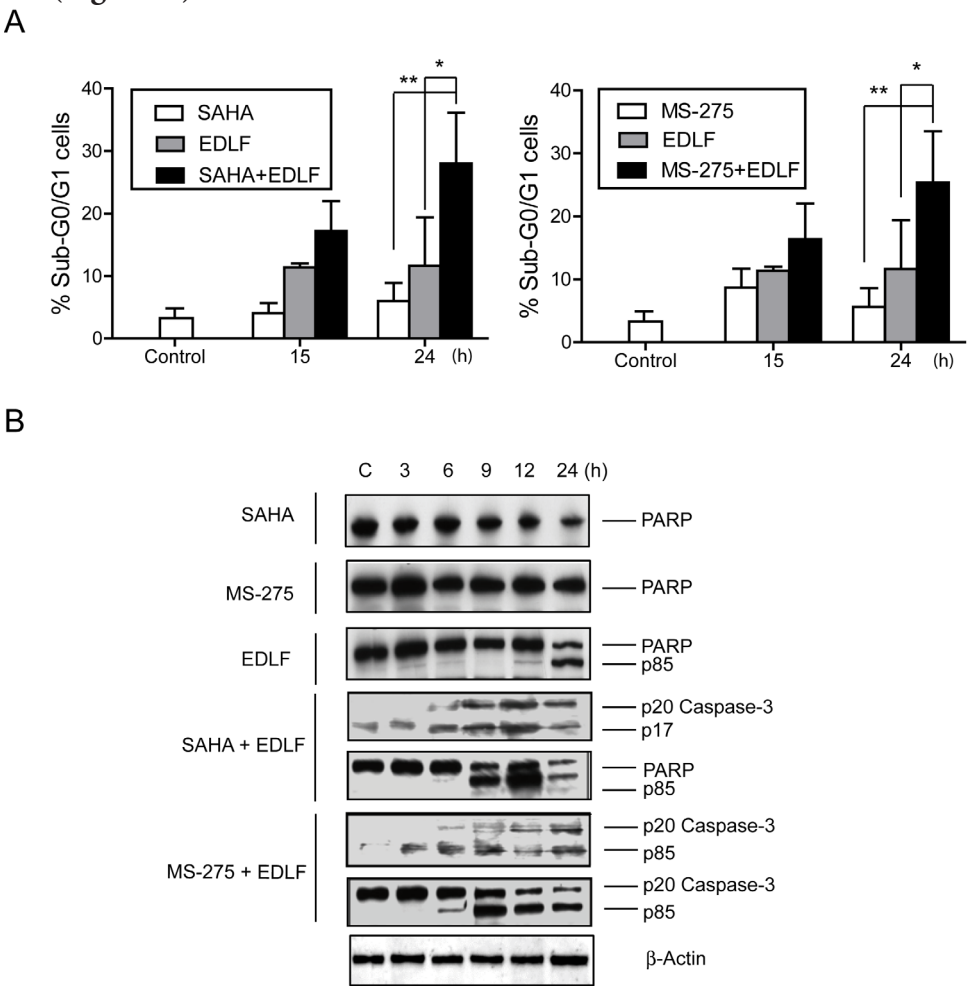

Figure 47. Combination of edelfosine and HDAC inhibitors potentiate apoptosis in MM cells. (*A*) MM1S cells were untreated or treated with 5 μM SAHA, 5 μM edelfosine, 5 μM SAHA + 5 μM edelfosine, 0.5 μM MS-275 or 0.5 μM MS-275 + 5 μM edelfosine for the indicated times, and then apoptosis was quantited by flow cytometry. Data shown are means ± SD of three independent experiments (*, $P < 0.05$; **, $P < 0.01$). (*B*) MM1S cells were untreated or treated with 5 μM edelfosine, 5 μM SAHA, 0.5 μM MS-275, 5 μM SAHA + 5 μM edelfosine or 0.5 μM MS-275 + 5μM edelfosine for the indicated times, and then analyzed by immunobloting for the indicated proteins.

5.3.2.2. Combination of edelfosine with bortezomib potentiates the anti-myeloma activity

Bortezomib induces apoptosis in MM cells through a mechanism of action different of that of edelfosine and independent of Fas/CD95 [145,150,151]. We found that co-treatment of edelfosine and bortezomib highly potentiated the proapoptotic activity exerted by each individual drug against a number of MM cell lines, including MM144, as well as dexamethasone-sensitive MM1S cells and dextamethasone-resistant MM1R cells (**Fig. 48**). Because all the three MM cell lines showed similar percentages of apoptotic cell death (**Fig. 48**), it is suggested that edelfosine + bortezomib treatment circumvents dexamethasome resistance. Since the combined use of edelfosine and bortezomib had a synergistic effect on apoptosis (**Fig. 48**), this combination therapy procedure shows promise in the treatment of MM.

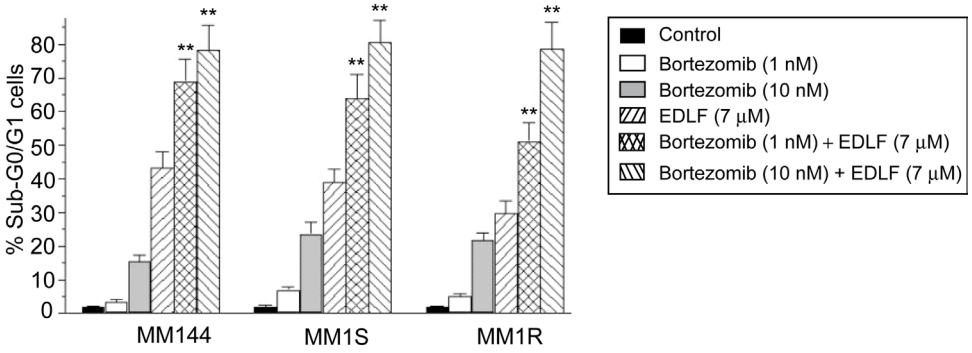

Figure 48. **Synergistic effect of the combination of edelfosine and bortezomib in the killing of MM cells.** MM144, MM1S and MM1R cells untreated or treated with 1 nM bortezomib, 10 nM bortezomib, 7 μM edelfosine (EDLF), 1 nM bortezomib + 7 μM edelfosine (EDLF) or 10 nM Bortezomib + 7 μM edelfosine (EDLF) for 24 h. Apoptosis was then assessed by flow cytometry as the percentage of cells with a DNA content less than G_0/G_1. Data shown are means ± SD of tree independent experiments. Asterisks indicate values that are significantly different from untreated control cells or cells treated individually with edelfosine or bortezomib at $p < 0.01$ (**) level by Student's t-test.

5.3.2.2. Combination of two raft-targeting drugs does not potentiate apoptosis induction

We have previously found that resveratrol promoted apoptosis in MM cells by co-clustering Fas/CD95 and rafts in MM cells [115] in a similar way as edelfosine did[64,69]. Resveratrol was less efficient than edelfosine in the induction of apoptosis in MM cells, and the combination of both agents resveratrol and edelfosine did not significantly increased the apoptotic action of the ether lipid (**Fig. 49**). These data suggest that both drugs induce cell death through a similar raft-mediated process and therefore no significant antitumor action potentiation is observed upon their combined use.

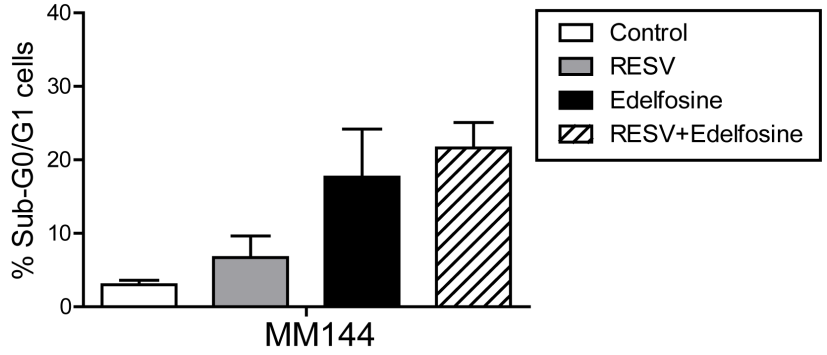

Figure 49. **Combination of resveratrol and edelfosine does not further potentiate apoptosis in MM cells.** MM144 cells were untreated or treated with 10 μM resveratrol, 5 μM edelfosine or 10 μM resveratrol + 5 μM edelfosine, and apoptosis were quantited by flow cytometry as the percentage of cells with a DNA content less than G_0/G_1.

5.3.2.3. INF-γ potentiates edelfosine action in MM cells

Previous reports have shown that pretreatment of tumor cells with INF-γ induced an increase in Fas/CD95 cell surface level, thus potentiating the anticancer action of resveratrol in MM cells [115] and Fas/CD95-FasL/CD95L-mediated apoptosis in allergen-activated T cells [152]. Likewise, here we found that IFN-γ increased the expression of cell surface Fas/CD95 expression in MM144 cells (**Fig. 50 A**), and potentiated edelfosine-induced apoptosis (**Fig. 50 B**). Similarly, IFN-γ pretreatment also enhanced the apoptotic ability of edelfosine in MM1S cells (47% increase).

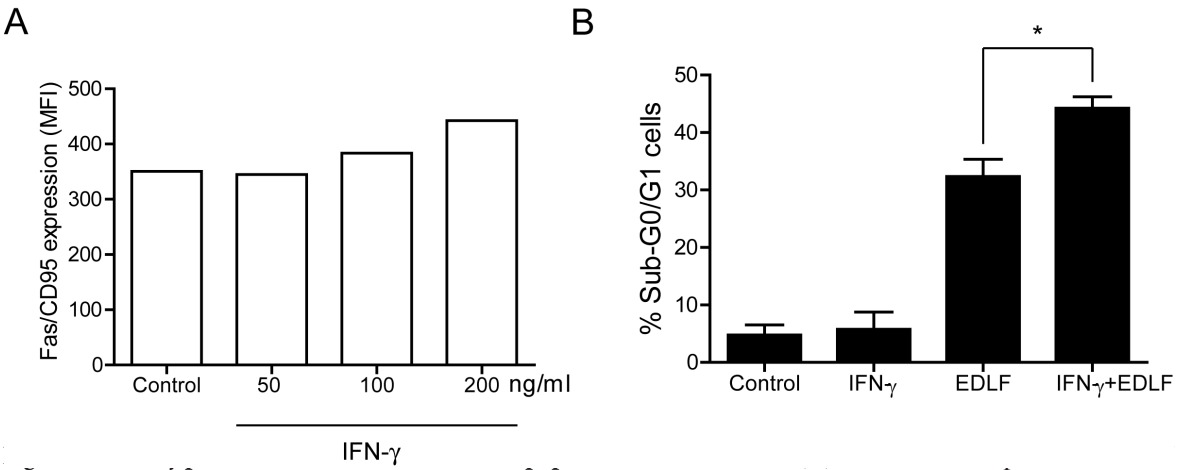

CD95 was determined by immunofluorescence flow cytometry as mean fluorescence intensity (MFI) values in cells untreated (Control) and treated with the indicated concentrations of IFN-γ for 24 h. (*B*) MM144 cells were pretreated with 200 ng/ml IFN-γ for 24 h, and then incubated with 7 μM edelfosine for 48 h. Apoptosis was assessed by flow cytometry as the percentage of cells with a DNA content less than G_0/G_1. Untreated control cells, and cells treated only with IFN-γ or edelfosine were also analyzed for apoptosis. Data shown are means of two experiments performed (A) or means ± SD of tree independent experiments.

5.3.3.Discussion

The data reported here show that bortezomib and HDAC inhibitors can potentiate the action of edelfosine on the killing of MM cells. Interestingly, the combination of bortezomib and edelfosine rendered a synergistic effect, which might be of interest as bortezomib is widely used in the current therapies for MM treatment [102,143,144]. The potentiation of the anti-myeloma activity of the above drug combinations seems to lie in the different mechanisms of action of each drug. Thus, edelfosine-induced apoptosis is mediated by a raft-mediated, whereas bortezomib and HDAC inhibitors mainly use different signaling routes [145,150,151]. This notion is supported by the weak potentiation of the combined use of resveratrol and edelfosine, as both agents have been shown to promote Fas/CD95 and raft co-clustering [64,69,115]. While the combination of edelfosine and bortezomib led to a synergistic effect, the potentiation of the apoptotic activity following the combination of HDAC inhibitors and edelfosine was less dramatic. In this regard, a recent report has shown that MS-275 sensitizes osteosarcoma cells to FasL-induced cell death by increasing the localization of Fas/CD95 in membrane lipid rafts [153]. These authors showed that cholesterol depletion by MCD inhibited the sensitization of cells to FasL, but did not affect MS-275-induced cell killing in osteosarcoma cells [153]. Here, we did not find co-localization of Fas/CD95 and rafts upon HDCA inhibitors treatment in MM cells, suggesting that the intensity of the action of HDAC inhibitors on raft organization might be cell dependent. However, it might be envisaged that the mechanism of action of bortezomib differs more from the mode of action of edelfosine than HDAC inhibitors, thus explaining the synergistic effect of the combined use of bortezomib and edelfosine

ATLs are a family of compounds that do not target DNA but cell membranes, and quickly disseminate to membrane organelles [56,57,65,66,81,82]. Edelfosine is considered the prototype of ATLs and accumulates in membrane rafts of hematopietic cancer cells, including MM cells [64,69]. Membrane rafts function as platforms for recruitment of death signaling proteins, forming the so-called CASMERs [42,73,80,154], from which death signaling is launched. Edelfosine was the first chemotherapeutic agent shown to target lipid rafts in hematological cancers [38,39]. Subsequently, a number of additional antitumor drugs have been shown to promote Fas/CD95 recruitment in lipid rafts [37,80], including cisplatin [78], resveratrol [115], aplidin [42] and the ATL perifosine [69]. On these grounds, it is envisaged that lipid rafts can constitute a major target for cancer therapy [8,37,64,80].

Despite a number of advances in new treatments that improve patient survival, MM is still an incurable disease [154]. ATLs have been shown as promising drugs in killing MM cells [64,69,87], and previous data have indicated that ATLs can circumvent drug resistance in MM. Thus, edelfosine readily induces cell death in MM cells resistant to dexamethasone [69], doxorubicin, melphalan, mitoxantrone, VP-16, cytoxan, and vincristine [155]; and perifosine has been reported to be cytotoxic to MM cells resistant to dexamethasone and melphalan [156]. In addition, ATLs have been shown to be effective antitumor drugs in mouse MM models [64,156]. Perifosine, in combination with bortezomib and dexamethasone, has shown encouraging activity in a multicenter phase I/II trial in relapsed/refractory MM, and a phase III clinical trial is underway [146,157]. We have also found here that IFN-γ upregulated Fas/CD95 cell surface expression and potentiated edelfosine-induced apoptosis in MM cells, further supporting the involvement of Fas/CD95 in the action of edelfosine in MM.

The data reported here suggest that edelfosine might be a valuable drug in combination therapy. Particularly, the synergistic combination of bortezomib and edelfosine might be clinically relevant as bortezomib is currently used in the clinics. Thus, the raft-mediated mechanism of action of edelfosine seems to be an interesting and promising way to potentiate cell death in combination therapy regimens and to circumvent drug resistance.

6. GENERAL DISCUSSION

In this work we provide evidence that rafts can be an important target for cancer therapy. ATLs can use rafts as gateways and then accumulate into the cell. ATLs and resveratrol lead tumor cells to death by recruiting and activating apoptotic signaling in rafts (**Fig. 9)** [37,56,76,77]. The use of MCD can be problematic to assess the role of rafts in Fas/CD95 triggering during ATL or resveratrol mediated-apoptosis. Since cholesterol is essential for raft formation/functionality, MCD interference with rafts can block drug incorporation in cancer cells and for that reason apoptosis could be abrogated [56]. Data obtained with MCD need to be supported with additional experimental approaches because changes in cholesterol levels can lead to pleiotropic effects in cells. MCD assays demonstrate only cholesterol dependence [14,19]. For that reason we additionally used FADD-dominant negative Jurkat cells to unravel the role of Fas/CD95 in resveratrol-mediated apoptosis. FADD-DN cells are specifically unable to trigger Fas/CD95 mediate apoptotic death. Following this approach, we were able to demonstrate that Fas/CD95 pathway is critical for edelfosine [67] and resveratrol-mediated apoptosis in Jurkat cells (**Fig. 15**). In addition, silencing of Fas/CD95 by RNA interference prevented the apoptotic response triggered by edelfosine in Jurkat cells [67], further supporting the involvement of Fas/CD95-mediated signaling in the antitumor action of the ether lipid. Nevertheless, ATLs can induce death in cells lacking Fas/CD95 or other death receptors such as yeast [66] and *Leishmania* [158], suggesting that Fas/CD95 is not a pre-requisite for ATL-induced cytotoxicity. Furthermore, edelfosine induces apoptosis in a number of solid tumor cells through an ER stress response [57,81,82]. Thus, Fas/CD95 not an universal requirement for ATL citotoxicity, and several signaling routes could be involved depending on the cell type context (see **Fig. 51**).

The putative use of the physiological FasL/CD95L as a cancer therapeutic agent is hampered because of its severe liver toxicity [159]. However, ATLs have the potential

to active Fas/CD95 pathway in cancer cells even in the absence of FasL, by promoting death receptor clustering in lipid rafts. In this regard, it has been shown that Fas/CD95 can became activated by proximity leading to a potent apoptotic response [37].

It has been suggested that redistribution of Fas/CD95 into lipid rafts can be a consequence of PI3K/Akt pathway inhibition, since Akt inhibitors lead cancer cells to apoptosis by co-clustering of Fas/CD95 and rafts [84], similarly to what is observed after treatment with resveratrol (**Fig. 9**) and ATLs [38]. In this regard, it is worth to note that one of the reported antitumor mechanisms of resveratrol [160] and ATLs is the inhibition of Akt pathway (**Fig. 28**), suggesting a relationship between Akt inhibition and Fas/CD95 redistribution. An increased Akt activity can lead to JNK suppression, through a direct interaction of Akt with JIP-1 (c-Jun-amino-terminal kinase-interacting protein-1) a JNK interacting protein [28,161-163] . This can be related with our data on edelfosine-treated MCL cells, where JNK phosphorylation was increased whereas Akt phosphorylation levels decreased (**Figs. 28 and 31**). JNK activation has been also related with death receptor mediated apoptosis[37], and edelfosine is a potent inducer of persistent JNK activation [118].

Taking together all data, it seems plausible to suggest that ATLs have multiple targets in cancer cells. They can induce ER stress, inhibit PC synthesis, inhibit survival/proliferation pathways (Akt and ERK) and activate intrinsic and extrinsic apoptotic pathways. Interestingly, ATL and lipid accumulation in membranes can lead to stress responses promoting special damage of metabolizing lipid organelles such as ER and probably mitochondria. A kind of cell death called lipoptosis can be triggered [22], and some similarities can be found between this kind of cell death and ATL-induced death in solid tumors as ATLs are synthetic lipids. ATL incubation triggers an ER stress apoptotic response in solid tumors [81,82]. During lipoptosis, the generation of ROS inactivates phosphatases leading to persistent activation of JNK [164] which in turn it has been described in many cancer cells after ATL-incubation [37]. ROS generation can also promote apoptosis by upregulation of Fas/CD95 and FasL/FasC95L [22]. In this regard, ATL incubation has been shown to generate ROS in cancer cells [71]. Additional work is needed to understand the putative role of ROS in ATL-induced apoptosis and Fas/CD95-raft co-clustering. Figure 51 summarizes the major pathways that ATLs can target in cancer cells.

Interestingly, we observed an increased in ERK phosphorylation levels, instead inhibition, in MCL cells at early ATL incubation times (**Fig. 31**). This could be explained

in part by a possible compensatory mechanism due to the ATL-induced inhibition of Akt signaling. However, it is also tempting to speculate that, similarly to what happens with Akt/PI3K signaling proteins, MAPK upstream molecules or receptors could also be displaced from rafts by the action of ATLs, thus leading to activation. This is consistent with the finding that the kinase activity of epidermal growth factor receptor (EGFR) is suppressed when associated with lipid rafts. It has been proposed that EGFR migration out of rafts allows changes in the structural configuration of the receptor promoting its phosphorylation and leading to the stimulation of ERK and JNK signaling pathways [1,165]. ATLs displace proteins from MCL rafts and it could be envisaged that this process does not occur in a specific way for proteins only from the PI3K/Akt signaling pathway.

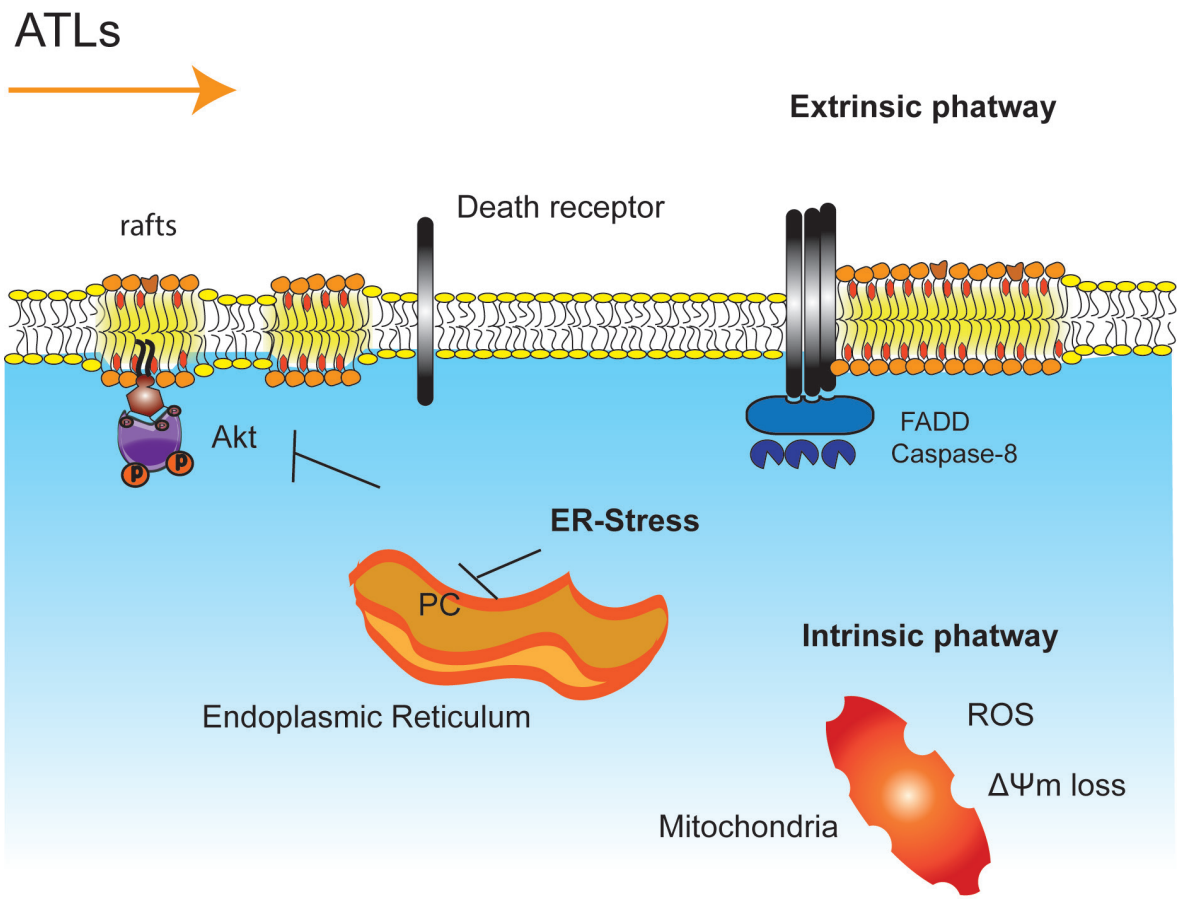

Figure 51- ATL mechanism of action is cell-type dependent. ATLs are able to activate a number of processes that eventually lead to cell death, namely: activation of apoptotic extrinsic, death receptor-mediated, and intrinsic, mitochondria-mediated, signaling pathways; induction of ER stress response together with inhibition of PC synthesis; and inhibition of survival pathways (Akt in the figure). ATL incubation can lead to the activation and recruitment of death receptors and apoptotic signaling (forming the so-called CASMER) into lipid rafts.

Cancer cells can become "addicted to" some oncogenes [166]. For that particular reason, cancer cells might undergo apoptosis by targeting one gene or a signaling route. Because of that, cancer cells may be more dependent on the activity of specific oncogenes and more sensitive to certain growth-inhibitory effects [166]. This could explain the fact that the inhibition of a single signaling pathway in MCL can lead cells to apoptosis (**Figs. 28 y 33**).

Statins and cholesterol-depleting agents can inhibit Akt signaling in rafts [48,49,51]. Our data suggest that ATLs can also target Akt activation in rafts on Ser473 phosphorylation being the most affected phosphorylation residue. Akt can become activated in other non-raft localizations in of cell membrane depending on the stimulus [34]. On these grounds, it is tempting to speculate that MCL cells are dependent on raft environment for Akt activation, and thereby MCL cells are sensitive to ATL therapy (**Fig. 38**). Our data support the notion that PDK2 activation is raft dependent [50], as the levels of p-Akt (Ser473) are rapidly decreased after ATL incubation. Consistent with our results on the critical role of Akt for MCL cell survival, it has been reported that ATL-resistant mouse lymphoma cells lack phosphoinositide phosphatase SHIP-1, a known regulator of the Akt survival pathway [135].

Edelfosine has affinity to cholesterol [61,63], and its saturated acyl chain probably facilitates its raft incorporation and subsequent internalization to intracellular membranes. In fact, edelfosine has been reported to locate in intracellular organelles, such as ER [57,81,82] and mitochondria [65]. *In vivo* experiments have shown that edelfosine biodistribution is spread over several organs [167], but when a tumor was present, edelfosine accumulates in the xenograft tumors [64]. The fact that edelfosine accumulates in the tumor tissue rather than in liver and kidney suggests that is affinity for cholesterol cannot explain by itself its selectivity for cancer cells, as liver and kidney are organs enriched in cholesterol. Additional alterations in the tumor lipid profile as well as in certain proteins are probably the underlying basis for edelfosine selectivity for tumor cells [8,59]. The selective mechanism of ATLs uptake remains to be fully understood.

As mentioned above ATLs target cell membranes of cancer cells rather than DNA. For that reason ATL-incubation can have a synergistic or additive effect in combination with conventional chemotherapy that usually target DNA. ATLs sensitizes tumor cells to radiotherapy [56,168]. Despite the promising potential of these compounds, the only clinical applications until now for ATLs in cancer therapy are purgation of leukemic cells from bone marrow before transplantation, and treatment

of skin metastasis in breast cancer and cutaneous lymphoma. So far, ATL clinical trials have not reveled an advantage of ATL therapy as compared to conventional therapies [56,58]. However, the use of nanoparticules to deliver the drug seems to improve bioavailability and decrease toxicity [169,170]. Furthermore, treatment with perifosine or edelfosine does not damage normal cells from bone marrow, which is one of the main adverse effects of conventional cancer therapy [38,56]. In addition, the date presented here indicate that edelfosine could be a promising anticancer drug for combination therapy, in particular combination of edelfosine and bortezomib for MM.

Recently, it has been reported that ATLs disrupt lipid rafts using model membranes [171]. It may look contradictory, but previous studies have shown that when rafts cluster to form bigger platforms they become unstable, and then endocytosis occurs and raft constituents are recycled back to the plasma membrane [19]. Nevertheless, it could be also argued that rafts do not behave in model membranes the same way as in living cells.

Due to technical limitations related to lipid raft isolation, it is not possible to discriminate between rafts from plasma membrane and those from intracellular organelles. In spite of plasma membranes are especially enriched in cholesterol as compared to other membranes from intracellular organelles, rafts have been reported in additional organelles such as mitochondria, Golgi and ER, despite being less studied due to these technical limitations [13,65,165,172]. In this regard, we cannot ensure that Bid and JNK are plasma membrane located after ATL or resveratrol treatment, since those proteins have been found in other intracellular organelles that might contain putative raft domains. New approaches are needed to discriminate between intracellular and plasma membrane rafts.

The results reported in this work suggest that lipid rafts can be an important target for cancer therapy. As shown here, raft-targeting drugs can induce apoptosis through PI3K/Akt inhibition and death receptor activation; and additional evidence also suggests that they could prevent metastasis [18].

7. CONCLUSIONS

1- Resveratrol induces apoptosis in MM and T-cell leukemic cell lines by a raft- and Fas/CD95- dependent mechanism, inducing co-clustering of rafts and Fas/CD95 as well as recruiting downstream apoptotic signaling molecules into rafts.

2- ATLs displace PI3K/Akt signaling proteins from lipid rafts in MCL cell lines, leading to apoptosis. Akt phosphorylation at Ser473 takes place mainly in lipid rafts and is critical for MCL cell survival.

3- Microenvironment stimuli do not prevent ATL-induced apoptosis. Sensitivity of MCL cell lines and primary cultures to ATLs is highly dependent on the basal Akt phosphorylation level of the cells.

4-Taking together, the data reported here support the involvement of lipid rafts as a promising target in cancer therapy, by regulating survival and death signaling pathways.

5-This raft-targeted therapy seems to be promising also for combination therapy, especially through its combination with bortezomib in hematopoietic cancers, such as T-cell leukemia and MM, rendering synergistic effects.

8. SPANISH SUMMARY

Lipid rafts como dianas terapéuticas en el tratamiento del cáncer

8.1. Introducción

8.1.1. Colesterol y cáncer

La continua proliferación de las células tumorales implica una gran demanda de síntesis de los componentes lipídicos que forman parte de la membrana, siendo el colesterol uno de esos componentes esenciales. A principios del siglo XX se observó que tanto en las células tumorales, como los tejidos adyacentes, acumulan mayor cantidad de colesterol que los tejidos normales de donde derivan [2,3] (**Fig. 1 A and B**). Sin embargo, a día de hoy todavía no está claro si la acumulación de colesterol en los tejidos es la causa o la consecuencia de la aparición de neoplasia [4]. Algunos estudios epidemiológicos apuntan a que el nivel de colesterol está asociado con el grado de malignidad tumoral. Así, el uso prolongado de estatinas (fármacos que reducen el nivel de colesterol) puede estar asociado con la prevención de ciertos tipos de tumores, sugiriendo estos datos que la acumulación de colesterol en los tejidos podría estar contribuyendo a la aparición de un estado tumoral maligno [5,6,9] .

El aumento de colesterol en las células tumorales se debe a irregularidades en diferentes mecanismos de biosíntesis y metabolismo de este lípido, Así, se ha observado: 1- aumento endógeno de la biosíntesis de colesterol, como consecuencia del aumento de la actividad de la enzima HMG-CoA-reductasa (*3-hydroxy-3-methylglutaryl CoA-reductase*), enzima perteneciente a la vía metabólica del mevalonato; 2- mayor *uptake* de colesterol exógeno, debido a la sobreexpresión de receptores de lipoproteínas LDL

(*low-density lipoproteins*), transportadores de colesterol en el torrente sanguíneo a los diferentes tipos celulares; 3- aumento de la actividad de la enzima ACAT (*acyl-coenzyme A:cholesterol acyltransferase*), que promueve el almacenamiento intracelular de colesterol; 4- Menor flujo de colesterol desde la célula, mediado por el receptor de lipoproteínas HDL (*high-density lipoproteins*) [9] (**Fig. 1 C**).

En condiciones normales, el colesterol es fundamental para la configuración de pequeños dominios en la membrana celular. El colesterol regula la organización lipídica promoviendo la segregación de los diferentes tipos de lípidos. Posibilita la organización de las cadenas acilo de los fosfolípidos formando plataformas más estables y rígidas en la membrana plasmática, estructuras conocidas por *lipid rafts* [4,7] (**Fig. 2 B**).

8.1.3. Lipid rafts

8.1.3.1. Historia

Las membranas celulares están compuestas de una amplia variedad de lípidos, todavía no identificados en su totalidad [12]. La membrana plasmática fue inicialmente definida como un *mar de lípidos* donde flotaban las proteínas que asumían el papel principal en la señalización. Este modelo fue conocido por el nombre de *mosaico fluido* o de Singer y Nicholson[13,14] (**Fig. 2 A**). Hoy se sabe que las membranas celulares no están desordenadas, sino compartimentadas en múltiples dominios con funciones especializadas [6]. En el año 1997 Kai Simons y Eliana Ikonen postularon el modelo *lipid raft* (**Fig. 2 B**), en el cual se defendía la existencia de pequeños dominios ricos en colesterol en la membrana celular [16]. Esta hipótesis fue desarrollada basándose en estudios de polaridad de membrana en células epiteliales (diferente composición lipídica en la parte apical y basolateral de la membrana) y en el comportamiento de mezclas lipídicas en membranas artificiales (segregación entre fases liquidas-ordenadas (L_o) y liquidas-desordenadas(L_d)) [14,16,17,19]. La función de estos *lipid rafts* estuvo en primer lugar asociada al transporte de ciertos componentes de las membranas y señalización celular [12,16].

8.1.3.2. Caracterización de los *lipid rafts*

Aunque los *lipid rafts* son más abundantes en la membrana plasmática también

se encuentran en orgánulos intracelulares. La caracterización de los dominios *rafts* ha estado envuelta en una gran controversia durante muchos años por las limitaciones técnicas empleadas en su estudio [12-14,17]. De hecho, se creía que se trataba de un artefacto ya que la resolución de los microscopios convencionales no permitia su detección sin recurrir a estímulos exógenos que conllevaban a la formación de plataformas-*raft* [14].

Los *lipid rafts* son muchas veces referidos en la literatura como dominios líquidos-ordenados o porciones de membrana resistentes a detergentes (DRMs). Las fases líquidas ordenadas fueron descritas en membranas artificiales y normalmente se emplea ese término en ese contexto; las DRMs son membranas aisladas que resultan insolubles en detergentes no-iónicos. De hecho, esta es la técnica más utilizada para el aislamiento y estudio de los *rafts*. Sin embargo, los DRMs no solo contienen *lipid rafts* sino tambíen agregados raft o plataformas-*rafts* y dominios caveola [12,14,19] (**Fig. 3**). Los dominios caveola se caracterizan por la presencia de la proteína caveolina las plataformas-*raft* se forman durante procesos de señalización, por ejemplo durante la sinapsis inmunológica. En términos de distribución parece que los *lipid rafts* son ubicuos en los diferentes tipos celulares; por el contrario, los dominios caveola son más abundantes en células musculares, endoteliales, adipocitos y fibroblastos. Las propiedades biofísicas de ambos dominios son similares y es posible que los *lipid rafts* reemplacen la función de los caveola en células en que éstos últimos no estén presentes [6,8,13,20,23].

8.1.3.3. Redefinición de los dominios raft y su función en la célula

Las técnicas de alta resolución *single particle tracking* (SPT), *single fluorophore video tracking* (SFVT), *fluorescence resonance energy transfer* (FRET) y homo-FRET han permitido la detección de los dominios *rafts* antes de la formación de las plataformas células vivas. Teniendo en cuenta los últimos datos obtenidos con estas técnicas, los *lipid rafts* se definen en la actualidad como dominios ordenados de agregados lípido-proteicos, altamente dinámicos, ricos en colesterol y esfingolípidos, de tamaño nanoscópico en reposo, que una vez estimulados pueden formar plataformas visibles en microscopios convencionales. Estas plataformas-*raft* se mantienen más estables mediante interacciones específicas entre lípidos y proteínas [14]. Son estructuras organizadas y especializadas en señalización, endocitosis, exocitosis, transporte de membranas y están también implicados en la infección viral [13,14,19].

8.1.3.4. ¿Cómo son seleccionadas las proteínas para los dominios *rafts*?

Muchas proteínas parecen asociarse de forma transitoria a los *lipid rafts* en respuesta a diferentes estímulos tanto intra como extracelulares. Esta segregación física de las proteínas puede regular el acceso de las mismas a otras proteínas efectoras y reguladoras. Esta localización de complejos proteicos en los *rafts* parece asegurar la transmisión de señales [13,19]. No se conoce todavía el mecanismo exacto por el cual las proteínas son seleccionadas en los *lipid rafts*. La hipótesis de los *lipid shells* o de las "capa/coberturas de lípidos" propone que las proteínas destinadas a los *rafts* estarían envueltas en una "cobertura de lípidos" que les conferiría especial atracción para los *lipid rafts* donde se fundirían. Sin embargo existe otra hipótesis que dice que las proteínas pueden estar funcionando como surfactantes que ayudan a estabilizar los *lipid rafts*, localizándose por lo tanto en los márgenes de estos dominios [19].

Existen otros factores que parecen condicionar la asociación de las proteínas a los *rafts*. El mismo colesterol, que al inducir un aumento del grosor de los dominios *raft* en comparación con locales de la membrana no-*raft*, excluiría las proteínas con dominios transmembrana muy cortos [4,12,13]. Existen, además determinadas modificaciones lipídicas en las proteínas ("colas hidrofóbicas") que condicionan la localización de las mismas en la membrana. Por ejemplo, las proteínas con anclajes de GPI (*gycosylphosphatidylinositol*) y las proteínas miristiladas o palmitoiladas tienen especial preferencia por los *rafts*, una vez que sus "colas hidrofóbicas" son cadenas acilo saturadas que promueven la asociación a los *rafts*; mientras que proteínas con "colas" insaturadas isoprenil se localizan de forma preferente en dominios no-*raft* (**Fig. 4**) [4,13,24].

Los dominios *raft* están involucrados en la señalización de numerosas rutas. Por lo tanto analizaremos en el siguiente apartado su papel en la señalización de la ruta de supervivencia/proliferación PI3K/Akt, y de la ruta muerte programada mediada por el receptor Fas/CD95. Posteriormente interpretaremos el efecto citotóxico de fármacos que interfieren con los *rafts* de las células tumorales, en función de estas rutas de señalización.

8.1.4. *Rafts* y señalización

8.1.4.1. Ruta de señalización de Akt

Akt tiene múltiples sustratos, cuyas funciones se relacionan directamente con

la proliferación y con el bloqueo de la apoptosis [26,27]. La ruta de Akt se encuentra sobreactivada en una gran cuantidad de tumores, favoreciendo la progresión de los mismos. Akt tiene un dominio PH que le confiere especial afinidad por los inositoles de membrana donde se ancla y se activa. En algunos tumores se ha observado una mutación en este dominio que conduce a una continua asociación de Akt con la membrana, resultando en una activación constitutiva de la proteína [27-30].

Las membranas plasmáticas de las células tumorales poseen una grand cantidad de dominios *raft*. Los dominios *raft* no solo son especialmente ricos en inositoles, factores clave para la activación de Akt [30-33], sino que además se han detectado algunas quinasas, como PI3K, mTOR y PDK1 [30,32,34], reguladoras de la ruta de Akt. Por último y reforzando la hipótesis de que los *rafts* están implicados en la protección del complejo proteico involucrado en la activación de Akt, recientemente, se ha podido detectar detectar *in vivo* el reclutamiento de Akt en *rafts* [30,32,34].

8.1.4.2. Ruta de señalización de Fas/CD95

La muerte celular programada o apoptosis, puede ser llevada a cabo por la activación de una ruta intrínseca, mediada por la mitocondria y/o por una ruta extrínseca, en la cual están implicados los receptores de muerte [35]. Uno de los receptores de muerte más importantes es el Fas/CD95, y su activación es necesaria para eliminación de células transformadas o con infecciones virales [36]. Fas/CD95, su ligando natural (FasL) así como otros receptores de la familia TRAIL (*tumor necrosis factor-related apoptosis-inducing ligand*) pueden palmitiolarse y esta "cola hidrofóbica" parece conferirles afinidad por los *rafts* [22,33,46]. De hecho, varios trabajos han detectado que los *lipid rafts* son importantes para la activación de Fas/CD95, ya sea inducida por su ligando, FasL[36,40,41] o por fármacos quimioterapéuticos [38]. Algunos de estos fármacos tienen la capacidad de inducir la distribución de Fas/CD95 en *rafts* de células tumorales conduciendo por lo tanto la apoptosis de la célula tumoral [35,37,38,44,45].

En el siguiente apartado se discute la posibilidad de utilizar como diana los *lipid rafts* en la terapia del cáncer, a través de fármacos que modulan los níveles de colesterol, u otros, cuya especial afinidad por *rafts* promueve la formación de plataformas-*raft* y el reclutamiento de la señalización apoptótica.

8.1.5. Modulación de *rafts* en células tumorales

8.1.5.1. Modulación de la ruta de Akt mediante alteración de los níveles de colesterol por estatinas y agentes quelantes

La manipulación del contenido de colesterol en una célula tumoral regula la supervivencia celular. Así, la reducción de los níveles de colesterol, ya sea inhibiendo su síntesis mediante el empleo de estatinas, o mediante su secuestro de la membrana por agentes quelantes de colesterol, provoca la muerte de algunos tipos de células tumorales [31,49-52]. La falta de colesterol, llevaría a la desconfiguración de los *rafts,* y con ello la inhibición del anclaje y activación de Akt [31,49-52].

Por otra parte, los niveles elevados de colesterol en circulación pueden promover el crecimiento tumoral en modelos animales de cáncer de próstata. Se detectó en este contexto, que en las células tumorales de animales con dietas ricas en colesterol ocurría una expansión de los *lipid rafts*, asociada a un aumento de la actividad de la proteína Akt.

La fosfatasa supresora de Akt, PTEN (*phosphatase and tensin homolog*), se encuentra mutada en muchos tumores, lo que se relaciona comúnmente con la activación constitutiva de Akt. Sin embargo, los trabajos referidos, indican que utilizando estatinas o quelantes de colesterol es posible inhibir la actividad de Akt, aun cuando la fosfatasa usptream Akt se encuentre suprimida [48,49,51] (**Fig. 5 A**).

Una vez localizada en los *lipid rafts,* Akt parece tener afinidad por sustratos diferentes a los que tiene en zonas no *raft*. La funciónde Akt en *rafts* parece estar relacionada con señalización anti-apoptotica y con la síntesis de componentes lipídicos pertenecientes a los *rafts*, como es el caso del colesterol. De esta forma, Akt tendría un feedback positivo, promoviendo su propia activación vía *rafts* [48,53] (**Fig. 5 B**).

8.1.5.2. Alquilfosfolipidos antitumorales (APLs) o lípidos antitumorales (ATLs)

Los ATLs son análogos metabólicamente estables de la fosfatidilcolina, sus propiedades antitumorales *in vivo* e *in vitro* fueron primeramente descritas por Munder y colaboradores [54,55]. Estos compuestos tienen como diana la membrana de las células tumorales, no el ADN, como la mayoría de los quimioterapéuticos. Su estructura les permite una fácil incorporación en la membrana y poseen especial afinidad por el colesterol. Esta afinidad lleva a que estos compuestos que hace que se localicen preferentemente en los *rafts* [37,39,56,57,61,63,64].

8.1.5.3. Mecanismo de acción de los ATLs en tumores hematológicos

El mecanismo de acción de los ATLs sobre las células tumorales es a través de la activación de la vía apoptótica. En concreto, se conoce que en tumores hematológicos, los ATLs actúan a través de la activación y reclutamiento del receptor Fas/CD95 en plataformas *raft,* de forma independiente de su ligando natural (FasL/CD95L). Además de Fas/CD95, el tratamiento con ATLs provoca la detección de otras proteínas apoptóticas que median la señalización *downstream* de este receptor. Algunas de estas proteínas incluyen a FADD (*Fas-associated death domain-containing protein*) y a procaspasa-8, que junto al receptor Fas/CD95 forman el complejo DISC (*death-inducing signaling complex*). Este *cluster* de proteínas apoptóticas en *rafts* ha sido llamado CASMER (*cluster of apoptotic signaling molecule-enriched rafts*), y su formación está relacionada de manera directa con la muerte celular de distintos tipos de canceres hematológicos [37-39,56,73] (**Fig. 6**).

La formación de CASMERs no parece ser un mecanismo exclusivo inducido por los ATLs, sino también por otros compuestos, como el resveratrol, aplidina o anandamida, entre otros; tratándose por lo tanto de un mecanismo apoptótico común a distintos compuestos antitumorales [37,73,76,77,79,173].

En los últimos años, se ha establecido una relación directa entre la acumulación de colesterol en tumores, la expansión de dominios *raft* y la activación de rutas relacionadas con la proliferación y supervivencia tumoral. Estos datos indican que los *lipid rafts* pueden estar implicados en procesos de tumorigénesis. Por ello, nos propusimos analizar el mecanismo de acción de compuestos antitumorales cuya acción citotóxica parece relacionarse con cambios en el contenido proteico de los *raft*; utilizando como modelo de estudio líneas celulares de mieloma múltiple (MM), leucemia de células T y células de linfoma de manto (MCL). Estas líneas se caracterizan por poseer defectos en las rutas apoptóticas y por carecer de una terapia efectiva [85,86,64,87].

En primer lugar evaluamos la implicación de los *raft* de membrana y del receptor Fas/CD95 en la apoptosis mediada por el resveratrol, en células de MM y leucemia de células T. Utilizamos el resveratrol un compuesto natural que ha demostrado tener propiedades antitumorales en células hematológicas [92] , activando mecanismos de muerte que implican a los rafts [76,91]. Con el objetivo de encontrar una posible aplicación terapéutica combinamos compuestos cuyo mecanismo de acción

implica a los *rafts* (resveratrol y edelfosina) con otros compuestos de interés clínico en el tratamiento de las referidas enfermedades hematológicas (bortezomib, perifosina y interferón gamma) [137,145,146,87].

Además, utilizamos células de MCL, en las cuales se ha descrito anteriormente la implicación de los dominios *rafts* en la acción antitumoral de los ATLs [70]. En estas células la vía de Akt se encuentra constitutivamente activada y es fundamental para su supervivencia, incluso se ha discutido anteriormente la posibilidad de inhibir esta vía como medida terapéutica [110,111]. Este modelo permite estudiar la ruta de activación de Akt y su relación con los *rafts* [34,114] en los procesos de muerte inducidos por ATLs.

8.2. Objetivos:

1. Conocer la implicación de los *lipid rafts* y del receptor de muerte Fas/CD95 en la citotoxicidad inducida por resveratrol en células de mieloma múltiple (MM) y leucemia de células T.

2. Caracterizar el papel de los *lipid rafts* en la activación de Akt y en la muerte inducida por ATLs en celulas de linfoma de manto (MCL).

3. Evaluación *in vitro* de una terapia combinada entre moléculas cuyo blanco son los rafts (Resveratrol y ATLs) + moléculas que no interfieren con los *rafts* (bortezomib, inhibidores de histona deacetilasas, interferón gamma (IFN-γ))

8.3. Resultados y discusión

8.3.1. La acción apoptótica del resveratrol sobre células de mieloma múltiple y de leucemia implica a la mitocondria y el reclutamiento de Fas/CD95 en *lipid rafts*

8.3.1.1. El resveratrol induce apoptosis en líneas celulares de mieloma múltiple (MM) y leucemia de células T

Para la consecución del primer y parte del tercero objetivo utilizamos líneas celulares de mieloma múltiple (MM144 y MM1S) y de leucemia de células T, (células Jurkat, JK) y las tratamos con resveratrol. La evaluación primera de la muerte celular por apoptosis se realizó mediante el análisis de la degradación del ADN. Nuestros resultados muestran que todas las líneas celulares estudiadas responden a concentraciones crecientes de resveratrol con un aumento en el porcentaje de degradación en su ADN. Además, las células JK tratadas con resveratrol presentan activación de caspasa-3 y del sustrato PARP (*Poly(ADP-ribose) polymerase*) (**Fig. 7**), parámetros indicadores de apoptosis. Estos datos demuestran que este fármaco desencadena el proceso de muerte celular por apoptosis en los dos tipos celulares de interés.

Con vistas a una posible aplicación clínica, tratamos con las mismas condiciones de resveratrol a células derivadas de pacientes con MM y a linfocitos de sangre periférica de voluntarios sanos, utilizados como control. Este análisis demostró que el resveratrol tiene una acción selectiva sobre las células tumorales, ya que el porcentaje de degradación de ADN en las muestras control fue inferior al 5% (**Fig. 8**).

8.3.1.2. Los *lipid rafts* están funcionalmente implicados en la apoptosis mediada por resveratrol en líneas celulares de mieloma múltiple y leucemia de células T

Algunos datos previos han demostrado que la incubación con resveratrol provoca la activación del receptor de muerte Fas/CD95 en *lipid rafts* [76]. Para comprobar si esto podía estar sucediendo también en los tumores hematológicos de estudio, realizamos inmunofluorescencia para la detección de Fas/CD95 y utilizamos la subunidad B de la toxina colérica unida a FITC (*fluorescein isothiocyanate*), cuya afinidad por el ganglíosido GM1 nos permite localizar los *rafts* en la membrana plasmática de las líneas MM144 y JK. Nuestros resultados demuestran que el tratamiento con resveratrol

provoca la formación de plataformas *raft* y la redistribución en ellas del receptor de muerte Fas/CD95 **(Fig. 9**). Por otra parte, si impedimos la formación de *rafts,* mediante la pre-incubación con un quelante de colesterol (MCD-*methyl*-β-*cyclodextrin*), se inhibe la apoptosis inducida por resveratrol (**Fig. 10**). Todos estos datos sugieren que los *lipid rafts* están directamente implicados en el proceso apoptótico mediado por resveratrol, posiblemente mediante el reclutamiento del receptor Fas/CD95.

8.3.1.3. El resveratrol induce el reclutamiento en lipid rafts de receptores de muerte y proteínas apoptóticas señalizadoras downstream

El aislamiento de *lipid rafts* de células JK y MM144 tratadas y sin tratar con resveratrol confirmó la translocación de Fas/CD95 a *rafts* tras el tratamiento con resveratrol. Además de Fas/CD95, en estas estructuras membranosas hemos detectado diversos receptores de la familia TRAIL, otros tipos de receptores de muerte. Así, en células JK se encuentra el receptor TRAIL [42], DR5 (*death receptor 5*) y en células MM144 los receptores TRAIL, DR4 (*death receptor 4*) y DR5. Además de los receptores, en los *lipid rafts* también se acumulan proteínas *downstream* a los receptores de muerte pertenecientes al complejo DISC (FADD y procaspasa-8) y otras proteínas involucradas en señalización apoptótica (caspasa-10, Bid y JNK). El complejo DISC es clave en la iniciación de la apoptosis y la proteína Bid puede servir de puente entre la apoptosis mediada por Fas/CD95 y la apoptosis mediada por la mitocondria. Estos resultados sugieren que el resveratrol induce una reorganización del contenido proteico de los *lipid rafts* (**Fig. 11**).

Para analizar en detalle cuales podían ser las rutas implicadas en la apoptosis mediada por resveratrol llevamos a cabo la preincubación de las células con distintos inhibidores moleculares. Así, la preincubación con inhibidores de JNK y caspasas provocó una inhibición de la apoptosis inducida por resveratrol. El inhibidor general de caspasas (z-VAD-fmk) produjo la inhibición casi total de la apoptosis en células JK, MM144 y MM1S, implicando la activación de caspasas en la transmisión de la señal apoptótica. Sin embargo, el pre-tratamiento con el inhibidor de JNK (SP600125) inhibe la apoptosis de forma parcial. Estos datos indican que la activación de las caspasas es necesaria mientras que JNK contribuye, pero no parece ser esencial en la transmisión de la señal apoptótica inducida por resveratrol (**Fig. 12**).

8.3.1.4. La mitocondria está implicada en la apoptosis inducida por resveratrol

Para estudiar el papel de la mitocondria en la apoptosis inducida por resveratrol analizamos el papel de la proteína mitocondrial anti-apoptótica Bcl-X_L en células MM144 tras el tratamiento con nuestro fármaco de interés. Para ello obtuvimos células MM144 transfectadas con el vector control pSFFV-Neo, y células transfectadas con Bcl-$X_{L,}$ que sobreexpresan la proteína. El tratamiento de las células control (MM144-Neo) con resveratrol conduce a la degradación del ADN, a la pérdida del potencial de membrana mitocondrial ($\Delta\Psi_m$) y a la formación de especies reactivas de oxígeno, ROS; mientras que el tratamiento con resveratrol en las células MM144-Bcl-X_L no produjo ni degradación del ADN, ni pérdida en el potencial de membrana mitocondrial pero sí la formación de ROS. Estos resultados indican que la disipación de $\Delta\Psi_m$ pero no la formación de ROS, es fundamental para que se dé el proceso apoptótico inducido por resveratrol (**Fig. 13**).

El hecho de que Bid se movilizara hacia los *rafts* tras el tratamiento de resveratrol estaba indicando que podría existir una conexión entre las rutas apoptóticas [96]. Para demostrar esta hipótesis, utilizamos células JK que sobreexpresan una forma dominante negativa de FADD (FADD-DN), la proteína adaptadora de Fas/CD95. En estas células la señalización vía Fas/CD95 se encuentra bloqueada. Nuestros resultados muestran que el tratamiento con el resveratrol de las células JK-FADD-DN no produjo ni degradación del ADN, ni perdida del $\Delta\Psi_m$ (**Fig. 14**). Además, células JK deficientes en Fas/CD95, las cuales se mostraron totalmente resistentes al tratamiento con resveratrol (**Fig. 15**). Estos datos indican que la falta de activación de Fas/CD95 provoca el bloqueo de los eventos apoptóticos mitocondriales, ya que no ocurren cuando éste no se activa.

8.3.1.5. El interferon gamma (IFN-γ) induce la expresión de Fas/CD95 y de la casapasa-8 y potencia la apoptosis inducida por resveratrol

Teniendo en cuenta que la activación de Fas/CD95 está directamente relacionada con el proceso apoptótico mediado por el resveratrol y que el IFN-γ induce la expresión de Fas/CD95 en células de MM [87,174] quisimos comprobar si el uso de IFN-γ tiene algún efecto sobre la apoptosis en nuestras células de interés. Nuestros resultados mostraron que el tratamiento de células MM1S con IFN-γ aumenta los niveles proteicos tanto de Fas/CD95 como de procaspasa-8. Este aumento puede estar directamente relacionado con la sensibilización de estas células a la apoptosis inducida por resveratrol observada en estas células cuando las pretratamos con INF-γ (**Fig. 16**).

8.3.1.6. Resveratrol induce el reclutamiento de Fas/CD95 en *lipid rafts* en células U266 de mieloma múltiple

La línea de mieloma múltiple U266 se caracteriza por expresar un receptor Fas/CD95 que no es activable por anticuerpos agonistas de Fas/CD95 ni por el ligando natural (FasL/CD95L). Por lo tanto, el objetivo de esta parte del trabajo fue determinar si el reveratrol sigue ejerciendo su efecto apoptótico cuando el receptor Fas/CD95 no es capaz de activarse por su ligando natural. Como indicador de muerte celular por apoptosis cuantificamos la degradación del ADN. De manera similar que para las células JK, MM144 y MM1S, las células U266 responden a concentraciones crecientes de resveratrol con un aumento en el porcentaje de degradación de su ADN. Estos resultados estarían de acuerdo con datos previos obtenidos con ATLs, en los que se observó que la redistribución de Fas/CD95 en *lipid rafts*, con independencia de su activación por ligando para el desencadenar del proceso apoptótico [75]. En concordancia con esto hemos observado la formación de plataformas-*raft* y redistribución de Fas/CD95 mediante tratamiento con resveratrol (**Fig. 17**). Sin embargo, mediante preincubación con MCD, que previne la formación de plataformas-*raft*, apenas hemos detectado una discreta inhibición de la apoptosis inducida por resveratrol. Estos datos indican que en células U266 el resveratrol induce la formación de plataformas-*rafts* y la redistribución de Fas/CD95 pero para que la apoptosis se produzca son necesarios otros mecanismos adicionales (**Fig. 18**), probablemente relacionados con la *down-regulation* de STAT3 (*signal transducer and activator of transcription 3*) y del factor nuclear-κB previamente documentado durante la muerte apoptótica de células MM mediante tratamiento con resveratrol [92].

8.3.1.6.7. Efectos en la apoptosis por combinación del resveratrol con bortezomib ó perifosina

Debido a que el efecto apoptótico del resveratrol solo se consigue a dosis altas del mismo, quisimos saber si la combinación de resveratrol con otros compuestos de interés clínico resultaría en un incremento de la apoptosis en las líneas celulares utilizadas en el presente estudio. Con este fin hemos escogido la perifosina perteneciente al grupo de los ATLs, compuestos que parecen actuar de forma similar al resveratrol en las células de MM y JK; y el inhibidor de proteasoma bortezomib, utilizado en la actualidad en clínica en el tratamiento de diferentes neoplasias sanguíneas, incluido el MM [69,102]. Tratamos a todas nuestras líneas de estudio (JK, MM144, MM1S y U266)

con las combinaciones anteriores. Nuestros datos demuestran que la combinación de resveratrol con perifosina (**Fig. 19**) resulta en un efecto apoptótico aditivo, mientras que la combinación con bortezomib resulta en un efecto apoptótico sinérgico (**Fig. 20**). El efecto aditivo resultante de la combinación del resveratrol con perifosina refuerza la idea de que estos compuestos comparten, al menos parte, el mismo mecanismo de acción. Nuestros resultados fueron similares en todas las líneas celulares utilizadas, excepto en las U266, en las cuales no se ha observado ningún efecto aditivo. La combinación entre el resveratrol y el bortezomib resultó en un efecto sinérgico probablemente porque el resveratrol ejerce su efecto apoptótico actuando sobre los *rafts* mientras que el bortezomib actua sobre el proteasoma. Estos resultados indican que la terapia combinada de resveratrol con otros compuestos podría ser considerada para su empleo en clínica. Para que el reveratrol ejerza su efecto citotoxico son necesarias dosis muy elevadas, siendo esta una de las limitaciones a su empleo clínico. Sin embargo, en combinación con otros compuestos, como hemos visto, dosis más bajas podrían ser consideradas. Además, dos oligomeros naturales del resveratrol, ε-viniferin y myabenol C se encuentra en estudio exactamente por el hecho de que a dosis más bajas están obteniendo resultados prometedores en líneas celulares de tumores linfoides y mieloides [106].

8.3.2. La activación de Akt mediada por *rafts* como diana terapéutica en células de MCL

8.3.2.1. Los ATLs inhiben la via de señalización de Akt y activan la vía apoptótica mitocondrial en líneas celulares de MCL

Para alcanzar el segundo objetivo de esta tesis utilizamos las siguientes líneas celulares de linfoma de manto: Z-138, JVM-2 y Jeko-1, las cuales tratamos con los ATLs perifosina y edelfosina. Empezamos describiendo la sucesión de eventos apoptóticos después de la incubación con los referidos ATLs. Los primeros parámetros apoptóticos detectados se relacionan con la activación de la vía intrínseca: perdida de $\Delta\Psi_m$ (**Fig. 22**), generación de ROS (**Fig. 23)** y activación de la caspasa-9 (**Fig. 24**)**.** Por último, detectamos la degradación del ADN (**Fig. 25**). Para determinar el papel de las caspasas en este proceso de muerte, preincubamos las células con el inhibidor general de caspasas z-VAD-fmk, y los resultados muestran que z-VAD-fmk inhibe la apoptosis inducida por ATLs (**Fig. 26**).

Datos previos relacionan la inhibición de la ruta PI3K/Akt tanto con la activación de la vía intrínseca de la apoptosis como con la muerte celular inducida por ATLs [29,70]. Por tal motivo, analizamos el efecto de la edelfosina sobre la fosforilación de Akt y de quinasas relacionadas, a diferentes intervalos de tiempo. Para realizar este ensayo seleccionamos las células más sensibles a la acción de los ATLs, según nuestros datos las células Z-138, y entre los dos ATLs (edelfosina y perifosina), la edelfosina que posee un efecto apoptótico fue potente (**Figs. 25 y 29**). Nuestros datos muestran que a las primeras horas (3 h) de tratamiento disminuyeron los niveles de fosforilación de Akt en Ser473. Además comprobamos que lo mismo ocorría con la mayoría de sus substratos, para ello utilizamos un anticuerpo que reconoce los sustratos de Akt fosforilados que poseen el motivo RXRXXS/T [119]. Sin embargo, los niveles de fosforilación de Akt en el residuo Thr308 solo disminuyeron transcurridas 15 h de incubación con la edelfosina (**Fig. 28 A**).

Posteriormente quisimos saber que ocurría con dos de los sustratos más conocidos de Akt: GSK3 y Bad, durante el tratamiento con edelfosina. Normalmente Akt inhibe a ambos mediante fosforilación mientras este activada. Datos previos implican a GSK3 en la degradación proteosómica de la ciclina D1, la cual se encuentra sobreexpresada en células de MCL [110]. Bad está relacionada con la activación de la

ruta intrínseca de la apoptosis [112], activada en nuestros ensayos mediante incubación con ATLs. Nuestros resultados muestran que los niveles de fosforilación de GSK3 no disminuyen. Incluso cuando preincubamos las células con el inhibidor de GSK3 LiCl detectamos un incremento en la apoptosis inducida por ATLs (**Fig. 28 B**), sugiriendo que los ATLs actúan sobre una vía independiente a GSK3. Esto coincide con resultados previos, donde el tratamiento de células de MCL con ATLs no disminuían los niveles de ciclina D1 [70], lo que podría implicar que GSK3 sea regulada por una vía alternativa a la de Akt [131]. Con respecto a Bad, se observó inhibición de su fosforilación 24 horas después de la incubación con los ATLs, cuando ya se habían iniciado los procesos apoptóticos, lo que sugiere que Bad no está implicada en la supervivencia de estas células por activación de Akt, como ya se ha descrito en células hematopoyéticas [112].

Además, analizamos lo que ocurría con los niveles de fosforilación de mTOR (*mammalian target of rapamycin*), una vez que, cuando forma parte del complejo mTORC1 (*mammalian target of rapamycin complex 1*) se convierte en un sustrato *downstream* de Akt [113]. Según nuestros datos, el tratamiento con edelfosina bajó los niveles de fosforilación tanto de mTOR como de 4E-BP1, proteína *dowstream* mTORC1, confirmando así, que el complejo mTORC1 se ve afectado por el tratamiento con edelfosina (**Fig. 28**).

A continuación, quisimos evaluar los niveles basales de fosforilación de Akt en Ser473 entre las diferentes líneas de MCL. Los niveles basales más altos fueron detectados en las células HBL-2, seguidas de Jeko-1, y luego de Z-138 y JVM-2, cuyos niveles detectados fueron similares. Después del tratamiento con ATLs, observamos que la línea celular HBL-2 era resistente al tratamiento (**Fig. 29**), indicando que altos niveles de p-Akt confieren resistencia al tratamiento por ATLs. Estos datos sugieren una relación entre los niveles de fosforilación de Akt y la sensibilidad o resistencia a la muerte inducida por ATLs.

8.3.2.2. Efectos de la edelfosina en la fosforilación de ERK y JNK

Datos previos relacionan la vía de señalización de JNK con la muerte inducida por ATLs [118] y con la patogénesis de MCL [120]. Igualmente, la activación de ERK se ha descrito como un mecanismo de compensación en células donde la señalización vía Akt se encontraba comprometida [121]. Por ello, quisimos analizar en detalle si estas rutas de señalización podrían estar implicadas en la apoptosis mediada por ATLs. Detectamos el estado de fosforilación de las proteínas JNK y ERK tras la incubación

con edelfosina a diferentes tiempos. Nuestros resultados mostraron un aumento de los niveles de fosforilación de la proteína JNK, sin embargo, al preincubar con el inhibidor de JNK, SP, se observó una disminución en la apoptosis inducida por ATLs, pero no una inhibición total. Con respecto a ERK, detectamos un pequeño incremento de los niveles de fosforilación de proteína, y la preincubación de las células con el inhibidor de ERK, PD98059 (PD) no indujo cambios en la viabilidad de las células con respecto a la muerte inducida por ATLs (**Fig. 31**). Estos resultados indican que las vías de señalización de ERK y JNK no son esenciales en la muerte celular inducida por ATLs en células de MCL.

8.3.2.3. La inhibición de PI3K potencia la apoptosis inducida por ATLs

Teniendo en cuenta los datos previos presentados anteriormente en este trabajo, en los cuales detectamos inhibición de Akt y de algunos de sus sustratos *downstream* tras la incubación con ATLs, quisimos saber si la inhibición de PI3K (quinasa *upstream* Akt) tiene algún efecto en la muerte inducida por los ATLs. Detectamos un aumento de la apoptosis inducida por los ATLs, así como de un incremento en la inhibición de Akt y del sustrato mTOR. Estos datos sugieren que la inhibición de la ruta de PI3K/Akt puede sensibilizar las células al tratamiento por ATLs, potenciando la respuesta apoptótica (**Fig. 32**).

8.3.2.4. Inhibidores de Akt inducen apoptosis en la línea celular de MCL Z-138

Utilizamos diferentes inhibidores específicos de Akt (**Fig. 33**) con el objetivo de comparar sus efectos apoptóticos con respecto a los de los ATLs, tanto a nivel de degradación de ADN como de la activación/inhibición de las quinasas previamente descritas. Todos los inhibidores empleados indujeron pérdida del $\Delta\Psi_m$, degradación del ADN, disminución de los niveles de p-mTOR, aumento de los de p-JNK y un pequeño aumento en la fosforilación de GSK3. Todos los eventos observados son similares a los ya descritos con ATLs. Estos datos sugieren, que tanto los inhibidores de Akt como los ATLs estarían actuando sobre la misma vía de señalización para la inducción de apoptosis en células de MCL (**Figs. 34 y 35**).

8.3.2.5. La estimulación por CD40 no protege las células de MCL de la muerte inducida por ATLs

Los estímulos del microambiente tumoral son claves para la supervivencia

de las células de MCL y para su resistencia a agentes quimioterapéuticos [110,124]. Para estudiar el efecto de uno de los estímulos del microambiente tumoral, preincubado dos líneas celulares JVM-2 y Z-138 con la inmunoglobulina anti-CD40, que funciona estímulando la proliferación celular por activación de CD40. Nuestros datos muestran que la fosforilación de Akt se incrementó mediante la incubación con la inmunoglobulina anti-CD40, sin generar cambios en el porcentaje de apoptosis entre células estimuladas y no estimuladas, tras la incubación con ATLs. Estos datos indican que este tipo de estímulación del microambiente tumoral de las MCL no sería suficiente para inhibir la muerte celular mediada por ATLs (**Figs. 36 y 37**).

8.3.2.6. Los *rafts* están implicados en la señalización de Akt en células de MCL

Nuestros resultados muestran una inhibición de Akt desencadenada por acción de los ATLs, dado que estudios previos han demostrado la implicación de *rafts* en la activación de la ruta PI3K/Akt [34], encontrándose esta vía constitutivamente activada en células de MCL [110,111], y que, una de las dianas descritas de los ATLs en células tumorales son los *lipid rafts* [73], aislamos *rafts* de células de MCL control y tratadas con ATLs. En los *rafts* de células Z-138 control detectamos preferentemente Akt activada (fosforilada en Ser473 y Th308) así como otras quinasas reguladoras de la vía de señalización de Akt: PI3K, mTOR y p-PDK1 (**Fig. 38**). Sin embargo, Akt y PDK1 no fosforiladas se encontraron igualmente distribuidas entre las fracciones *rafts* y no-*rafts.* Estos datos indican que los dominios de membrana pueden tener un papel clave en la activación de la ruta PI3K/Akt en células de MCL.

Se ha descrito que los ATLs tienen como diana los *rafts* de distintos tumores hematológicos [73]. Nuestros resultados muestran que en distintas líneas de MCL tratadas con edelfosina ocurre un desplazamiento hacia las fracciones no-*raft* de las proteínas pertenecientes a la vía PI3K/Akt. De igual modo, los substratos *downstream* de Akt en *rafts* se vieron especialmente afectados, indicando que la edelfosina al incorporarse en los *rafts* estaría bloqueando la señalización de la ruta PI3K/Akt en células de MCL (**Figs. 38 y 39**).

La preincubación de las células Z-138 con pervanadato, el activador más potente de Akt que se conoce [125], aumentó los niveles de fosforilación de Akt en la membrana, y además inhibió la muerte celular inducida por edelfosina de forma significativa. Estos datos apoyan la teoria de que la inhibición de la señalización de Akt, localizada en los *rafts,* es un paso importante para la inducción de muerte mediada por los ATLs

(**Fig. 40**).

Los datos presentados en este trabajo sugieren que la incorporación de edelfosina en los dominios rafts conlleva a un desplazamiento de las proteínas quinasas Akt, PI3K, PDK1 y mTOR hacia zonas no-raft, inhibiendo la fosforilación de Akt y de sus sustratos, resultando en la pérdida ΔΨm, degradación del ADN y finalmente a la muerte celular (**Fig. 44**).

Se ha descrito que la inhibición de la ruta de Akt puede originar una distribución de receptores de muerte en *lipid rafts* [84], lo que coincide con los datos presentados en este trabajo y con datos anteriores en cuanto a la movilización de Fas/CD95 inducida por ATLs [70]. Sin embargo, en la línea celular Z-138 no se detecto un aumento de la apoptosis en presencia del anticuerpo agonista de Fas/CD95, el CH11 (**Fig. 41**). Estos datos coinciden con estudios anteriores, donde se demuestra que la edelfosina es capaz de activar Fas/CD95 a nivel intracelular, aunque el receptor no responda al estimulo con el anticuerpo agonista o el ligando natural [39].

En estudios previos se ha localizado la quinasa responsable de fosforilación de Akt en la Ser473 en los dominos *rafts* [134]. Este dato explicaría por qué en este trabajo detectamos en primero lugar una disminución de la fosforilación en Ser473, antes que en Thr308. La quinasa responsable de fosforilar Akt en Ser473 puede ser mTORC2, lo cual detectamos que se desplaza de los *rafts* hacia localizaciones no-*rafts* mediante el tratamiento con ATLs.

8.3.2.7. Edelfosina y perifosina son eficaces en el tratamiento de MCL en modelos *in vivo*

Con la idea de extrapolar la toxicidad obtenida *in vitro* con los ATLs a ensayos con animales, realizamos un ensayo *in vivo* en ratones SCID a través de un modelo animal *xenograft*. Después de la inoculación de la línea celular Z-138 y de la detección de la generación de tumores incipientes, los ratones fueron tratados por vía oral con perifosina y edelfosina durante 3 semanas. Comparando el índice de crecimiento tumoral de los ratones control (tratados solamente con el vehículo, agua) *vs* tumores de ratones tratados con ATLs observamos una disminución en peso y volumen de los tumores en aquellos animales tratados con ATLs (30 mg/kg edelfosina y 25.45 mg/kg) (**Fig. 42**).

8.3.2.8. Los ATLs inducen muerte celular e inhiben Akt en células derivadas de pacientes

con MCL

Con el fin de extrapolar los datos obtenidos en líneas celulares a células derivadas de pacientes, recurrimos a células de 9 pacientes con MCL (**Tabla 1**). Las células de los pacientes 8 y 9 no respondieron al tratamiento y no se detectó una inhibición de la fosforilacion de Akt tras la incubación con ATLs, efecto igualmente observado en la línea resistente HBL-2. Por el contrario, en las células del paciente 3, sensible a ATLs se ha detectó una disminución en los niveles de p-Akt (**Fig. 43**), siendo estos datos similares a los obtenidos en las líneas celulares sensibles a los ATLs.

8.3.3. Edelfosina en terapia combinada en el tratamiento del mieloma múltiple

8.3.3.1. Los inhibidores de histona deacetilasas (HDAC) inducen apoptosis in líneas celulares de mieloma múltiple

Para alcanzar el último objetivo de esta tesis hemos utilizado las siguientes líneas celulares de mieloma múltiple: MM144 y MM1S y las tratamos con los inhibidores de histona deacetilasas (HDAC) SAHA y MS-275. Comenzamos por caracterizar el tipo de muerte celular inducida por los inhibidores de HDAC en células de mieloma múltiple. La incubación con SAHA y MS-275 resultó en la degradación del ADN, activación de la caspasa-3 y degradación de su típico sustrato PARP. Adicionalmente, recurriendo a un ensayo colorimétrico se detectó la activación de las caspasas 8 y 9, pertenecientes a las rutas extrínseca y intrínseca de la apoptosis respectivamente (**Fig. 45**).

8.3.3.1. La activación de la apoptosis mediante inhibidores de HDAC en células de MM ocurre por un mecanismo independiente al reclutamiento de Fas/CD95 en plataformas-*rafts*

En resultados anteriores observamos como compuestos como el resveratrol y los ATLs promueven la formación de plataformas *raft* y Fas/CD95 activando una respuesta apoptótica. Sin embargo, los inhibidores de HDAC no activan dicho mecanismo de muerte en células MM144. Además, si impedimos da formación de *rafts*, mediante la preincubación con en quelante de colesterol MCD, tampoco se inhibió la muerte inducida por los inhibidores de HDAC. Estos datos sugieren que los inhibidores de HDAC inducen una apoptosis independiente de *raft* en células de MM (**Fig. 46**).

8.3.3.2 La combinación entre edelfosina e inhibidores de HDAC tiene un efecto potenciador de la apoptosis

Con vista a una posible aplicación terapéutica, estudiamos el efecto en la apoptosis resultante de la combinación entre compuestos que tienen como diana los *rafts* de membrana, en este caso la edelfosina, en combinación con compuestos que actúan de forma independiente de *rafts*, los inhibidores de HDAC. Detectamos utilizando dosis bajas de cada uno de los compuestos SAHA, MS-275 o EDLF, un aumento de la aptoptosis cuando se añadían de forma combinada EDLF+SAHA o

EDLF+MS-275. Comprobamos la activación temprana de la apoptosis mediante activación de caspasa-3 y la degradación de su sustrato PARP en los periodos de 3 a 6 h posteriores a la incubación (**Fig. 47**).

8.3.3.3. La combinación entre edelfosina y bortezomib resulta en una respuesta apoptótica sinérgica.

Quisimos saber si la combinación de edelfosina con el bortezomib, un inhibidor del proteasoma que se encuentra en clínica para el tratamiento del MM, resultaba en un aumento de la apoptosis. Para ello utilizamos líneas celulares de MM sensibles (MM1S y MM144) o resistentes (MM1R) al tratamiento por dexametasoma, compuesto igualmente utilizado en clínica. Combinamos bajas dosis de edelfosina y bortezomib solas o combinadas, en las referidas líneas celulares de MM. Todas las líneas celulares empleadas respondieron de forma similar, en términos de degradación de ADN (apoptosis), cuando se incubaron con los compuestos solos o en estudios combinatorios. Se obtuvo una respuesta sinérgica resultante de la combinación entre edelfosine y bortezomib, lo que podría ser de interés clínico para el tratamiento de pacientes resistentes al tratamiento con dexametasona (**Fig. 48**).

8.3.3.4. La combinación entre dos compuestos cuya diana son los *lipid rafts* no tiene un efecto potenciador de la apoptosis

La combinación entre el resveratrol y la edelfosina no se ha reflejado en el incremento de la apoptosis lo que sugiere que pueden estar actuando a través de la misma ruta apoptótica (**Figura 49**).

8.3.3.5. La pre-incubación con interferón gamma potencia la acción apoptótica de la edelfosina en células de MM

Datos anteriores (**Fig. 16**) demuestran que la incubación de células de MM con interferón gamma resulta en el aumento de Fas/CD95 y caspasa-8.Teniendo en cuenta el papel que desempeña Fas/CD95 en el proceso apoptótico mediado por edelfosina, utilizamos el IFN-γ en células de MM. Nuestros datos indican que el tratamiento de células MM con IFN-γ sensibiliza estas células a la apoptosis inducida por edelfosina (**Fig. 50**).

8.4. Conclusiones:

1- El resveratrol induce apoptosis en células de MM y de leucemia de células T por un mecanismo dependiente de *rafts* y de Fas/CD95. Este mecanismo implica el reclutamiento en plataformas-*raft* de Fas/CD95 así como de proteínas apoptóticas *downstream rafts*.

2- Los ATLs en líneas celulares de MCL desplazan quinasas pertenecientes a la ruta PI3K/Akt de dominios de membranas *raft* a otros no-*raft*, induciendo una muerte celular apoptótica. La fosforilación de Akt en el residuo Ser473 ocurre principalmente en dominios de membrana *raft*, lo que es fundamental para la supervivencia de las células de MCL.

3- Los ATLs en presencia de estímulos del microambiente tumoral mantienen su acción apoptótica en células de MCL. Su acción antitumoral en estas células es dependiente de los niveles basales de fosforilación de Akt, tanto en líneas celulares como en células aisladas de pacientes.

4- En su conjunto los datos presentados en este trabajo revelan que los *rafts* son potenciales dianas terapéutica en cáncer, estando implicados en la regulación de la señalización de rutas de vida y muerte.

5- Esta terapia dirigida a dominios *raft* parece mostrarse como una herramienta prometedora en terapia combinada para el tratamiento del cáncer. La combinación entre moléculas que tienen como diana los *rafts* y bortezomib resulta en un efecto apoptótico sinérgico en células de MM y leucemia de células T

9. AGRADECIMIENTOS

En primer lugar quiero agradecer a mi director de tesis, **Dr. Faustino Mollinedo**, por la oportunidad de realizar este trabajo en su laboratorio, por haberme recibido y por tratarme desde el primer al último día con toda su amabilidad. A parte de sus enseñanzas, la ilusión con la que realiza su trabajado me ha motivado en mis primeros pasos. A la **Drª Consuelo Gajate** agradezco su contribución en los trabajos publicados.

Le agradezco a la **Drª Dolors Colomer** y al **Dr. Gaël Roué** por recibirme en vuestro grupo de trabajo, por vuestra colaboración en la realización de uno de los objetivos de esta tesis. He aprendido mucho en el poco tiempo que estuve allí.

Agradeço à minha **família**, à minha mãe **Lucília**, ao meu pai **Henrique**, à minha irmã **Joana** e à mais recente aquisição, o meu sobrinho **Henrique** (com menos anos que esta tese), todo o vosso apoio! Obrigada por terem respeitado sempre as minhas decisões e por entender as minhas consecutivas ausências em datas importantes. Uma tese é um conjunto de resultados que tomam forma numa historia, eu sou a vossa história, por isso este trabalho é vosso! Obrigada!

A todos mis compañeros del **laboratorio 6**, no los voy a nombrar a todos porque hemos sido muchos a lo largo de estos años...A los que empezamos juntos, **Álvaro**, **Rubén**, **Janny**, **Ximena** y **Rósula**, he pasado en suma más tiempo con vosotros que con mi propia familia, entre horas dentro y fuera del laboratorio. Al final hemos sido unos para los otros, apoyo, amistad y compañerismo. Ha sido un privilegio compartir mi tiempo con vosotros, fue algo muy afortunado haber empezado este camino con vosotros ¡gracias por todo! Será imposible recordar a Salamanca sin que no me acuerde de vosotros. También a **Sarita**, **Vero** y **Ale,** entre tartas y risas les agradezco los momentos de "relax". **Adolfo** y **Alberto**, ha sido menos tiempo pero lo suficiente para que os recuerde con todo el cariño, gracias por el ánimo, consejos y toda la ayuda en mis últimos tiempos en Salamanca. A **Ana,** muchas gracias por la paciencia, atención y cuidado, he tenido la suerte de compartir contigo no solo un piso sino una amistad duradera.

Al **laboratorio 1**! A los vecinos más solidarios y animados! En especial quiero agradecer a la dulce **Alicia**, lo que empezó por un sencillo intercambio de ideas (total que esto de las quinasas es un lio), pronto se transformó en largas horas de debates socio-psicológicos…!Como lo he disfrutado! A **Carmela** muchas gracias por la ayuda, por compartir conmigo tu alegría, tu sabiduría y tus estupendas apreciaciones criticas. A **Fer**, gracias por toda tu ayuda, animo, amistad y compañía a cualquier hora! No tenéis precio!

A mi amigo **Carlos Rojas** gracias por la paciencia, amistad y valorados concejos. Por acompañarme y disfrutar conmigo esas mil horas de partidos de futbol.

Aos meus amigos de Portugal, que me acompanham praticamente desde a infância, obrigada por participarem da minha vida mesmo à distancia, graças a vocês nunca me sinto só...Os quilómetros que nos separam são pormenores em relação ao que está estabelecido entre nós! Aos meus bens mais preciosos: **Raquel**, **Joana**, **Carlos**, **Heitor** e **Luís**. Obrigada pela vossa amizade!

A los chicos del equipo de *ultimate* **Quimera** de Salamanca, muchas gracias por todos los momentos deportivo-sociales que me han proporcionado.

10. REFERENCES

1. Mulas MF, Abete C, Pulisci D, et al. Cholesterol esters as growth regulators of lymphocytic leukaemia cells. Cell Prolif. 2011;44:360-371.

2. Jowett M. The phosphatide and cholesterol contents of normal and malignant human tissues. Biochem J. 1931;25:1991-1998.

3. Yasuda M, Bloor WR. Lipid Content of Tumors. J Clin Invest. 1932;11:677-682.

4. Maxfield FR, Tabas I. Role of cholesterol and lipid organization in disease. Nature. 2005;438:612-621.

5. Freeman MR, Solomon KR. Cholesterol and benign prostate disease. Differentiation. 2011;82:244-252.

6. Lutchman M, Solomon KR, Freeman MR. Cholesterol, Cell Signaling, and Prostate Cancer. Prostate Cancer. In second ed: Prostate Cancer Biology, Genetics, and the New Therapeutics.Totowa NJ: Humana Press, 2007: 119-137.

7. Maxfield FR, van Meer G. Cholesterol, the central lipid of mammalian cells. Curr Opin Cell Biol. 2010;22:422-429.

8. Freeman MR, Di Vizio D, Solomon KR. The Rafts of the Medusa: cholesterol targeting in cancer therapy. Oncogene. 2010;29:3745-3747.

9. Tosi MR, Tugnoli V. Cholesteryl esters in malignancy. Clin Chim Acta. 2005;359:27-45.

10. Dessi S, Batetta B, Anchisi C, et al. Cholesterol metabolism during the growth of a rat ascites hepatoma (Yoshida AH-130). Br J Cancer. 1992;66:787-793.

11. Rudling M, Collins VP. Low density lipoprotein receptor and 3-hydroxy-3-methylglutaryl coenzyme A reductase mRNA levels are coordinately reduced in human renal cell carcinoma. Biochim Biophys Acta. 1996;1299:75-79.

12. Lingwood D, Simons K. Lipid rafts as a membrane-organizing principle. Science. 2010;327:46-50.

13. Lucero HA, Robbins PW. Lipid rafts-protein association and the regulation of protein activity. Arch Biochem Biophys. 2004;426:208-224.

14. Simons K, Gerl MJ. Revitalizing membrane rafts: new tools and insights. Nat Rev Mol Cell Biol. 2010;11:688-699.

15. Harding AS, Hancock JF. Using plasma membrane nanoclusters to build better signaling circuits. Trends Cell Biol. 2008;18:364-371.

16. Simons K, Ikonen E. Functional rafts in cell membranes. Nature. 1997;387:569-572.

17. Simons K, Toomre D. Lipid rafts and signal transduction. Nat Rev Mol Cell Biol. 2000;1:31-39.

18. Caldieri G, Buccione R. Aiming for invadopodia: organizing polarized delivery at sites of invasion. Trends Cell Biol. 2010;20:64-70.

19. Hancock JF. Lipid rafts: contentious only from simplistic standpoints. Nat Rev Mol Cell Biol. 2006;7:456-462.

20. Carver LA, Schnitzer JE. Caveolae: mining little caves for new cancer targets. Nat Rev Cancer. 2003;3:571-581.

21. Freeman MR, Cinar B, Lu ML. Membrane rafts as potential sites of nongenomic hormonal signaling in prostate cancer. Trends Endocrinol Metab. 2005;16:273-279.

22. Morgan MJ, Kim YS, Liu Z. Lipid rafts and oxidative stress-induced cell death. Antioxid Redox Signal. 2007;9:1471-1483.

23. Carver LA, Schnitzer JE, Anderson RG, Mohla S. Role of caveolae and lipid rafts in cancer: workshop summary and future needs. Cancer Res. 2003;63:6571-6574.

24. Sprong H, van der Sluijs P, van Meer G. How proteins move lipids and lipids move proteins. Nat Rev Mol Cell Biol. 2001;2:504-513.

25. Staubach S, Hanisch FG. Lipid rafts: signaling and sorting platforms of cells and their roles in cancer. Expert Rev Proteomics. 2011;8:263-277.

26. Crowell JA, Steele VE, Fay JR. Targeting the AKT protein kinase for cancer chemoprevention. Mol Cancer Ther. 2007;6:2139-2148.

27. Hill MM, Hemmings BA. Inhibition of protein kinase B/Akt. implications for cancer therapy. Pharmacol Ther. 2002;93:243-251.

28. Franke TF. PI3K/Akt: getting it right matters. Oncogene. 2008;27:6473-6488.

29. Brazil DP, Hemmings BA. Ten years of protein kinase B signalling: a hard Akt to follow. Trends Biochem Sci. 2001;26:657-664.

30. Wymann MP, Schneiter R. Lipid signalling in disease. Nat Rev Mol Cell Biol. 2008;9:162-176.

31. Li YC, Park MJ, Ye SK, Kim CW, Kim YN. Elevated levels of cholesterol-rich lipid rafts in cancer cells are correlated with apoptosis sensitivity induced by cholesterol-depleting agents. Am J Pathol. 2006;168:1107-1118; quiz 1404-1105.

32. Lasserre R, Guo XJ, Conchonaud F, et al. Raft nanodomains contribute to Akt/PKB plasma membrane recruitment and activation. Nat Chem Biol. 2008;4:538-547.

33. Brown DA. Lipid rafts, detergent-resistant membranes, and raft targeting signals. Physiology (Bethesda). 2006;21:430-439.

34. Gao X, Zhang J. Spatiotemporal analysis of differential Akt regulation in plasma membrane microdomains. Mol Biol Cell. 2008;19:4366-4373.

35. George KS, Wu S. Lipid raft: A floating island of death or survival. Toxicol Appl Pharmacol. 2012;259:311-319.

36. Guardiola-Serrano F, Rossin A, Cahuzac N, et al. Palmitoylation of human FasL modulates its cell death-inducing function. Cell Death Dis. 2010;1:e88.

37. Mollinedo F, Gajate C. Fas/CD95 death receptor and lipid rafts: new targets for apoptosis-directed cancer therapy. Drug Resist Updat. 2006;9:51-73.

38. Gajate C, Mollinedo F. The antitumor ether lipid ET-18-OCH(3) induces apoptosis through translocation and capping of Fas/CD95 into membrane rafts in human leukemic cells. Blood. 2001;98:3860-3863.

39. Gajate C, Del Canto-Janez E, Acuna AU, et al. Intracellular triggering of Fas aggregation and recruitment of apoptotic molecules into Fas-enriched rafts in selective tumor cell apoptosis. J Exp Med. 2004;200:353-365.

40. Chakrabandhu K, Herincs Z, Huault S, et al. Palmitoylation is required for efficient Fas cell death signaling. Embo J. 2007;26:209-220.

41. Cahuzac N, Baum W, Kirkin V, et al. Fas ligand is localized to membrane rafts, where it displays increased cell death-inducing activity. Blood. 2006;107:2384-2391.

42. Gajate C, Mollinedo F. Cytoskeleton-mediated death receptor and ligand concentration in lipid rafts forms apoptosis-promoting clusters in cancer chemotherapy. J Biol Chem. 2005;280:11641-11647.

43. Mollinedo F, Gajate C. Fas signaling. In: FasL-independent activation of Fas. Georgetown, TX, USA: Landes Bioscience and Springer Science; 2006:13-27.

44. Muppidi JR, Siegel RM. Ligand-independent redistribution of Fas (CD95) into lipid rafts mediates clonotypic T cell death. Nat Immunol. 2004;5:182-189.

45. Legembre P, Mollinedo F. The plasma membrane: a catalyst in the decision to die or not to die? Recent Pat Anticancer Drug Discov. 2011;6:271-273.

46. Rossin A, Derouet M, Abdel-Sater F, Hueber AO. Palmitoylation of the TRAIL receptor DR4 confers an efficient TRAIL-induced cell death signalling. Biochem J. 2009;419:185-192, 182 p following 192.

47. Miyaji M, Jin ZX, Yamaoka S, et al. Role of membrane sphingomyelin and ceramide in platform formation for Fas-mediated apoptosis. J Exp Med. 2005;202:249-259.

48. Adam RM, Mukhopadhyay NK, Kim J, et al. Cholesterol sensitivity of endogenous and myristoylated Akt. Cancer Res. 2007;67:6238-6246.

49. Zhuang L, Kim J, Adam RM, Solomon KR, Freeman MR. Cholesterol targeting alters lipid raft composition and cell survival in prostate cancer cells and xenografts. J Clin Invest. 2005;115:959-968.

50. Calay D, Vind-Kezunovic D, Frankart A, Lambert S, Poumay Y, Gniadecki R. Inhibition of Akt signaling by exclusion from lipid rafts in normal and transformed epidermal keratinocytes. J Invest Dermatol. 2010;130:1136-1145.

51. Zhuang L, Lin J, Lu ML, Solomon KR, Freeman MR. Cholesterol-rich lipid rafts mediate akt-regulated survival in prostate cancer cells. Cancer Res. 2002;62:2227-2231.

52. Elhyany S, Assa-Kunik E, Tsory S, et al. The integrity of cholesterol-enriched microdomains is essential for the constitutive high activity of protein kinase B in tumour cells. Biochem Soc Trans. 2004;32:837-839.

53. Porstmann T, Griffiths B, Chung YL, et al. PKB/Akt induces transcription of enzymes involved in cholesterol and fatty acid biosynthesis via activation of SREBP. Oncogene. 2005;24:6465-6481.

54. Andreesen R, Modolell M, Munder PG. Selective sensitivity of chronic myelogenous leukemia cell populations to alkyl-lysophospholipids. Blood. 1979;54:519-523.

55. Modolell M, Andreesen R, Pahlke W, Brugger U, Munder PG. Disturbance of phospholipid metabolism during the selective destruction of tumor cells induced by alkyl-lysophospholipids. Cancer Res. 1979;39:4681-4686.

56. van Blitterswijk WJ, Verheij M. Anticancer Alkylphospholipids: Mechanisms of Action, Cellular Sensitivity and Resistance, and Clinical Prospects. Curr Pharm Des. 2008;14:2061-2074.

57. Nieto-Miguel T, Gajate C, Mollinedo F. Differential targets and subcellular localization of antitumor alkyl-lysophospholipid in leukemic versus solid tumor cells. J Biol Chem. 2006;281:14833-14840.

58. Gajate C, Mollinedo F. Biological activities, mechanisms of action and biomedical prospect of the antitumor ether phospholipid ET-18-OCH(3) (edelfosine), a proapoptotic agent in tumor cells. Curr Drug Metab. 2002;3:491-525.

59. Mollinedo F, Fernandez-Luna JL, Gajate C, et al. Selective induction of apoptosis in cancer cells by the ether lipid ET-18-OCH3 (Edelfosine): molecular structure requirements, cellular uptake, and protection by Bcl-2 and Bcl-X(L). Cancer Res. 1997;57:1320-1328.

60. Mollinedo F, Gajate C, Martin-Santamaria S, Gago F. ET-18-OCH3 (edelfosine): a selective antitumour lipid targeting apoptosis through intracellular activation of Fas/CD95 death receptor. Curr Med Chem. 2004;11:3163-3184.

61. Ausili A, Torrecillas A, Aranda FJ, et al. Edelfosine is incorporated into rafts and alters their organization. J Phys Chem B. 2008;112:11643-11654.

62. Torrecillas A, Aroca-Aguilar JD, Aranda FJ, et al. Effects of the anti-neoplastic agent ET-18-OCH3 and some analogs on the biophysical properties of model membranes. Int J Pharm. 2006;318:28-40.

63. Busto JV, Del Canto-Janez E, Goni FM, Mollinedo F, Alonso A. Combination of the anti-tumour cell ether lipid edelfosine with sterols abolishes haemolytic side effects of the drug. J Chem Biol. 2008;1:89-94.

64. Mollinedo F, de la Iglesia-Vicente J, Gajate C, et al. Lipid raft-targeted therapy in multiple myeloma. Oncogene. 2010;29:3748-3757.

65. Mollinedo F, Fernandez M, Hornillos V, et al. Involvement of lipid rafts in the localization and dysfunction effect of the antitumor ether phospholipid edelfosine in mitochondria. Cell Death Dis. 2011;2:e158.

66. Cuesta-Marban A, Botet J, Czyz O, et al. Drug uptake, lipid rafts, and vesicle trafficking modulate resistance to an anticancer lysophosphatidylcholine analogue in yeast. J Biol Chem. 2013;288:8405-8418.

67. Gajate C, Gonzalez-Camacho F, Mollinedo F. Involvement of raft aggregates enriched in Fas/CD95 death-inducing signaling complex in the antileukemic action of edelfosine in Jurkat cells. PLoS One. 2009;4:e5044.

68. Van der Luit AH, Budde M, Zerp S, et al. Resistance to alkyl-lysophospholipid-induced apoptosis due to downregulated sphingomyelin synthase 1 expression with consequent sphingomyelin- and cholesterol-deficiency in lipid rafts. Biochem J. 2007;401:541-549.

69. Gajate C, Mollinedo F. Edelfosine and perifosine induce selective apoptosis in multiple myeloma by recruitment of death receptors and downstream signaling molecules into lipid rafts. Blood. 2007;109:711-719.

70. Mollinedo F, de la Iglesia-Vicente J, Gajate C, et al. In vitro and In vivo selective antitumor activity of Edelfosine against mantle cell lymphoma and chronic lymphocytic leukemia involving lipid rafts. Clin Cancer Res. 2010;16:2046-2054.

71. Gajate C, Santos-Beneit AM, Macho A, et al. Involvement of mitochondria and caspase-3 in ET-18-OCH(3)-induced apoptosis of human leukemic cells. Int J Cancer. 2000;86:208-218.

72. Gajate C, Gonzalez-Camacho F, Mollinedo F. Lipid raft connection between extrinsic and intrinsic apoptotic pathways. Biochem Biophys Res Commun. 2009;380:780-784.

73. Mollinedo F, Gajate C. Lipid rafts, death receptors and CASMERs: new insights for cancer therapy. Future Oncol. 2010;6:491-494.

74. Nieto-Miguel T, Gajate C, Gonzalez-Camacho F, Mollinedo F. Proapoptotic role of Hsp90 by its interaction with c-Jun N-terminal kinase in lipid rafts in edelfosine-mediated antileukemic therapy. Oncogene. 2008;27:1779-1787.

75. Gajate C, Fonteriz RI, Cabaner C, et al. Intracellular triggering of Fas, independently of FasL, as a new mechanism of antitumor ether lipid-induced apoptosis. Int J Cancer. 2000;85:674-682.

76. Delmas D, Rebe C, Lacour S, et al. Resveratrol-induced apoptosis is associated with Fas redistribution in the rafts and the formation of a death-inducing signaling complex in colon cancer cells. J Biol Chem. 2003;278:41482-41490.

77. Colin D, Limagne E, Jeanningros S, et al. Endocytosis of resveratrol via lipid rafts and activation of downstream signaling pathways in cancer cells. Cancer Prev Res (Phila). 2011;4:1095-1106.

78. Lacour S, Hammann A, Grazide S, et al. Cisplatin-induced CD95 redistribution into membrane lipid rafts of HT29 human colon cancer cells. Cancer Res. 2004;64:3593-3598.

79. DeMorrow S, Glaser S, Francis H, et al. Opposing actions of endocannabinoids on cholangiocarcinoma growth: recruitment of Fas and Fas ligand to lipid rafts. J Biol Chem. 2007;282:13098-13113.

80. Mollinedo F, Gajate C. Lipid rafts and clusters of apoptotic signaling molecule-enriched rafts in cancer therapy. Future Oncol. 2010;6:811-821.

81. Nieto-Miguel T, Fonteriz RI, Vay L, Gajate C, Lopez-Hernandez S, Mollinedo F. Endoplasmic reticulum stress in the proapoptotic action of edelfosine in solid tumor cells. Cancer Res. 2007;67:10368-10378.

82. Gajate C, Matos-da-Silva M, Dakir el H, Fonteriz RI, Alvarez J, Mollinedo F. Antitumor alkyl-lysophospholipid analog edelfosine induces apoptosis in pancreatic cancer by targeting endoplasmic reticulum. Oncogene. 2012;31:2627-2639.

83. Ruiter GA, Zerp SF, Bartelink H, van Blitterswijk WJ, Verheij M. Anti-cancer alkyl--lysophospholipids inhibit the phosphatidylinositol 3-kinase-Akt/PKB survival pathway. Anticancer Drugs. 2003;14:167-173.

84. Beneteau M, Pizon M, Chaigne-Delalande B, et al. Localization of Fas/CD95 into the lipid rafts on down-modulation of the phosphatidylinositol 3-kinase signaling pathway. Mol Cancer Res. 2008;6:604-613.

85. Barille-Nion S, Barlogie B, Bataille R, et al. Advances in biology and therapy of multiple myeloma. Hematology Am Soc Hematol Educ Program. 2003:248-278.

86. Lonial S. Multiple myeloma: novel approaches for relapsed disease. Clin Lymphoma Myeloma. 2007;8 Suppl 1:S18-23.

87. Mollinedo F. Death Receptors in Multiple Myeloma and Therapeutic Opportunities. In: Lonial S, ed. Contemporary Hematology Myeloma Therapy. Totowa, NJ: Humana Press; 2009;393-419.

88. Aziz MH, Kumar R, Ahmad N. Cancer chemoprevention by resveratrol: in vitro and in vivo studies and the underlying mechanisms (review). Int J Oncol. 2003;23:17-28.

89. Jang M, Cai L, Udeani GO, et al. Cancer chemopreventive activity of resveratrol, a natural product derived from grapes. Science. 1997;275:218-220.

90. Baur JA, Sinclair DA. Therapeutic potential of resveratrol: the in vivo evidence. Nat

Rev Drug Discov. 2006;5:493-506.

91. Delmas D, Rebe C, Micheau O, et al. Redistribution of CD95, DR4 and DR5 in rafts accounts for the synergistic toxicity of resveratrol and death receptor ligands in colon carcinoma cells. Oncogene. 2004;23:8979-8986.

92. Bhardwaj A, Sethi G, Vadhan-Raj S, et al. Resveratrol inhibits proliferation, induces apoptosis, and overcomes chemoresistance through down-regulation of STAT3 and nuclear factor-kappaB-regulated antiapoptotic and cell survival gene products in human multiple myeloma cells. Blood. 2007;109:2293-2302.

93. Schon A, Freire E. Thermodynamics of intersubunit interactions in cholera toxin upon binding to the oligosaccharide portion of its cell surface receptor, ganglioside GM1. Biochemistry. 1989;28:5019-5024.

94. Harder T, Scheiffele P, Verkade P, Simons K. Lipid domain structure of the plasma membrane revealed by patching of membrane components. J Cell Biol. 1998;141:929-942.

95. Christian AE, Haynes MP, Phillips MC, Rothblat GH. Use of cyclodextrins for manipulating cellular cholesterol content. J Lipid Res. 1997;38:2264-2272.

96. Luo X, Budihardjo I, Zou H, Slaughter C, Wang X. Bid, a Bcl2 interacting protein, mediates cytochrome c release from mitochondria in response to activation of cell surface death receptors. Cell. 1998;94:481-490.

97. Bennett BL, Sasaki DT, Murray BW, et al. SP600125, an anthrapyrazolone inhibitor of Jun N-terminal kinase. Proc Natl Acad Sci U S A. 2001;98:13681-13686.

98. Hofmann TG, Moller A, Hehner SP, Welsch D, Droge W, Schmitz ML. CD95-induced JNK activation signals are transmitted by the death-inducing signaling complex (DISC), but not by Daxx. Int J Cancer. 2001;93:185-191.

99. Shima Y, Nishimoto N, Ogata A, Fujii Y, Yoshizaki K, Kishimoto T. Myeloma cells express Fas antigen/APO-1 (CD95) but only some are sensitive to anti-Fas antibody resulting in apoptosis. Blood. 1995;85:757-764.

100. Westendorf JJ, Lammert JM, Jelinek DF. Expression and function of Fas (APO-1/CD95) in patient myeloma cells and myeloma cell lines. Blood. 1995;85:3566-3576.

101. Mollinedo F. Antitumor ether lipids: proapoptotic agents with multiple therapeutic indications. Expert Opin Ther Patents. 2007;17:385-405.

102. Orlowski RZ, Kuhn DJ. Proteasome inhibitors in cancer therapy: lessons from the first decade. Clin Cancer Res. 2008;14:1649-1657.

103. Ashkenazi A, Holland P, Eckhardt SG. Ligand-based targeting of apoptosis in cancer: the potential of recombinant human apoptosis ligand 2/Tumor necrosis factor-related apoptosis-inducing ligand (rhApo2L/TRAIL). J Clin Oncol. 2008;26:3621-3630.

104. Fulda S, Debatin KM. Resveratrol-mediated sensitisation to TRAIL-induced apoptosis depends on death receptor and mitochondrial signalling. Eur J Cancer. 2005;41:786-798.

105. Gill C, Walsh SE, Morrissey C, Fitzpatrick JM, Watson RW. Resveratrol sensitizes androgen independent prostate cancer cells to death-receptor mediated apoptosis through multiple mechanisms. Prostate. 2007;67:1641-1653.

106. Barjot C, Tournaire M, Castagnino C, Vigor C, Vercauteren J, Rossi JF. Evaluation of antitumor effects of two vine stalk oligomers of resveratrol on a panel of lymphoid and myeloid cell lines: comparison with resveratrol. Life Sci. 2007;81:1565-1574.

107. Jares P, Colomer D, Campo E. Genetic and molecular pathogenesis of mantle cell lymphoma: perspectives for new targeted therapeutics. Nat Rev Cancer. 2007;7:750-762.

108. Perez-Galan P, Dreyling M, Wiestner A. Mantle cell lymphoma: biology, pathogenesis, and the molecular basis of treatment in the genomic era. Blood. 2011;117:26-38.

109. Herrmann A, Hoster E, Zwingers T, et al. Improvement of overall survival in advanced stage mantle cell lymphoma. J Clin Oncol. 2009;27:511-518.

110. Dal Col J, Zancai P, Terrin L, et al. Distinct functional significance of Akt and mTOR constitutive activation in mantle cell lymphoma. Blood. 2008;111:5142-5151.

111. Rudelius M, Pittaluga S, Nishizuka S, et al. Constitutive activation of Akt contributes to the pathogenesis and survival of mantle cell lymphoma. Blood. 2006;108:1668-1676.

112. Duronio V. The life of a cell: apoptosis regulation by the PI3K/PKB pathway. Biochem J. 2008;415:333-344.

113. Zoncu R, Efeyan A, Sabatini DM. mTOR: from growth signal integration to cancer, diabetes and ageing. Nat Rev Mol Cell Biol. 2011;12:21-35.

114. Gao X, Zhang J. Akt signaling dynamics in plasma membrane microdomains visualized by FRET-based reporters. Commun Integr Biol. 2009;2:32-34.

115. Reis-Sobreiro M, Gajate C, Mollinedo F. Involvement of mitochondria and recruitment of Fas/CD95 signaling in lipid rafts in resveratrol-mediated antimyeloma and antileukemia actions. Oncogene. 2009;28:3221-3234.

116. van der Luit AH, Budde M, Ruurs P, Verheij M, van Blitterswijk WJ. Alkyl-lysophospholipid accumulates in lipid rafts and induces apoptosis via raft-dependent endocytosis and inhibition of phosphatidylcholine synthesis. J Biol Chem. 2002;277:39541-39547.

117. Berggren MI, Gallegos A, Dressler LA, Modest EJ, Powis G. Inhibition of the signalling enzyme phosphatidylinositol-3-kinase by antitumor ether lipid analogues. Cancer Res. 1993;53:4297-4302.

118. Gajate C, Santos-Beneit A, Modolell M, Mollinedo F. Involvement of c-Jun NH2--terminal kinase activation and c-Jun in the induction of apoptosis by the ether phospholipid 1-O-octadecyl-2-O-methyl-rac-glycero-3-phosphocholine. Mol Pharmacol. 1998;53:602-612.

119. Obata T, Yaffe MB, Leparc GG, et al. Peptide and protein library screening defines optimal substrate motifs for AKT/PKB. J Biol Chem. 2000;275:36108-36115.

120. Wang M, Atayar C, Rosati S, Bosga-Bouwer A, Kluin P, Visser L. JNK is constitutively active in mantle cell lymphoma: cell cycle deregulation and polyploidy by JNK inhibitor SP600125. J Pathol. 2009;218:95-103.

121. Serra V, Scaltriti M, Prudkin L, et al. PI3K inhibition results in enhanced HER signaling and acquired ERK dependency in HER2-overexpressing breast cancer. Oncogene. 2011;30:2547-2557.

122. Castillo SS, Brognard J, Petukhov PA, et al. Preferential inhibition of Akt and killing of Akt-dependent cancer cells by rationally designed phosphatidylinositol ether lipid analogues. Cancer Res. 2004;64:2782-2792.

123. Kumar CC, Madison V. AKT crystal structure and AKT-specific inhibitors. Oncogene. 2005;24:7493-7501.

124. Andersen NS, Larsen JK, Christiansen J, et al. Soluble CD40 ligand induces selective proliferation of lymphoma cells in primary mantle cell lymphoma cell cultures. Blood. 2000;96:2219-2225.

125. Conus NM, Hannan KM, Cristiano BE, Hemmings BA, Pearson RB. Direct identification of tyrosine 474 as a regulatory phosphorylation site for the Akt protein kinase. J Biol Chem. 2002;277:38021-38028.

126. Mollinedo F, Gajate C, Morales AI, et al. Novel anti-inflammatory action of edelfosine lacking toxicity with protective effect in experimental colitis. J Pharmacol Exp Ther. 2009;329:439-449.

127. Garrido SM, Appelbaum FR, Willman CL, Banker DE. Acute myeloid leukemia cells are protected from spontaneous and drug-induced apoptosis by direct contact with a human bone marrow stromal cell line (HS-5). Exp Hematol. 2001;29:448-457.

128. Cardone MH, Roy N, Stennicke HR, et al. Regulation of cell death protease caspase-9 by phosphorylation. Science. 1998;282:1318-1321.

129. Plumas J, Jacob MC, Chaperot L, Molens JP, Sotto JJ, Bensa JC. Tumor B cells from non-Hodgkin's lymphoma are resistant to CD95 (Fas/Apo-1)-mediated apoptosis. Blood. 1998;91:2875-2885.

130. Clodi K, Snell V, Zhao S, Cabanillas F, Andreeff M, Younes A. Unbalanced expression of Fas and CD40 in mantle cell lymphoma. Br J Haematol. 1998;103:217-219.

131. Vilimek D, Duronio V. Cytokine-stimulated phosphorylation of GSK-3 is primarily dependent upon PKCs, not PKB. Biochem Cell Biol. 2006;84:20-29.

132. Kondapaka SB, Singh SS, Dasmahapatra GP, Sausville EA, Roy KK. Perifosine, a novel alkylphospholipid, inhibits protein kinase B activation. Mol Cancer Ther. 2003;2:1093-1103.

133. Hope HR, Pike LJ. Phosphoinositides and phosphoinositide-utilizing enzymes in detergent-insoluble lipid domains. Mol Biol Cell. 1996;7:843-851.

134. Hill MM, Feng J, Hemmings BA. Identification of a plasma membrane Raft-associa-

ted PKB Ser473 kinase activity that is distinct from ILK and PDK1. Curr Biol. 2002;12:1251-1255.

135. Alderliesten MC, Klarenbeek JB, van der Luit AH, et al. Phosphoinositide phosphatase SHIP-1 regulates apoptosis induced by edelfosine, Fas ligation and DNA damage in mouse lymphoma cells. Biochem J. 2011;440:127-135.

136. Kumar SK, Rajkumar SV, Dispenzieri A, et al. Improved survival in multiple myeloma and the impact of novel therapies. Blood. 2008;111:2516-2520.

137. Jagannath S, Dimopoulos MA, Lonial S. Combined proteasome and histone deacetylase inhibition: A promising synergy for patients with relapsed/refractory multiple myeloma. Leuk Res. 2010;34:1111-1118.

138. Lonial S, Kaufman JL. The Era of Combination Therapy in Myeloma. J Clin Oncol. 2012; 30: 2434-2436.

139. Gajate C, Mollinedo F. Lipid rafts and Fas/CD95 signaling in cancer chemotherapy. Recent Pat Anticancer Drug Discov. 2011;6:274-283.

140. Hueber AO, Bernard AM, Herincs Z, Couzinet A, He HT. An essential role for membrane rafts in the initiation of Fas/CD95-triggered cell death in mouse thymocytes. EMBO Rep. 2002;3:190-196.

141. Legembre P, Daburon S, Moreau P, et al. Amplification of Fas-mediated apoptosis in type II cells via microdomain recruitment. Mol Cell Biol. 2005;25:6811-6820.

142. Legembre P, Daburon S, Moreau P, Moreau JF, Taupin JL. Modulation of Fas-mediated apoptosis by lipid rafts in T lymphocytes. J Immunol. 2006;176:716-720.

143. Watanabe R, Tokuhira M, Kizaki M. Current approaches for the treatment of multiple myeloma. Int J Hematol. 2013;97:333-344.

144. Macbride A RPY. Proteasome inhibitors in the treatment of multiple myeloma. Expert Rev Anticancer Ther. 2013;13:339-358.

145. Hideshima T, Richardson PG, Anderson KC. Mechanism of action of proteasome inhibitors and deacetylase inhibitors and the biological basis of synergy in multiple myeloma. Mol Cancer Ther. 2011;10:2034-2042.

146. Richardson PG, Mitsiades CS, Laubach JP, et al. Preclinical data and early clinical experience supporting the use of histone deacetylase inhibitors in multiple myeloma. Leuk Res. 2013;37:829-837.

147. Hajek R, Siegel D, Orlowski RZ, Ludwig H, Palumbo A, Dimopoulos MA. The Role of Hdac Inhibitors in Patients with Relapsed/Refractory Multiple Myeloma. Leuk Lymphoma. 2013.

148. Cea M, Cagnetta A, Gobbi M, et al. New insights into the treatment of multiple myeloma with histone deacetylase inhibitors. Curr Pharm Des. 2013;19:734-744.

149. Hideshima T, Anderson KC. Histone deacetylase inhibitors in the treatment for multiple myeloma. Int J Hematol. 2013;97:324-332.

150. Hideshima T, Richardson P, Chauhan D, et al. The proteasome inhibitor PS-341 inhibits growth, induces apoptosis, and overcomes drug resistance in human multiple myeloma cells. Cancer Res. 2001;61:3071-3076.

151. Ottosson-Wadlund A, Ceder R, Preta G, et al. Requirement of apoptotic protease--activating factor-1 for bortezomib-induced apoptosis but not for Fas-mediated apoptosis in human leukemic cells. Mol Pharmacol. 2013;83:245-255.

152. De Rose V, Cappello P, Sorbello V, et al. IFN-gamma inhibits the proliferation of allergen-activated T lymphocytes from atopic, asthmatic patients by inducing Fas/FasL-mediated apoptosis. J Leukoc Biol. 2004;76:423-432.

153. Rao-Bindal K, Zhou Z, Kleinerman ES. MS-275 sensitizes osteosarcoma cells to Fas ligand-induced cell death by increasing the localization of Fas in membrane lipid rafts. Cell Death Dis. 2012;3:e369.

154. Borrello I. Can we change the disease biology of multiple myeloma? Leuk Res. 2012;36 Suppl 1:S3-12.

155. Glasser L, Dalton WS, Fiederlein RL, Cook P, Powis G, Vogler WR. Response of human multiple myeloma-derived cell lines to alkyl-lysophospholipid. Exp Hematol. 1996;24:253-257.

156. Hideshima T, Catley L, Yasui H, et al. Perifosine, an oral bioactive novel alkylphospholipid, inhibits Akt and induces in vitro and in vivo cytotoxicity in human multiple myeloma cells. Blood. 2006;107:4053-4062.

157. Richardson PG, Wolf J, Jakubowiak A, et al. Perifosine plus bortezomib and dexamethasone in patients with relapsed/refractory multiple myeloma previously treated with bortezomib: results of a multicenter phase I/II trial. J Clin Oncol. 2011;29:4243-4249.

158. Varela MR, Villa-Pulgarin JA, Yepes E, et al. In vitro and in vivo efficacy of ether lipid edelfosine against Leishmania spp. and SbV-resistant parasites. PLoS Negl Trop Dis. 2012;6:e1612.

159. Ogasawara J, Watanabe-Fukunaga R, Adachi M, et al. Lethal effect of the anti-Fas antibody in mice. Nature. 1993;364:806-809.

160. Vergara D, Simeone P, Toraldo D, et al. Resveratrol downregulates Akt/GSK and ERK signalling pathways in OVCAR-3 ovarian cancer cells. Mol Biosyst. 2012;8:1078-1087.

161. Kim AH, Yano H, Cho H, et al. Akt1 regulates a JNK scaffold during excitotoxic apoptosis. Neuron. 2002;35:697-709.

162. Berra E, Diaz-Meco MT, Moscat J. The activation of p38 and apoptosis by the inhibition of Erk is antagonized by the phosphoinositide 3-kinase/Akt pathway. J Biol Chem. 1998;273:10792-10797.

163. Cerezo A, Martinez AC, Lanzarot D, Fischer S, Franke TF, Rebollo A. Role of Akt and c-Jun N-terminal kinase 2 in apoptosis induced by interleukin-4 deprivation. Mol Biol Cell. 1998;9:3107-3118.

164. den Hertog J, Groen A, van der Wijk T. Redox regulation of protein-tyrosine phosphatases. Arch Biochem Biophys. 2005;434:11-15.

165. Pike LJ. Lipid rafts: bringing order to chaos. J Lipid Res. 2003;44:655-667.

166. Weinstein IB. Cancer. Addiction to oncogenes--the Achilles heal of cancer. Science. 2002;297:63-64.

167. Estella-Hermoso de Mendoza A, Campanero MA, Mollinedo F, Blanco-Prieto MJ. Comparative study of A HPLC-MS assay versus an UHPLC-MS/MS for anti-tumoral alkyl lysophospholipid edelfosine determination in both biological samples and in lipid nanoparticulate systems. J Chromatogr B Analyt Technol Biomed Life Sci. 2009;877:4035-4041.

168. Bruyneel EA, Storme GA, Schallier DC, Van den Berge DL, Hilgard P, Mareel MM. Evidence for abrogation of oncogene-induced radioresistance of mammary cancer cells by hexadecylphosphocholine in vitro. Eur J Cancer. 1993;29A:1958-1963.

169. Lasa-Saracibar B, Estella-Hermoso de Mendoza A, Mollinedo F, Odero MD, Blanco--Prieto MJ. Edelfosine lipid nanosystems overcome drug resistance in leukemic cell lines. Cancer Lett. 2013;334:302-310.

170. Estella-Hermoso de Mendoza A, Preat V, Mollinedo F, Blanco-Prieto MJ. In vitro and in vivo efficacy of edelfosine-loaded lipid nanoparticles against glioma. J Control Release. 2011;156:421-426.

171. Gomide AB, Thome CH, Dos Santos GA, et al. Disrupting membrane raft domains by alkylphospholipids. Biochim Biophys Acta. 2013;1828:1384-1389.

172. Pike LJ. The challenge of lipid rafts. J Lipid Res. 2009;50 Suppl:S323-328.

173. Gajate C, An F, Mollinedo F. Rapid and selective apoptosis in human leukemic cells induced by Aplidine through a Fas/CD95- and mitochondrial-mediated mechanism. Clin Cancer Res. 2003;9:1535-1545.

174. Spets H, Georgii-Hemming P, Siljason J, Nilsson K, Jernberg-Wiklund H. Fas/APO-1 (CD95)-mediated apoptosis is activated by interferon-gamma and interferon- in interleukin-6 (IL-6)-dependent and IL-6-independent multiple myeloma cell lines. Blood. 1998;92:2914-2923.